博士論文

論文題目**Bridge of Solution and Solid-state Chemistry through the Dynamic Nature of M_6L_4 Capsule**

（M_6L_4カプセルの動的性質を介した溶液化学と固相化学の架橋）

氏名　　寧 國宏

Ning Guo-Hong

CONTENTS

Chapter 4

Chapter 5

Chapter 6

Chapter 1

General Introduction

This chapter provides an overview of host-guest chemistry in solution or in the solid-state with either rigid or flexible (dynamic) synthetic hosts. In addition, the 'networking strategy' for bridging two physical states of chemistry through a pair of rigid M_6L_4 cage hosts is described. Finally, the aims and strategy of this thesis are given.

1.1 *Host-Guest Chemistry in Solution*

In the past few decades, chemists have prepared numerous molecular hosts that are capable of binding guest molecules in solution. This introduction does not intent to be an exhaustive review of all hosts to date, but rather is meant to provide an overview, which forces on the synthetic hosts that are able to completely isolate guests from external environments and correspondingly modulate their physical or chemical properties.[1]

In the early 1980s, Donald J. Cram et al. developed the chemistry of carcerands (Figure 1.1a), which accommodated various solvent guests (e.g. dimethylacetamide (DMA), dimethylformamide (DMF) and dimethylsulfoxide (DMSO)) within their inner space to form carceplexes.[2,3] These guests are permanently entrapped due to the closed surface of carcerands, and their release can only occur by decomposition of the hosts. The Cram group has also synthesized hemicarcerands (Figure 1.1b), which are structurally similar to carcerands, but they can generate portals that allow guests release and bind under different circumstance (e.g. temperature). For example, Cram and co-workers have stabilized cyclobutadiene in solution at room temperature within the unique microenvironment created by hemicarcerands (Figure 1.1c).[4] Warmuth et al. also reported the synthesis and stablization of *o*-benzyne within the inner phase of hemicarcerands at –75 °C (Figure 1.1d).[5]

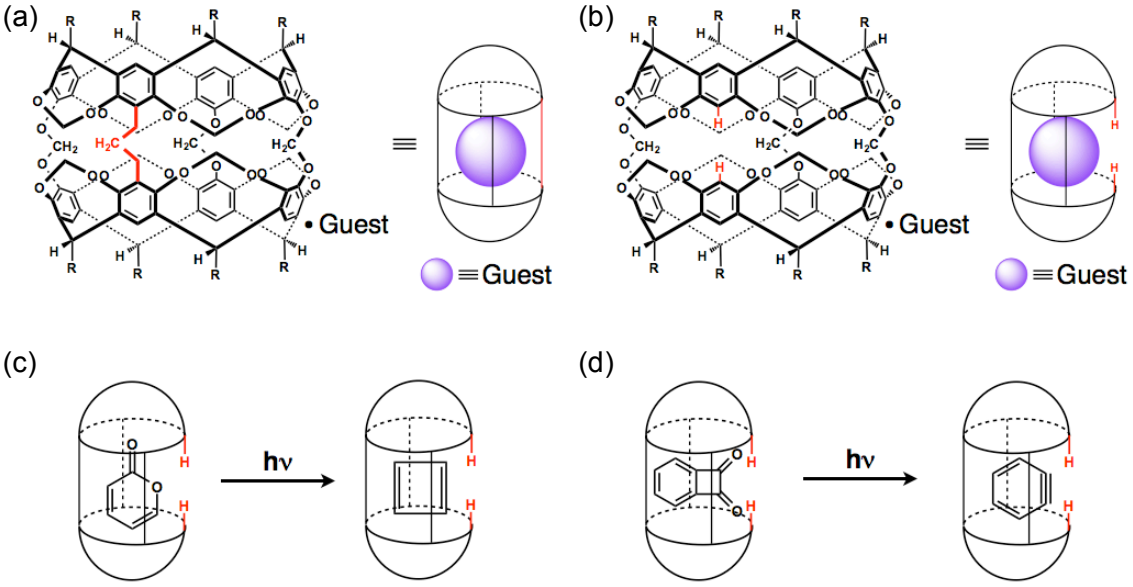

Figure 1.1. (a) Carceplex; (b) hemicarceplex; stabilization of (c) cyclobutadiene and (d) *o*-benzyne within hemicarcerands.

The group of Jerry L. Atwood has made major contributions to the field of supramolecular hosts with their multiple hydrogen bonded calixarene assemblies since the 1990s. They demonstrated that identical components could be formed into a 'molecular capsule' with a large cavity (~1375 Å^3) through sixty hydrogen bonds.[6] In the following investigations, the Atwood group found that the physical properties (i.e. volatility) of internalized ethyl acetate guests in the supramolecular capsule are totally different from the external bulk solvent (Figure 1.2).[7]

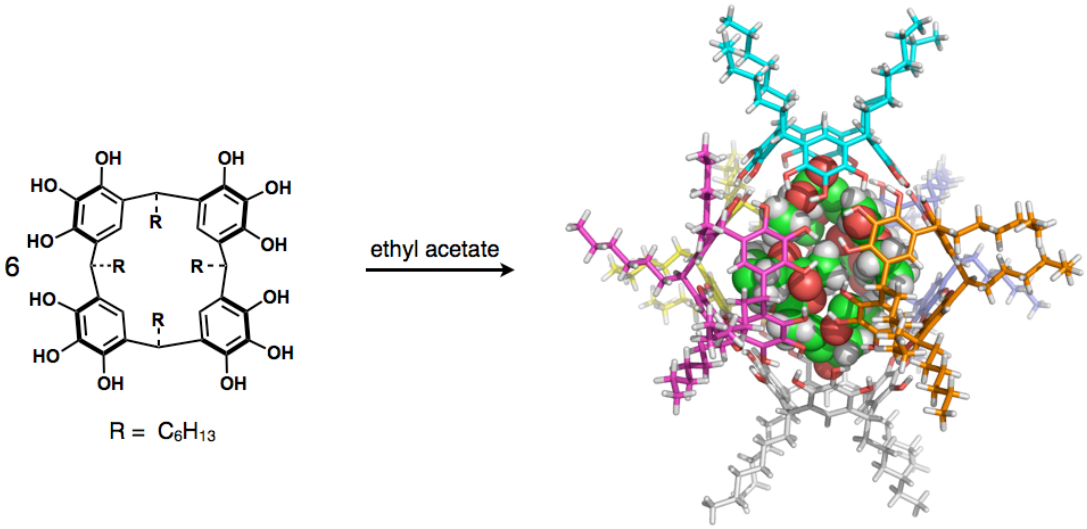

Figure 1.2. X-ray structure of hexameric assemblies that accommodating seven ethyl acetate molecules. (The six pyrogallolarene were shown in stick model with different color; the ethyl acetate molecules were shown as CPK model)

The Julius Rebek Jr. group has developed a series of organic capsule hosts such as tennis ball,[8] soft ball,[9] and cylindrical capsules[10, 11] (Figure 1.3a and b). These capsule hosts are not only able to bind various guests, but are also capable of mediating the chemical and physical properties of entrapped guest molecules. One of the most elegant examples to date is Rebek and co-workers' acceleration of a Diels-Alder reaction by encapsulation of the reactants within a softball capsule (Figure 1.3c).[12] Another distinct example from his group is 'social isomerism' caused by different arrangements among two co-encapsulated guests within the cylindrical capsules (Figure 1.3d).[13]

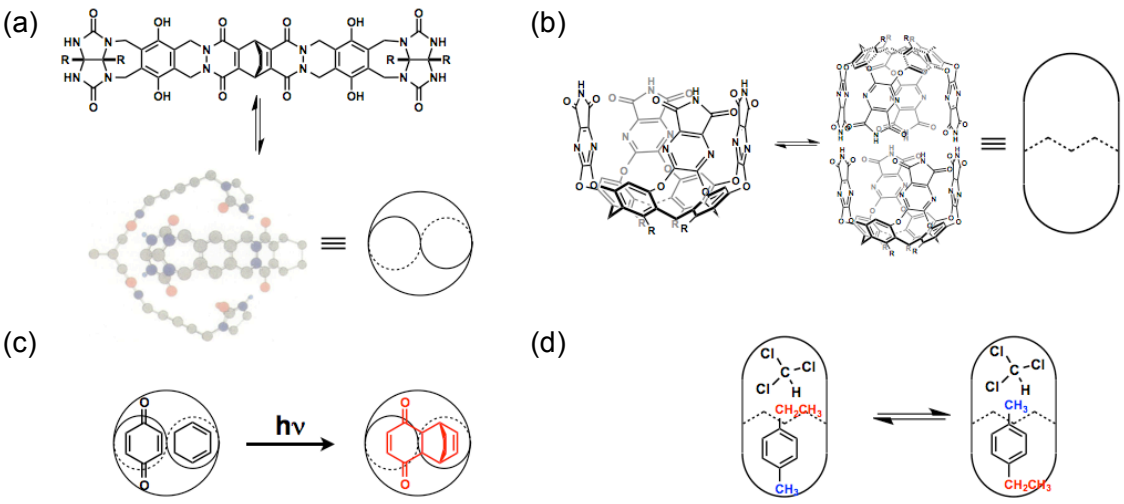

Figure 1.3. Self-assembly of (a) soft ball (From ref. 9. Reprinted with permission from AAAS) and (b) cylindrical capsule; (c) acceleration of D-A reaction in the soft ball; (d) social isomerism in the cylindrical capsule.

To construct more robust hosts than hydrogen-bonded organic assemblies, numerous groups have synthesized metallo-organic cages by utilizing metal-ligand coordination bonds. The Raymond group, for example, has investigated the host-guest chemistry of M_4L_6 (where L = N,N'-bis(2,3-dihydroxybenzoyl)-1,5-diaminonaphthalene and M = Ga^{III}, Fe^{III} or Ti^{III}) molecular capsule (Figure 1.4a).[14] For example, they have demonstrated that their Ga_4L_6 anionic capsule is able to bind and stabilize the reactive cationic species $[Me_2C(OH)PEt_3]^+$ in aqueous solution (Figure 1.4b).[15]

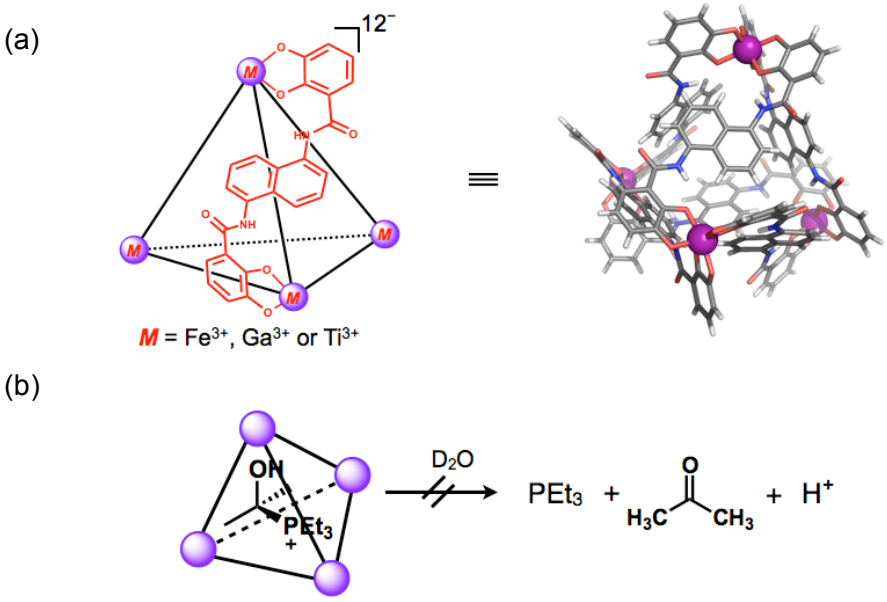

Figure 1.4. (a) Structure of M_4L_6 capsule; (b) stabilization of cationic species.

Very recently, the Nitschke group has prepared a self-assembled Fe_4L_6 capsule with a confined hydrophobic cavity (~140 Å^3) that accommodates the hazardous chemical white phosphorus (P_4) in water. Remarkably, P_4 becomes air-stable and water-soluble within the hollows of the tetrahedral container.[16]

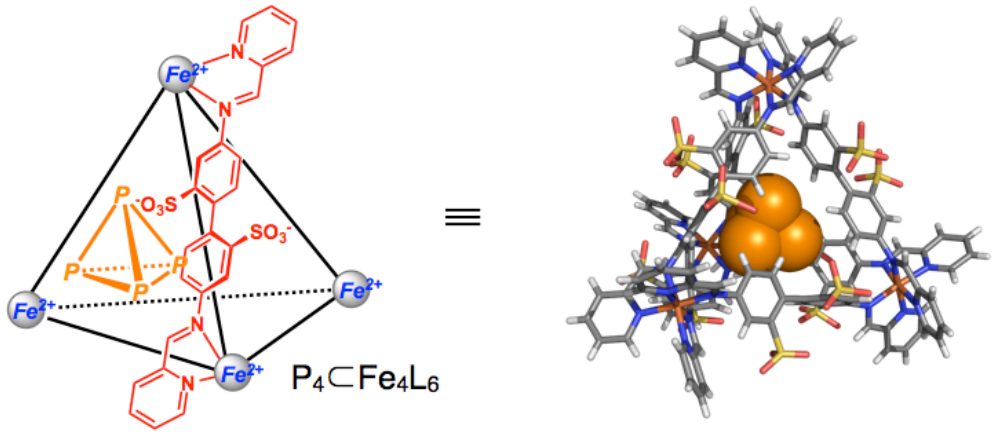

Figure 1.5. Fe_4L_6 capsule accommodating white phosphorus (right, X-ray structure)

Since 1995, the Fujita group has established the chemistry of cationic Pd_6L_4 cages in aqueous solution.[17] The Pd_6L_4 cage's nano-space is capable of binding various guests, including natural and ionic compounds. Due to the confined nature of cavity, Fujita and co-workers found that the *cis-trans* isomerization of a dinuclaer ruthenium complex could be controlled within the cage. Moreover, the cage showed an impressive stabilization effect for the entrapped guest, since the photosensitive ruthenium complex became stable for several months under ambient light (Figure 1.6).[18]

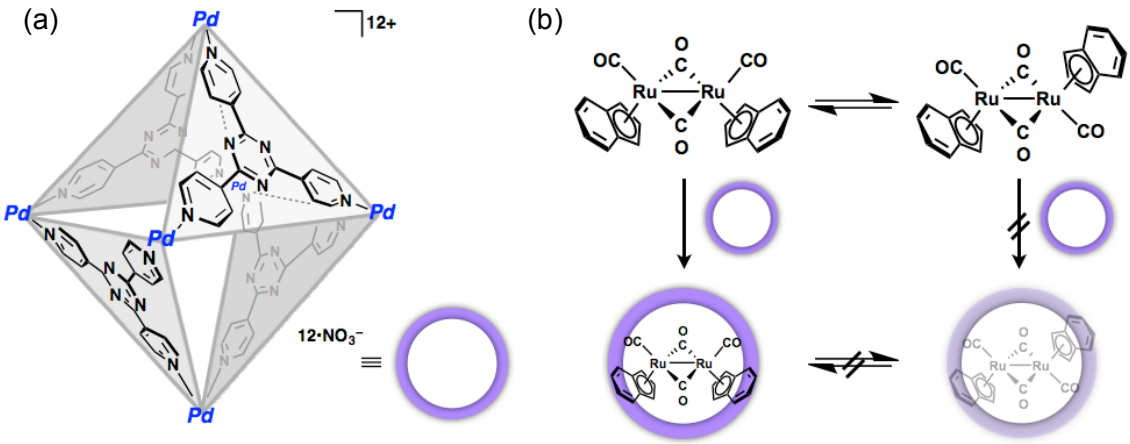

Figure 1.6. (a) Schematic structure of Pd_4L_6 cage and (b) only *cis*-bridged ruthenium complex was trapped within cage.

1.2 *Host-Guest Chemistry in the Solid-State*

Host-guest chemistry in the solid-state still remains immature compared with the well-established and rich host-guest chemistry in solution, and a brief overview of the solid-state host-guest chemistry is introduced in this section.

The zeolites, composed of a cage and channel (pore) structure, can serve as solid (crystalline) hosts to bind a large range of guests including small organic molecules, metal clusters, and organometallic compounds.[19] Dutta et al., for example, have prepared $[Ru(bpy)_3]^{2+}$ in the supercages of zeolite Y via a ship-in-a-bottle synthesis. The size of these guests ensured that once these molecules were synthesized in the cages, they cannot release through the narrow windows of the supercages (Scheme 1.1). As a consequence, the entrapped ruthenium complex shows high thermal stability.[20]

Scheme 1.1. Synthesis of the ruthenium complex encapsulated inside zeolite Y

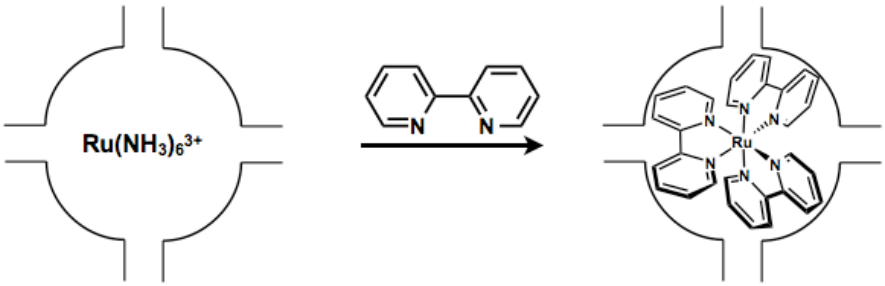

Very recently, the chemistry of metal-organic frameworks (MOFs) or porous coordination polymers (PCPs) constructed from metal connectors and organic linkers have been explored with extraordinary speed, and in most of cases, the chemists only employed the host-guest chemistry within the pores.[21] The porosity, pore size, pore shape and pore surface functionalization are key factors for determination of function and application of MOFs or PCPs. The Yaghi group, for example, has synthesized a series of nine IRMOFs with tunable pore sizes that can be enlarged by extension of the organic linker length (Figure 1.7). Because of the difference of pore volume in these frameworks, the profile of Ar gas uptake is also altered.[22]

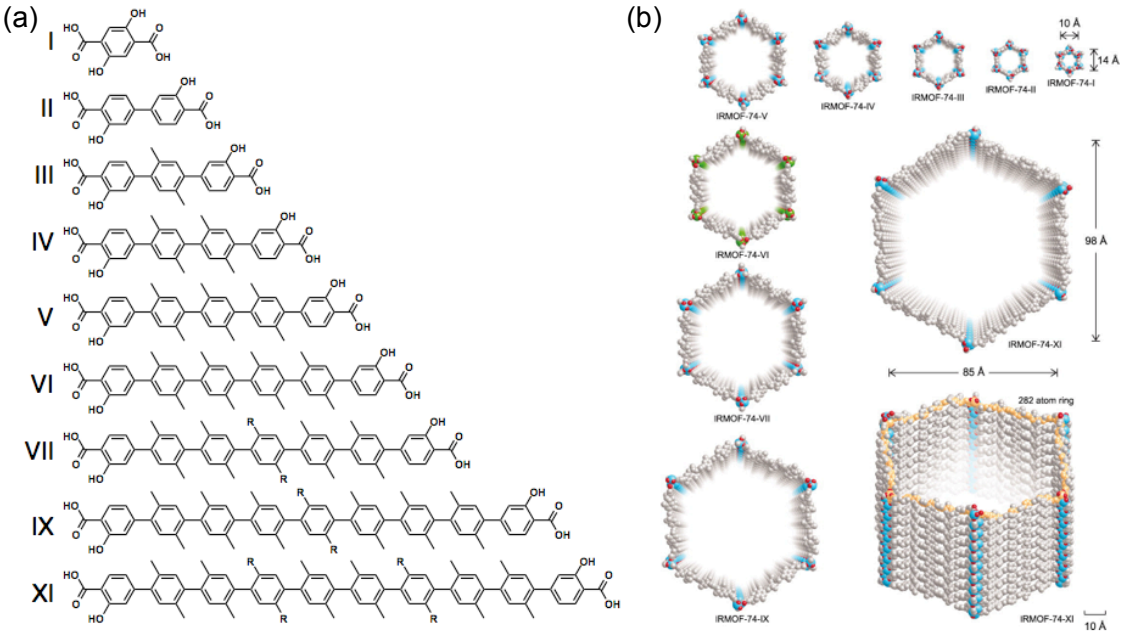

Figure 1.7. (a) Organic linkers and (b) crystal structures of IRMOF-74 series synthesized from the organic linker in (a). (From ref. 22. Reprinted with permission from AAAS)

Although the pores in MOFs or PCPs can affect the physical or chemical prosperities of guests to some extent, it is impossible to totally surround or isolate the guest molecules from the external environment. Therefore, the chemistry of MOFs or PCPs can generally be regarded as 'chemistry of the pores'. Can MOFs incorporate well-defined host cavities into its porous structure? In 1999, Williams et al. synthesized the HKUST-1 that consists of $Cu_{12}L_4$ (where L = benzene-1,3,5-tricarboxylate) octahedral secondary building units (SBUs) and pores (Figure 1.8a,b).[23] Unfortunately, their group and others only investigated the gas absorption of the HKUST-1 and there are no further studies on host-guest chemistry within the octahedral cavity.[24] Another analogous example has come from Long group; they have prepared a series of robust, sodalite-type MOFs $M_3[(M_4Cl)_3(btt)_8]_2$ (where M = Mn, Fe or Cu; btt = 1,3,5-benzenetristetrazolate) that consist of $M_{24}L_8$ truncated-octahedral cage SBUs and pores (Figure 1.8c and d).[25] Although they observed the encapsulation of $[Cu(DMF)_6]^{2+}$ cation within the inner cavity, as in HKUST-1, they only focused on the hydrogen storage and no further investigations of guest binding in the $M_{24}L_8$ cage were conducted. One possibility is that the portal of the robust $M_{24}L_8$ cage is too small to allow guest encapsulation (Figure 1.8e).

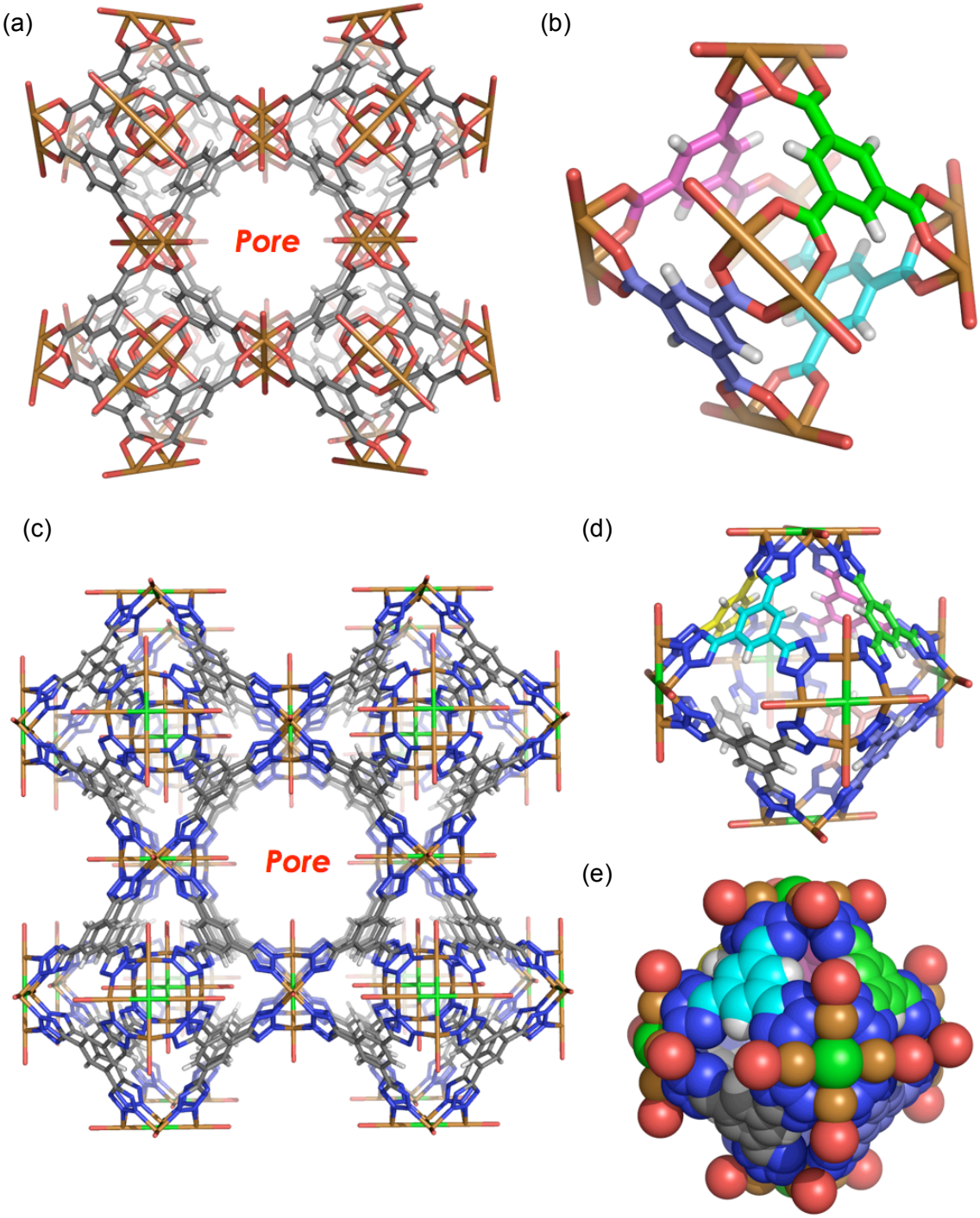

Figure 1.8. Structure of (a) HKUST-1; (b) stick model of the octahedral cage SBUs (the four ligands are shown as different color); Structure of (c) $Cu_3[(Cu_4Cl)_3(btt)_8]_2$; the $M_{24}L_8$ cage SBUs (d) in stick model and (e) in CPK model (the eight ligands are shown as different color)

These examples demonstrate that the incorporation of host cavities into MOFs or PCPs is possible. What new functions or advantages can be obtained from this strategy? Very recently, the Custelcean group has designed an unusual one-dimensional MOF from the self-assembly of Ag_2SO_4 and a tripodal urea linker with the SO_4^{2-} guest anions trapped within cavities instead of pores (Figure 1.9). Unlike other anion binding MOFs, the ion exchange of sulfate was prevented due to its exclusive encapsulation.[26] Therefore, two different environment for guests (e.g. guest in the host cavity and in the pore) can be expected by incorporation of a host cavity in MOFs or PCPs, and a strong encapsulation effect can be generated by host structure.

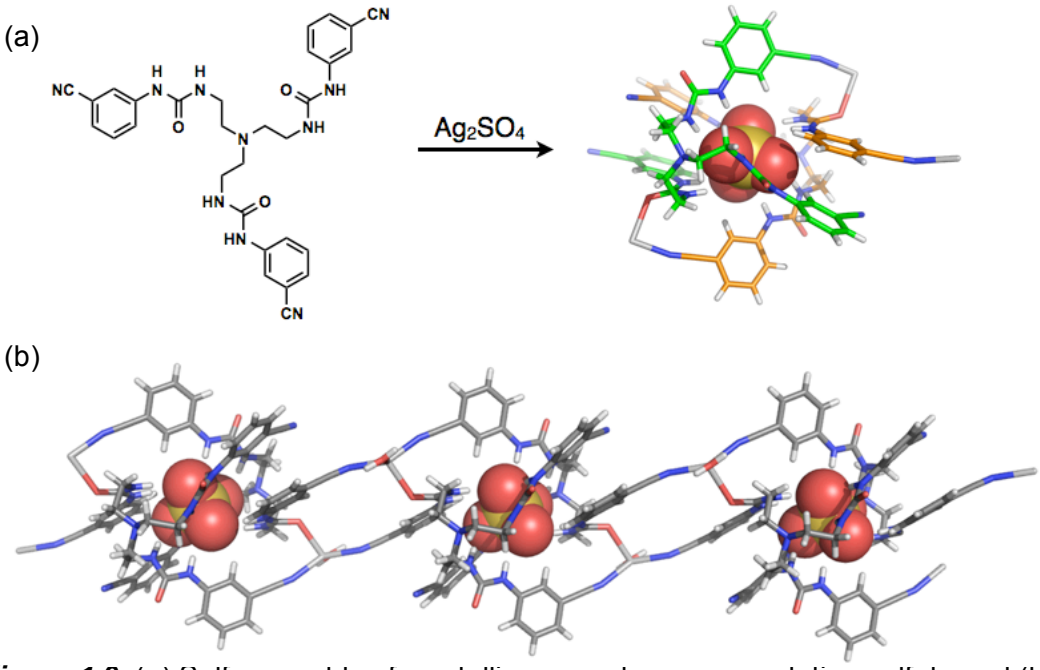

Figure 1.9. (a) Self-assembly of crystalline capsule accommodating sulfate and (b) capsule unit linked by sliver ion resulting in a coordination polymer.

1.3 *Bridge of Solution and the Solid-State Chemistry with Rigid Hosts*

Host-guest chemistry in solution or in the solid (crystalline) state has developed in parallel and independently since the environment for guest binding, major analysis methods, driving forces of guest encapsulation, and dynamic behavior of hosts are completely different in the two states (Table 1.1).

Table 1.1. Features of solution and solid-state host-guest chemistry

	Host-guest chemistry in	
	Solution	Solid-State
Environment for guest binding	Host cavities	Pores
Major analysis methods	Spectroscopy (NMR, MS)	X-ray crystallographic analysis
Driving forces of guest encapsulation	Host-guest interactions (molecular recognition)	Diffusion (fill the vacuum)
Dynamic behavior of hosts	Dynamic (flexible)	Rigid (crystal packing effect)

Take the difference in the dynamic behavior of the host as an example. A. I. Cooper and co-workers have prepared a pure organic molecular cage **CC3** from 1,3,5-triformylbenzene and *(R,R)*-1,2-diaminocyclohexane. They have found that in solution, the dynamic imine bond in **CC3** cage assists the ingress and egress of mesitylene guests (Figure 1.10a). However, in the solid-state, the dynamic dissociation of imine bonds in the **CC3** cage was totally suppressed by the crystal packing effect, therefore mesitylene guests could not be entrapped within the cavity of the organic cage (Figure 1.10b).[27]

Although a bridge between solution and the solid-state chemistry is a challenge, many benefits can be expected: (1) The solid-state chemistry can be predicted through studies in solution, and vice versa; (2) The advantages of both states can be combined synergistically, such as fast screening of suitable guests for the solid-state host by solution-state NMR spectroscopy or **visualization** of host-guest complexes by X-ray

without the need for further crystallization; (3) New functional crystalline hosts can be easily designed by inspiration from solution hosts, and vice versa.

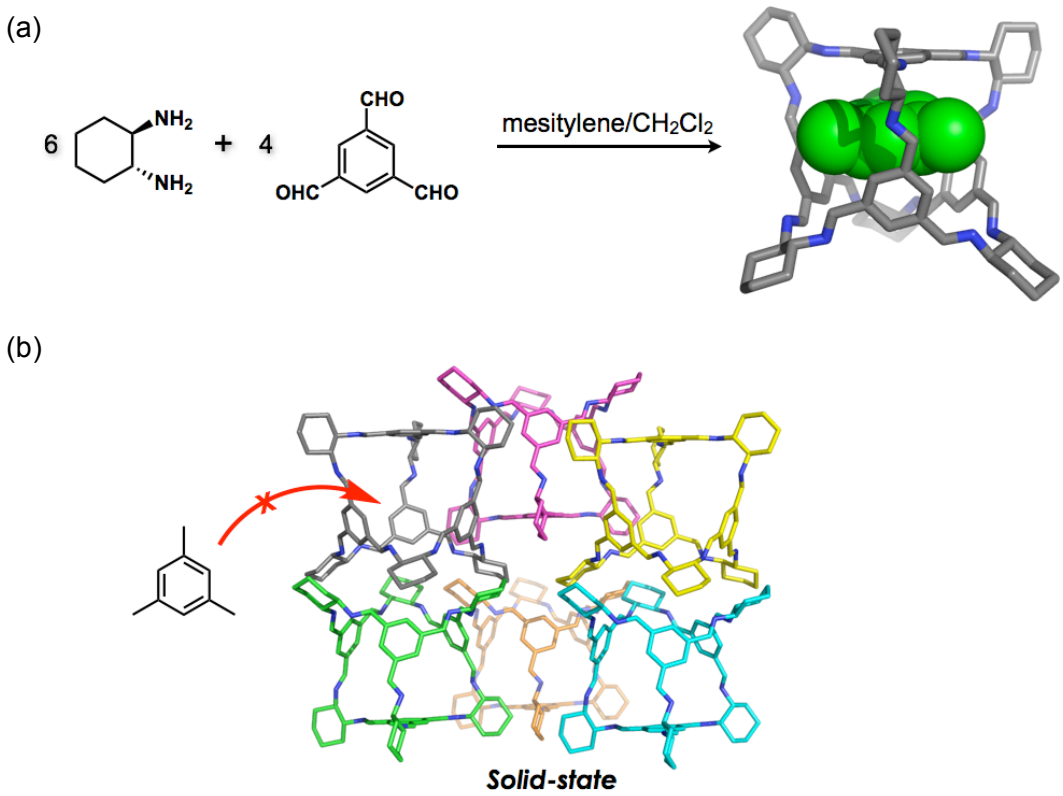

Figure 1.10. (a) Self-assembly of **CC3** molecular cage accommodating mesitylene in solution and (b) The exclusion of mesitylene molecules in the solid (crystalline) state.

The Fujita group has recently demonstrated that solution and solid-state chemistry can be bridged by clever design of common host cavities that are isostructural in solution and the solid state. The pair of a Pd_4L_4 molecular square (solution host) and Cd_4L_4 networked squares (crystalline host) constitute an early example.[28,29] A more distinct example demonstrated that a pair of discrete and networked M_6L_4 (where L = 2,4,6-tris(4-pyridyl)-1,3,5-triazine (**4-TPT**)) rigid cages performed exactly the same guest binding behavior.[30] The networked cages are composed of an infinite network of Co_6L_4 cages with six Co(II) vertexes and four **4-TPT** planes that are identical to discrete Pd_6L_4 cage (Figure 1.11a and b). Further investigations of host-guest chemistry with discrete and networked cages revealed some important insights for designing a complementary pair of solution and solid-state hosts. In this so called

'networking strategy': (1) the guest recognition highly depends on the organic ligand, **4-TPT**, and not on the metal center (i.e. cobalt for networked cages and palladium for discrete cage); (2) the porosity of networked structure is essential for guest encapsulation; (3) it can only applied for metallo-organic hosts, since the change the metal center is curial point for networking discrete cage into networked cages.

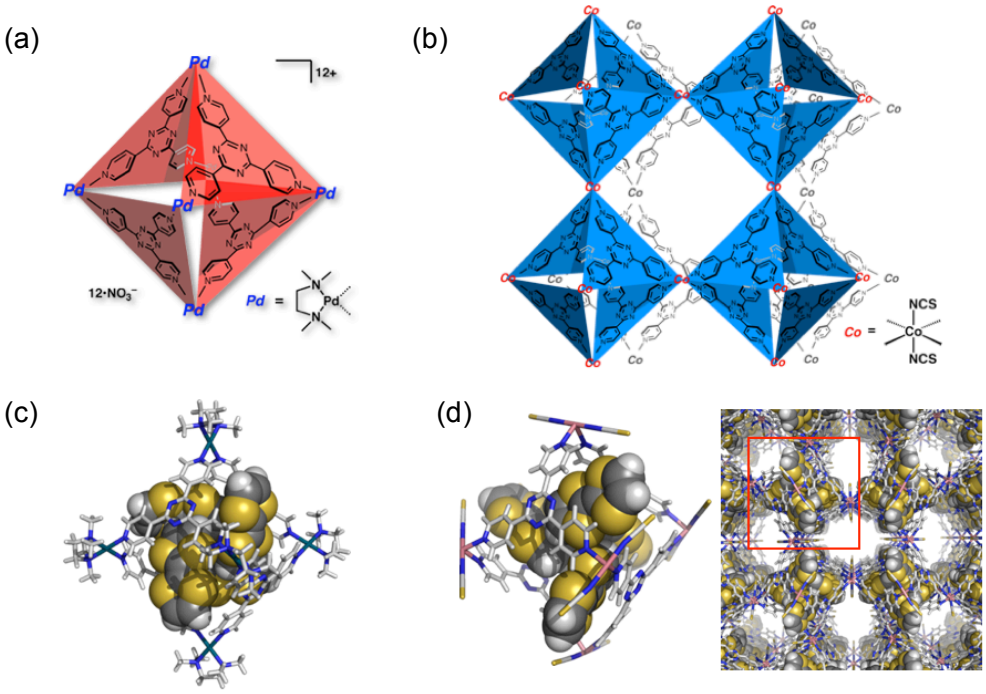

Figure 1.11. (a) Discrete Pd_6L_4 cage and (b) networked Co_6L_4 cages; X-ray structure of four TTF molecules encapsulated by (c) discrete and (d) networked cages (left, one M_6L_4 cage unit accommodating four TTF guests represented by red square; right, the networked structure)

So far, these examples have only employed rigid hosts (dynamic nature of solution hosts is not reproduced into crystals) and only common guest encapsulation was investigated. I have envisioned that rich and diverse solution chemistry can be introduced into solid-state by construction of a pair of ***dynamic*** discrete and networked host in solution and in crystals, and the common host-guest properties can be found in two physical states. The following section presents an overview of dynamic host-guest chemistry in solution and the solid-state.

1.4 *Dynamic Hosts in Solution*

First I would like to define the deformation of host structure that change the guest binding properties can be regard as '***dynamic behavior***' of hosts.

The Fujita group has established a dynamic receptor that undergoes a reversible conformation switch upon the guest exchange. Upon the addition of the unfavorable flat guest molecule, *p*-xylene, the highly symmetric Pd_3L_2 cage with a spherical cavity transfers to a low symmetry cage with a flat cavity. The re-conversion between two cages can be achieved by addition of a spherical guest molecule, $CBrCl_3$, into the low symmetry cage (Figure 1.12).[31]

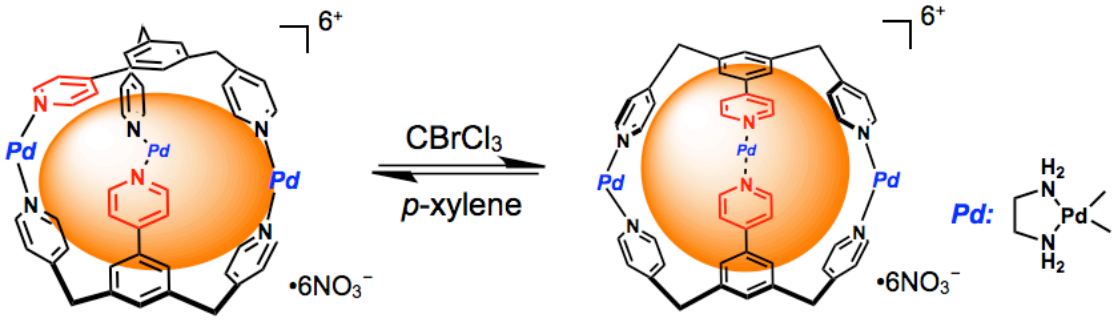

Figure 1.12. Conformational change upon guest binding (left, low symmetry cage; right, high symmetry cage).

Raymond et al. have investigated the mechanism of guest exchange with their M_6L_4 tetrahedral cages. Based on the guest exchange rate and molecular modeling studies, they emphasized that despite the hemi-labile metal-catecholate interaction, the cage remains intact and the apertures of the cage expand to allow guest ingress and egress during the guest exchange process (Scheme 1.2).[32]

Scheme 1.2. Schematic of non-associative guest exchange mechanism (The yellow and gray balls represent different guests).

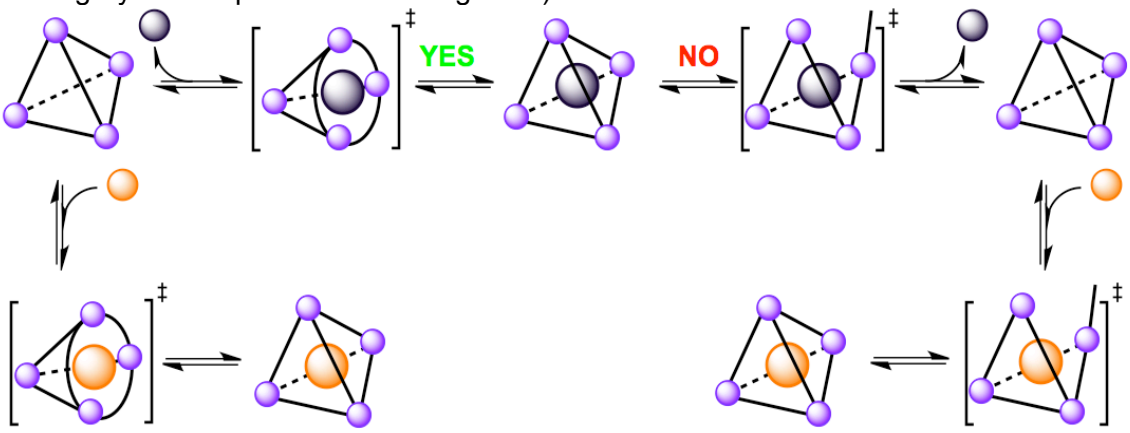

1.5 *Dynamic Host in the Solid-State*

One of the most interesting phenomena in MOFs or PCPs is the dynamic structure transformations of flexible porous frameworks, a process which often involves the uptake, removal, or exchange of guest molecules.[33] The Fujita group has prepared a 3D-coodination network by self-assembly of **4-TPT** and ZnI_2 that showed reversible conversion of two frameworks in a single-crystal-to-single-crystal (SCSC) fashion (Figure 1.13). When the nitrobenzene guest molecules were removed from the crystals, the new structure was produced by compression of networks, and it reverts back to the original one after the reabsorption of nitrobenzene guests.[34]

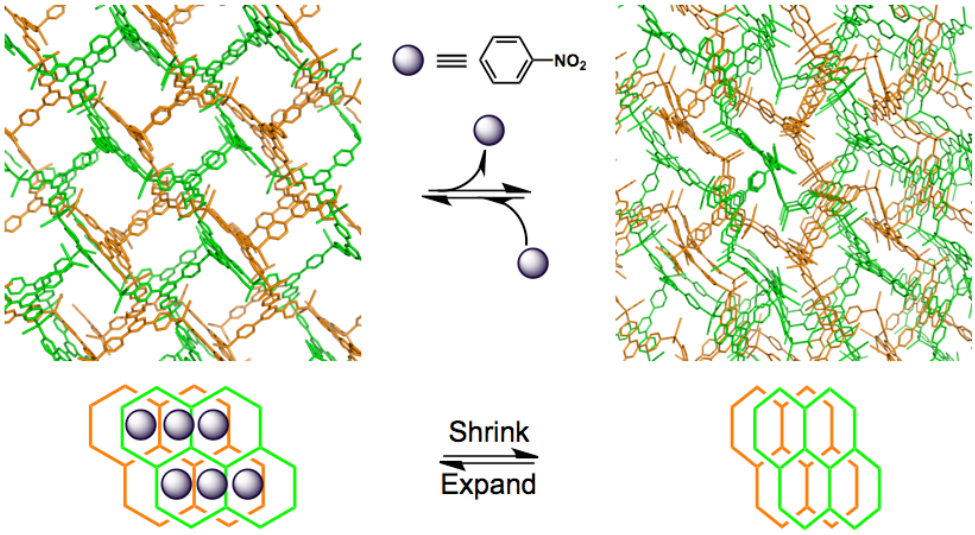

Figure 1.13. Schematic of guest exchange mechanism (The yellow and gray balls represent different guests).

The Kitagawa group has emphasized that the framework flexibility of MOFs or PCPs will play a key role in the development of next generation of PCPs.[21c, 33a] One of their recent work has demonstrated that a isocynaurate-functionalized PCP prepared from a highly flexible tripodal ligand and cerium or gadolinium metal ions exhibited sponge-like dynamic behavior upon the uptake or removal of water guest molecules (Figure 1.14).[35]

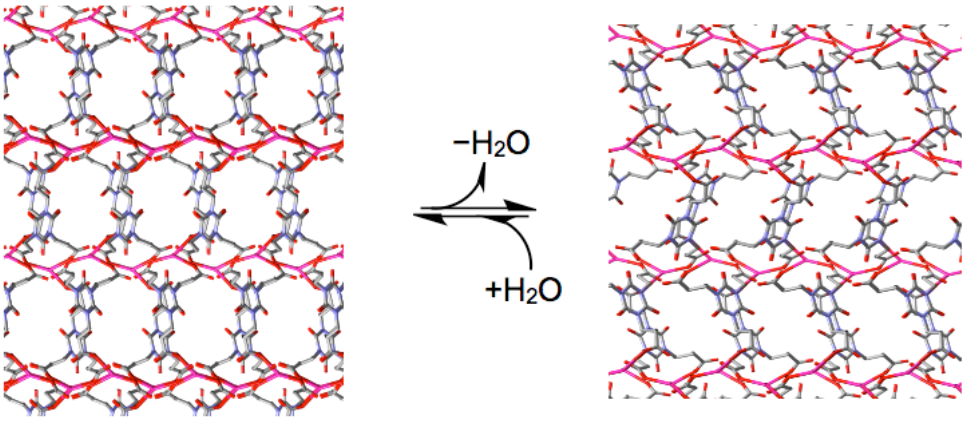

Figure 1.14. Structure change introduced by uptake or removal of water molecules.

Although the dynamic behavior of porous frameworks is quite common in MOFs or PCPs, the dynamic behavior of host structure incorporated into MOFs or PCPs is rarely investigated.

1.6 *Overview of this Thesis*

In principle, when the solution hosts, such as cages or capsules, were crystallized as crystals, the solution chemistry can be expected to transfer into the solid-state identically. However, the fact is the crystalline hosts often lose their ability to reproduce their solution chemistry, because the strong and tight packing effect in the solid-state not only suppress their dynamic behavior (such as partially dissociation-reassociation of hosts), but also block the host porters, preventing the ingress and egress of guests. From the overview above, the Fujita group developed a 'networking strategy' and constructed equivalent host cavity in solution and in crystals. The cage cavities in the networked cages are well-separated in crystal lattices and the guests can easily access to the host cavities.[30] However, there are still some problems need to be solved: 1) only rigid host frameworks are employed therefore the dynamic (flexible) motion of solution hosts is not introduced into solid-state; 2) only common guest encapsulation is achieved and no further common host-guest properties are found in two states. In the thesis, I will explore the 'networking strategy' in the context of flexible or dynamic hosts and find the common host-guest properties in solution and in crystals. In addition, as application of 'cream skimming' of host-guest chemistry, the

networked capsules are employed to develop a 'crystalline reagent' for easy and safe handling of volatile reagent (i.e. CH_3NCS).

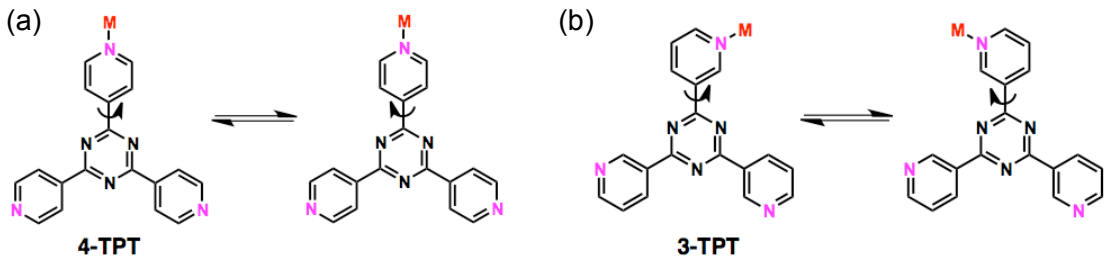

Figure 1.15. Conformational (a) rigidity of **4-TPT** and (b) flexibility of **3-TPT**.

The dynamic behavior of metallo-organic hosts is largely dependent on the flexibility of the organic ligand. Whereas **4-TPT** is a rigid ligand, the 2,4,6-tris(4-pyridyl)-1,3,5-triazine (**3-TPT**) is conformationally flexible (Figure 1.15).

In addition, molecular modeling studies suggested that complexation of **3-TPT** and a metal ion with near 90° coordination angle afforded a M_6L_4 capsule structure that showed remarkable dynamic behavior due to the rotation of **3-TPT** (Scheme 1.3).

Scheme 1.3. Dynamic behavior of M_6L_4 capsule.

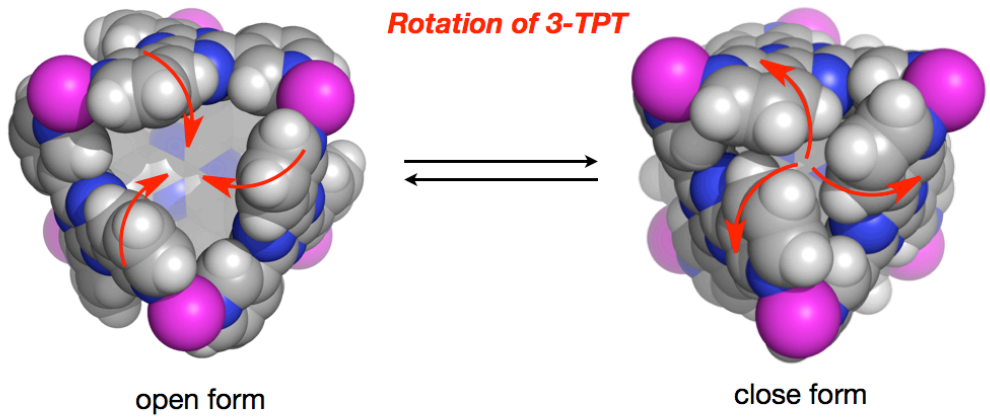

There are four main chapters apart from the introduction and summary.

Chapter 2 targets the construction of dynamic capsule cavity in solution. The complexation of **3-TPT** and a ruthenium metal complex affords a Ru_6L_4 molecular capsule in solution that is able to expand and shrink its windows upon the guest encapsulation.

Chapter 3. targets the networked capsules in crystals. The self-assembly of **3-TPT** and $Co(NCS)_2$ produces networked Co_6L_4 capsules that are composed of infinite Co_6L_4 capsule unit and interstitial pore. The dynamic behavior of networked capsules confirmed by a single-crystal-to-single-crystal guest exchange experiment.

Chapter 4 compares the structural features of solution and crystalline capsules based on X-ray crystallographic analysis. The detailed structural analysis reveals that Ru_6L_4 molecular capsule is isostructral with the capsule unit in the networked capsules. Due to the common dynamic capsule cavities, same guest molecule, THF, are accommodated with in cavity of capsules either in solution or in crystals. These results demonstrated that the qualitatively same host-guest chemistry is achieved via common dynamic capsule host, although the inclusion number is diffident (one for solution capsule and four for crystalline capsules). In addition, common host-guest properties are found in solution and in crystals, such as 1) guest screening 2) suppression of volatility; 3) suppression of D-A dimerization; 4) suppression of polymerization and 5) control of guest delivery.

Through the solution studies, I have found interesting host-guest properties for the networked capsules. Given these advantages of networked capsules, including stabilization of reactive guests and dynamic control of guest delivery, Chapter 5 develops a 'crystalline reagent' by pre-installation of troublesome reagents (i.e. CH_3NCS) into the networked capsules, and the encapsulated reagents can be stable stored and easily handled during the synthesis.

In Chapter 6, summary and perspectives are given.

Chapter 2

Construction of Dynamic Capsule Cavity in Solution

In this chapter I have synthesized a discrete Ru_6L_4 molecular capsule **1** in solution from the self-assembly of **3-TPT** and *cis*-[$Ru^{III}Cl_2$(cyclen)]Cl (where cyclen = 1,4,7,10-tetraazacyclododecane). During the complexation, redox reaction of *cis*-[$Ru^{III}Cl_2$(cyclen)]Cl took place. Although the experimental investigation of dynamic guest binding mechanism was difficult due to the extremely complicate and broad proton signal of capsule **1**, molecular modeling studies were conducted to probe the flexibility of **1**. Finally, the capsule **1** was able to bind various guests, and the cavity calculation revealed the dynamic cavity change of **1** upon guest encapsulation.

2.1 *Introduction*

Rotation of **3-TPT** reduces its C3 symmetry and generates isomerism during complexation of **3-TPT** with metal ion (Figure 1.13). Therefore, the synthesis and characterization of discrete and well-defined supramolecular structure using **3-TPT** is unexpected difficult and few examples have been reported so far.[36~39] The Fujita group, for example, has prepared a Pd_6L_4 bowl structure by complexation of **3-TPT** with $[Pd(en)]^{2+}(NO_3)_2$ (where en = ethylenediamine) (Figure 2.1).[40,41] By inspiration from the Pd_6L_4 bowl structure, I assumed that increase of steric hindrance around metal ion in the bowl would prevent the formation of bowl and afford capsule structure.

In this chapter, a bulky metal complex, *cis*-$[Ru^{III}Cl_2(cyclen)]Cl$ (cyclen = 1,4,7,10-tetraazacyclododecane) is used to construct a Ru_6L_4 molecular capsule. In addition, the dynamic nature of the Ru_6L_4 capsule in solution is discussed in details.

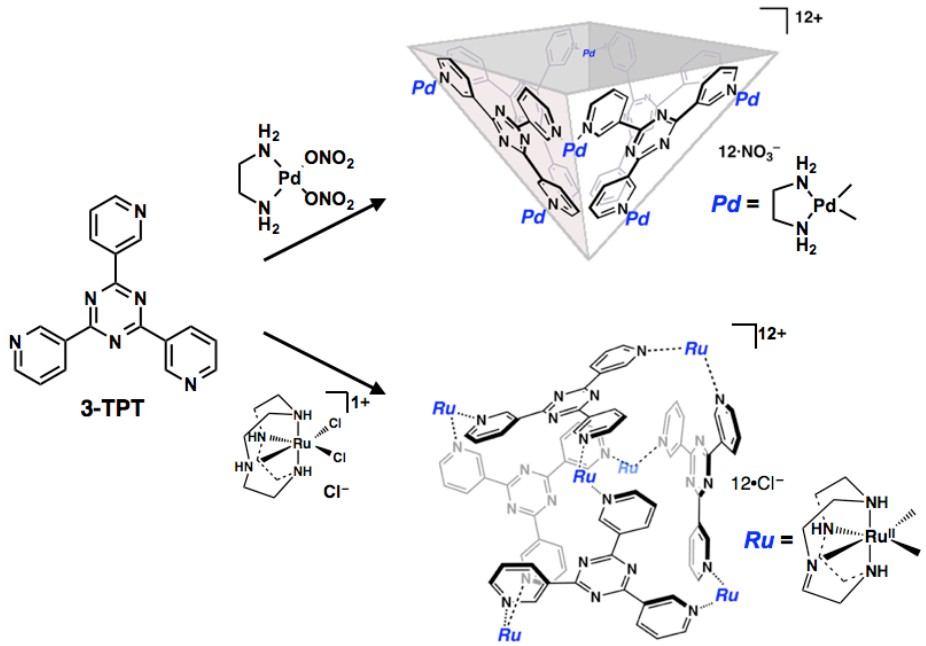

Figure 2.1. Synthesis of Pd_6L_4 bowl (top) and Ru_6L_4 capsule (bottom).

2.2 *Synthesis and Characterization*

Ru_6L_4 capsule **1** was synthesized from the self-assembly of **3-TPT** and *cis*-[$Ru^{III}Cl_2$(cyclen)]Cl (**3**) in H_2O at 100 °C for 30 h under neutral conditions. Although ^{1}H NMR of capsule **1** was complicate and broad, diffusion-ordered NMR spectroscopy (DOSY) unambiguously showed a single band with an identical diffusion coefficient $D = 1.51 \times 10^{-10}$ m^2s^{-1} (log D = -9.82) (Figure 2.2), indicating the formation of one species in high yield (> 90 %, a Ru_3L_2 clam-like structure was obtained as by-product under this reaction condition, the detailed characterization see the experimental section). Cold-spray ionization mass spectrometry (CSI-MS) analysis of **1** showed intense signals for [**1** – $(Cl^-)_m]^{m+}$ (m = 8 ~ 2), *e.g.* m/z = 436.6, 515.1, 625.1, 790.1 and 1065.2, which well-matched with the simulation for Ru(II)-hinged M_6L_4 capsule [**1**– $(Cl^-)_7]^{7+}$, [**1** – $(Cl^-)_6]^{6+}$, [**1** – $(Cl^-)_5]^{5+}$, [**1** – $(Cl^-)_4]^{4+}$ and [**1** – $(Cl^-)_3]^{3+}$.

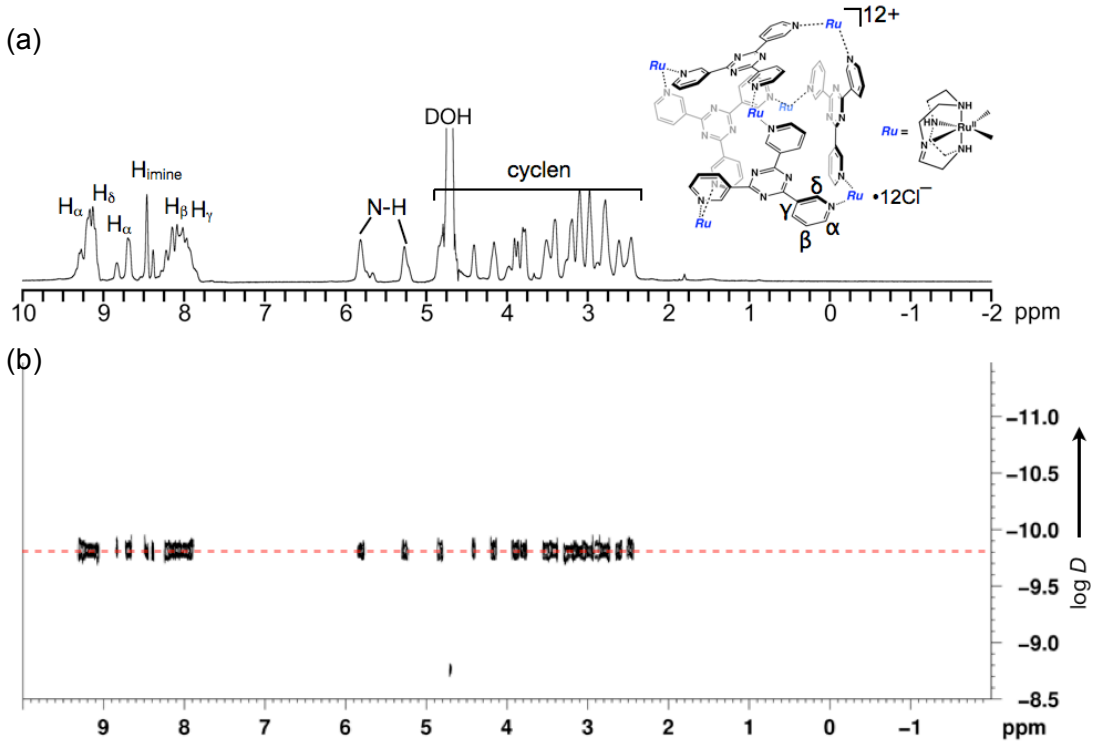

Figure 2.2. (a) ^{1}H NMR (500 MHz, D_2O, 300 K) of discrete Ru_6L_4 capsule **1**; (b) DOSY spectroscopy (500 MHz, D_2O, 300 K) of **1**.

The CSI-MS data suggested that the metal centers were reduced (Ru(III) to Ru(II)) while the cyclen ligand was dehydrogenated as previously reported for other Ru(III)-cyclen complexes.[42] In addition, heteronuclear multiple quantum coherence

(HMQC) and correlation spectroscopy (COSY) analyses revealed that the N=CH moiety was present in **1** at 8.38–8.46 ppm (Figure S2.6). Due to the existence of many diastereomers arising form the oxidized cyclen ligands, the intricately split signals in ^{1}H NMR were reasonable.

The structure of the Ru_6L_4 capsule **1** was confirmed by X-ray crystallographic analysis as a tetrahydrofuran (**4**)–inclusion complex **1⊃4** (where ⊃ denotes encapsulation) after diffusion of **4** into an aqueous solution of as-synthesized **1**. The complex **1** showed a M_6L_4 capsule topology that featured six imcyclen-capped Ru^{II} centers situated at vertices of a slightly twisted octahedron with edge lengths ranging from 11.126 to 11.421 Å (avg. 11.269 Å) (Figure 2.3). In addition, the Ru-N_{py} distances were ranged from 2.088 – 2.107 Å, which were lying the range of 2.053 – 2.125 Å reported of Ru^{II}–N_{py} bond distances,[43] and the N–Ru–N angles were ranged from 85.60 to 86.53° (avg. 86.07°) were considerable smaller than idea 90°. Moreover, the short C_{cyclen}–N_{cyclen} distances were ranged from 1.289 to 1.375 Å (avg. 1.348 Å) that were attributable to the C=N bond, indicating the cyclen was oxidized to imcyclen.

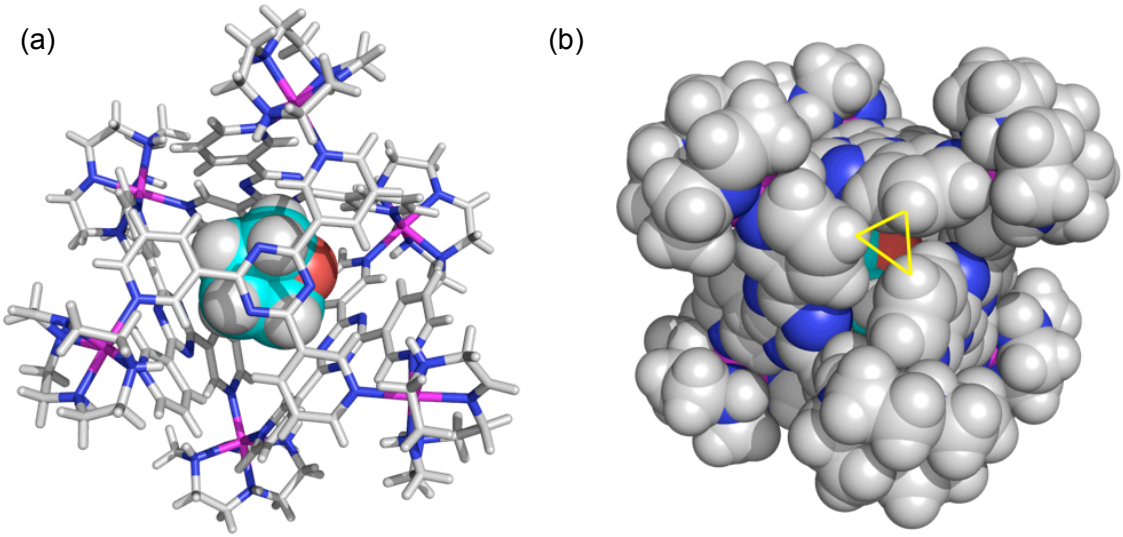

Figure 2.3. X-ray structure of capsule **1⊃4** (a) capsule framework is shown in stick model while the THF guest in CPK model; (b) CPK model revealing the aperture of **1** is narrower than the size of the THF guest (yellow triangle with 3.22 × 3.16 × 3.42 Å^3 size represent the aperture of **1** constructed by the three hydrogen atoms).

2.3 *Dynamic Guest Encapsulation*

Examination of the crystal structure of **1⊃4** (Figure 2.3b) leads to the conclusion that the encapsulated THF guest is completely isolated from the external environment (water) by aromatic backbones of the capsule **1** and large openings do not exist in the host shell. In addition, guest encapsulation occurs without major disruption to the host structure and no intermediate structures are detected in ^{1}H NMR.

Based on the spectroscopic and structural evidences, one most reasonable guest encapsulation mechanism is considered: Guest encapsulation occurs without any ligand dissociation, therefore the host needs to expand its aperture to accommodate guest, and then squeeze its aperture to make tight packing of guest. However, considering the liability of Ru-N_{cyclen} and Ru-N_{py} bond, there are two possible dissociation mechanism: (1) the dissociation of the Ru-N_{cyclen} bond can reduce the steric repulsion between cyclen and **3-TPT** ligand during the rotation of **3-TPT** ligand and assist the expansion of host aperture; (2) the internal cavity of host is momentarily opened to the external environment due to the dissociation of the Ru-N_{py} bond.

In this thesis, only non-dissociation guest encapsulation mechanism is discussed in details. Is the host deformation required for the non-dissociative guest encapsulation realistic? Since the intermediate deformed structures were not been observed, molecular modeling was employed to evaluate the flexibility of the Ru_6L_4 host with respect to stretching of its apertures.

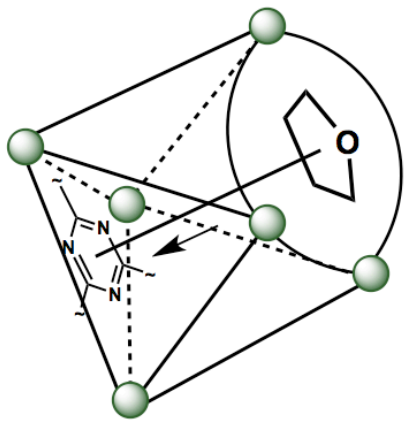

Figure 2.4. Schematic representation of intermediate structures corresponding to the passage of the THF guest through the Ru_6L_4 host aperture were generated by fixing the distance between the center of THF guest and the **3-TPT** ligand opposite to the active aperture.

An initial host-guest model was based on the crystal structure of **1⊃4**, and a series of structures in which the position of the guest was varied were minimized (Material Studio 4.4) to produce a track of guest passage through the host aperture. Specifically, the distance from the center of the THF guest to center of **3-TPT** opposite the active aperture (C_{THF} to C_{TPTopp}) was fixed in each structure (Figure 2.4)

Eleven of the calculated structures for THF guest are shown in Figure 2.5, with the distances of C_{THF} to C_{TPTopp} are ranged from 3.6 to 13.6 Å. Examination of the intermediate structures supports the conclusion that host dynamic deformation is a reasonable mechanism. To accommodate THF guest, host deforms by rotation of **3-TPT** ligand as mentioned in Chapter 1 (Scheme 1.3) and the enlargement of the active aperture can be measured by the distance between three hydrogen atoms as shown in Figure 2.3b. The molecular modeling studies revealed that active aperture could expand from 3.32 × 3.55 × 3.81 $Å^3$ at Figure 2.5k (THF guest just approached host) to 6.86 × 7.14 × 7.54 $Å^3$ for the largest enlargement (Figure 2.5h) and start shrinking to 3.22 × 3.16 × 3.42 $Å^3$ for X-ray structure at Figure 2.5a. The selected bond length and angle of these intermediate structures for comparison will be summarized in detail (Experimental Section Table S2.1)

The molecular modeling studies also indicated that the egress of THF guest would cause large strain on the host structure. Based on this, I expected that the THF guest would prefer stay in cavity even at hash condition. To my delight, the THF guest could not be released from capsule **1** when the crystals of **1⊃4** were re-dissolved into water, indicating the strong encapsulation effect that agreed with the observation in X-ray structure. To further test the strong encapsulation effect, the aqueous solution of **1⊃4** was heated at 80 °C, far above the boil point (b. p.) of guest molecules, the THF guest still remain enclathrated.

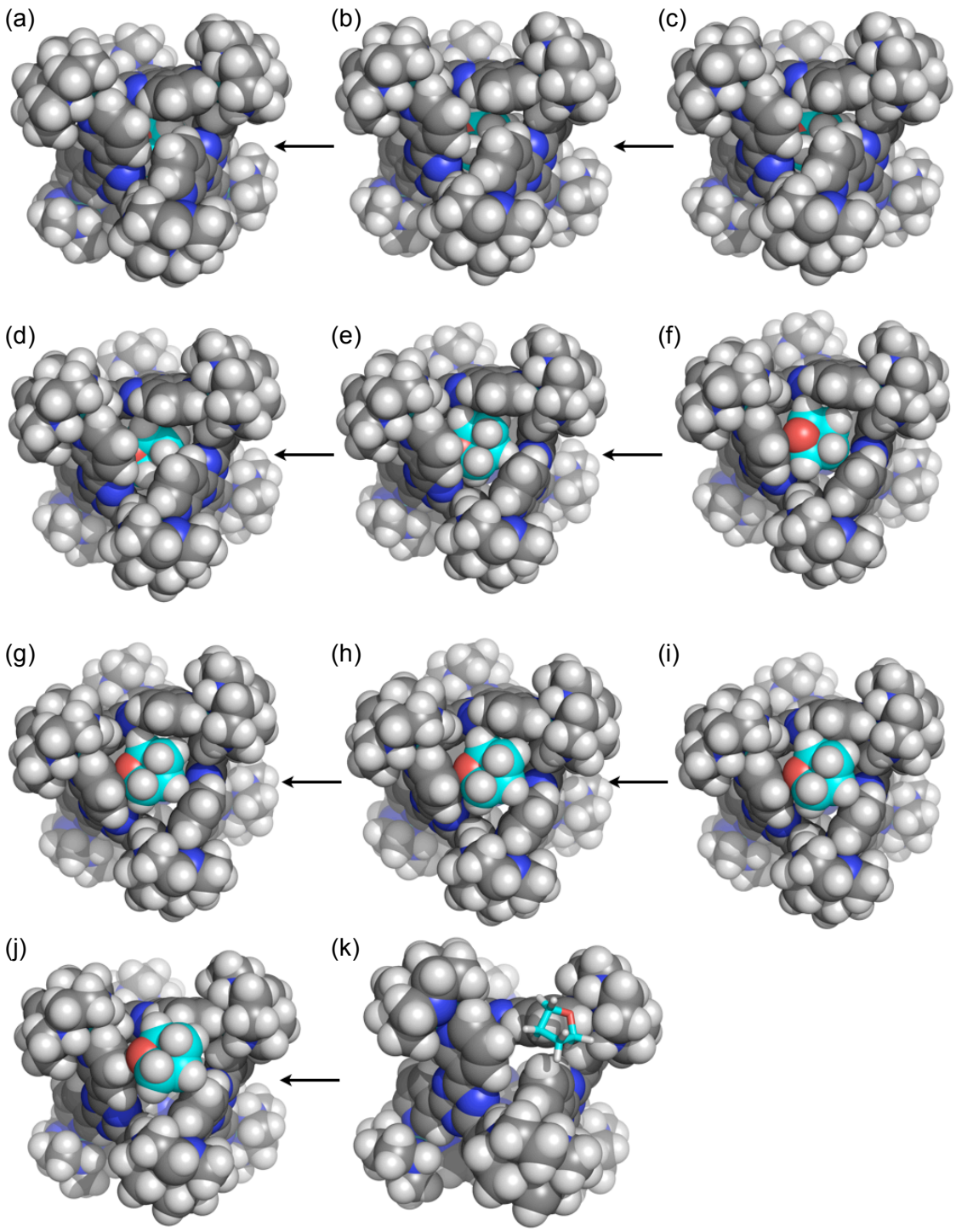

Figure 2.5. Calculated intermediate structures for the passage of THF guest through Ru_6L_4 host aperture. The models demonstrate the flexibility of the host, which appears able to expand its aperture. In each structure, the C_{THF} to C_{TPTopp} distance is fixed, and these distances increase by incensements of 1 Å from 3.6 Å at (a) to 13.6 Å at (k) (THF guest shown as stick model to clarify the active aperture in (k))

2.4 *Dynamic Cavity Change*

Another dynamic feature of capsule topology is dynamic cavity change upon guest encapsulation. To test this, various cyclic guests (i.e. THF, (**4**), cyclopentane (**5**) and cyclohexane (**6**)) with different molecule volume have introduced into the capsule **1**. The encapsulation of guests was confirmed by highly up-filed shifted guests' signal in ^{1}H NMR (Figure 2.6). For instance, the signals of encapsulated THF guest appeared at 0.77 and -1.49 ppm ($\Delta\delta$ = -2.96 and -3.33 ppm), respectively.

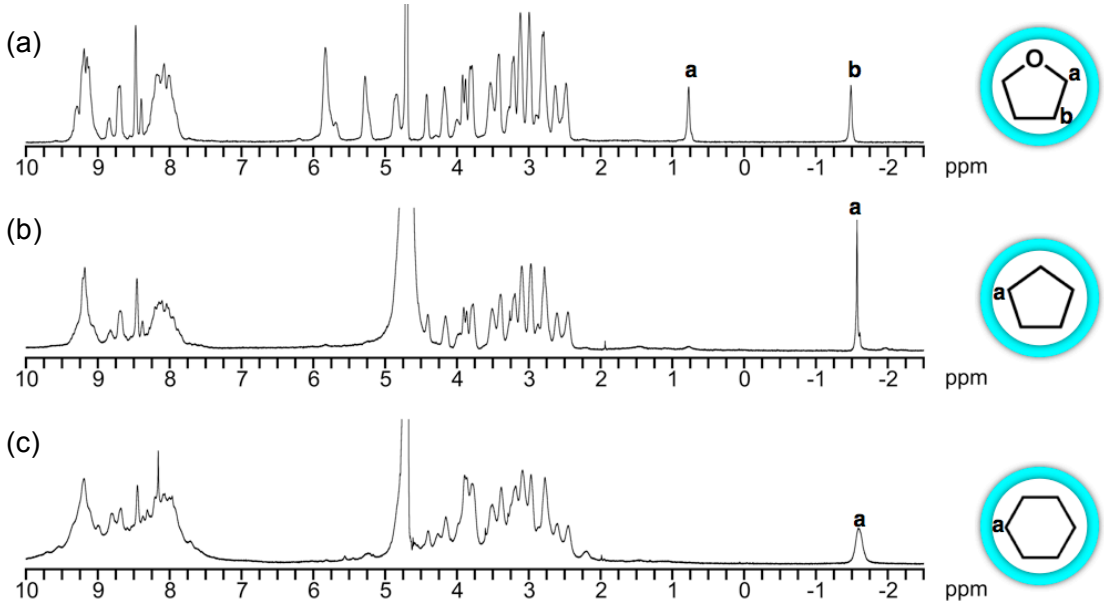

Figure 2.6. ^{1}H NMR (500 MHz, D_2O, 300K) of (a) **1⊃4**; (b) **1⊃5; (c) 1⊃6**.

The cavity volume of host **1** was calculated by VOIDOO program (detail introduction was discussed in experimental section),[44] based on the crystal structure of inclusion complex **1⊃4** and molecular modeling structure of **1⊃5** and **1⊃6**. The results clearly showed that the cavity volume of **1** are able to expand by ~ 75% from 141 Å^3 for **1⊃4** to 248 Å^3 for **1⊃6** (Table 2.1)

Table 2.1. Cavity volumes of Ru_6L_4 capsule with various guests

Guest	Guest volume (Å^3)^a	Host cavity (Å^3)^b
THF	86	141
Cyclopentane	95	206
Cyclohexane	112	248

^{a}van der Waals volumes calculated from structure optimized using SPARTAN'10 with MP2 using both a 6-311+G** basis set. ^{b}The cavity volumes calculated from VOIDOO program. (Probe radius = 1.4 Å)

2.5 *Conclusion*

In summary, a discrete Ru_6L_4 molecular capsule **1** was newly designed and synthesized. The X-ray crystallographic analysis confirmed that complex **1** adopted M_6L_4 capsule topology. The NMR and CSI-MS date revealed that the redox reaction of *cis*-[$Ru^{III}Cl_2$(cyclen)]Cl occurred during the complexation. Through the molecular modeling studies, a non-dissociative mechanism, which was agreement with the X-ray structure evidences, was proposed, revealing the capsule **1** exhibited flexible or dynamic guest encapsulation process via expansion and shrinking its aperture. Once the guest was encapsulation, the capsule **1** was able to shrink its aperture to completely isolate guest from external environment and mediate the physical properties of guest, such as suppression of volatility of THF guest. Finally, the cavity volume of the capsule **1** enlarged by ~ 75% upon the accommodation of guests with size increase, leading to induced-fit binding of guests.

2.6 *Experimental Section*

- **General procedures**

Solvent and reagents were purchased from TCI, WAKO Pure Chemical Industries, Furuya metal Co., Ltd. or Sigma-Aldrich. All chemicals were used without any further purification except where noted. ^{1}H, ^{13}C and 2D NMR spectra were recorded on Bruker DRX-500 (500 MHz) spectrometers. All the NMR spectra were collected at 300 K, and chemical shifts were reported as the delta scale in parts per million (ppm). IR measurements were carried out as KBr pellets using a DIGILAB FTS7000 instrument. Elemental analysis was performed on a YANACO MT-6. Single crystal X-ray diffraction data were made using a BRUKER APEX-Ⅱ/CCD diffractometer equipped with a focusing mirror (MoK_{α} radiation $\lambda = 0.71073$ Å) and a N_2 generator (Japan Thermal Eng. Co., Ltd.).

- **Preparation of Ru_6L_4 molecular capsule 1**

To a 10 mL test tube were added 2,4,6-tri(3-pyridyl)-1,3,5,-triazine (**3-TPT**) (36.0 mg, 0.115 mmol), *cis*-[Ru(cyclen)Cl_2]Cl (**3**) (66.0 mg, 0.174 mmol), distilled water (4 mL) and 160 μL of NaOH aq. (1.09 M). The mixture was heated at 100 °C for 30 h and the resulting red solution was concentrated to half of the volume by rotary evaporator. After vapour diffusion of THF into the resultant solution within one day, a by-product (Ru_3L_2 complex) precipitated as golden yellow powder (6.9 mg, 7%) was removed by filtration. Further addition of THF into the filtrate gave crude product **1⊃4** as black precipitate (67.0 mg, 70%). Further recrystallization from water/THF furnished black single crystals of **1⊃4** (28.0 mg, 29%).

Characterization data for THF complex **1⊃4**

^{1}H NMR (500 MHz, D_2O): δ 9.30-9.16 (br, 18H, Py_α and Py_δ), 8.85-8.71 (br, 6H, Py_α), 8.48-8.41 (br, 6H, imine), 8.19-7.91 (br, 24H, Py_γ and Py_β), 5.84-5.70 (br, 12H, NH), 5.29 (br, 6H, NH), 4.84 (br, 6H, -CH_2-), 4.43 (br, 4H, -CH_2-), 4.18 (br, 6H, -CH_2-), 3.93-3.80 (br, 14H, -CH_2-), 3.54-3.43 (br, 12H, -CH_2-), 3.22 (br, 6H, -CH_2-), 3.12 (br, 6H, -CH_2-), 3.00 (br, 6H, -CH_2-), 2.80 (br, 12H, -CH_2-), 2.64 (br, 6H, -CH_2-), 2.49 (br, 6H, -CH_2-) 0.77 (br, 4H, encapsulated THF), –1.49 (br, 4H, encapsulated THF). ^{13}C NMR (125 MHz, D_2O): δ 171.1 (imine), 169.1, 159.7, 159.5, 156.4, 155.8, 135.4, 134.9, 134.8, 132.1, 125.2, 65.19 (encapsulated THF) 62.9, 60.2, 57.2, 56.8, 56.6, 53.8, 47.8, 22.4 (encapsulated THF). IR (KBr) 3474 (s), 3114 (m), 2894 (m), 2353 (s), 1619 (m), 1525 (s), 1359 (m), 1123 (m) cm^{-1}; Elemental analysis (%): calculated for $C_{120}H_{156}N_{48}Ru_6Cl_{12}(C_4H_8O)(H_2O)_{37}$: C 36.85, H 5.94, N 16.64; found: C 36.56, H 5.91, N 17.03.

Guest removal from THF complex **1⊃4**

An aqueous solution of **1⊃4** (*ca*. 10 mM, 1 mL) was washed with $CHCl_3$ (1 mL × 2 times) to give host **1** quantitatively (confirmed by NMR). By freeze-drying, compound **1** was obtained as red powders.

Characterization data for **1**

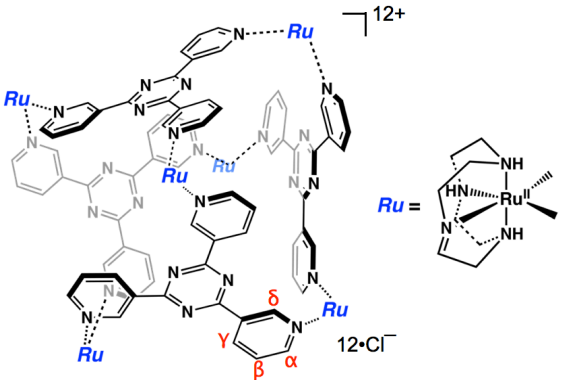

^{1}H NMR (500 MHz, D_2O): δ 9.27-9.13 (br, 18H, Py_α and Py_δ), 8.83-8.70 (br, 6H, Py_α), 8.46-8.38 (br, 6H, imine), 8.22-7.84 (br, 24H, Py_γ and Py_β), 5.81-5.66 (br, 12H, NH), 5.27 (br, 6H, NH), 4.84 (br, 6H, $-CH_2-$), 4.41 (br, 4H, $-CH_2-$), 4.16 (br, 6H, $-CH_2-$), 3.99-3.80 (br, 14H, $-CH_2-$), 3.51-3.40 (br, 12H, $-CH_2-$), 3.20 (br, 6H, $-CH_2-$), 3.10 (br, 6H, $-CH_2-$), 2.98 (br, 6H, $-CH_2-$), 2.78 (br, 12H, $-CH_2-$), 2.61 (br, 6H, $-CH_2-$), 2.46 (br, 6H, $-CH_2-$); ^{13}C NMR (125 MHz, D_2O): δ 171.1 (imine), 169.1, 159.7, 159.4, 156.5, 156.0, 135.4, 134.8, 134.7, 132.1, 125.5, 125.3, 125.2, 125.1, 62.8, 60.2, 57.1, 56.8, 53.7, 53.6, 47.8, 47.7. CSI-MS (MeOH): *m/z* calcd for $[\mathbf{1}-(Cl^-)_8]^{8+}$ 377.6, found: 377.3; calcd for $[\mathbf{1}-(Cl^-)_7]^{7+}$ 436.5, found: 436.6; calcd for $[\mathbf{1}-(Cl^-)_6]^{6+}$ 515.1, found: 515.2; calcd for $[\mathbf{1}-(Cl^-)_5]^{5+}$ 625.1, found: 625.8; calcd for $[\mathbf{1}-(Cl^-)_4]^{4+}$ 790.1, found: 790.1; calcd for $[\mathbf{1}-(Cl^-)_3]^{3+}$ 1065.2, found: 1065.8; calcd for $[\mathbf{1}-(Cl^-)_2+(MeOH)]^{2+}$ 1631.3, found: 1631.7. IR (KBr) 3437 (s), 3128 (m), 2353 (s), 1525 (s), 1357 (m), 1133 (m) cm^{-1}; Elemental analysis (%): calculated for $C_{120}H_{156}N_{48}Ru_6Cl_{12}(H_2O)_{39}$: C 35.98, H 5.89, N 16.79; found: C 35.86, H 5.95, N 16.67.

Characterization data for Ru_3L_2 complex

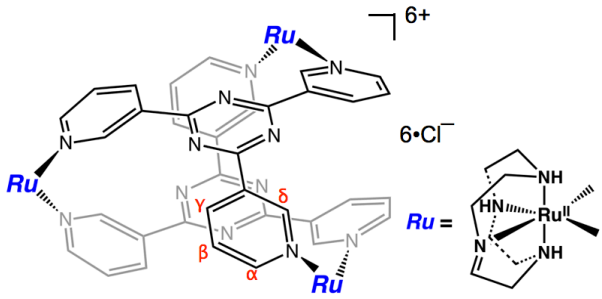

^{1}H NMR (500 MHz, D_2O): δ 9.11-8.82 (m, 9H, Py_α and Py_δ), 8.62-8.60 (br, 3H, imine), 8.53-8.49 (m, 3H, Py_α), 8.40-8.26 (m, 6H, Py_γ), 7.83-7.54 (m, 6H, Py_β), 5.95-5.87 (br, 6H, NH), 5.22 (br, 3H, NH), 4.82 (br, 3H, $-CH_2-$), 4.30 (br, 3H, $-CH_2-$), 3.98 (br, 6H, $-CH_2-$), 3.62 (br, 3H, $-CH_2-$), 3.50 (br, 3H, $-CH_2-$), 3.27 (br, 6H, $-CH_2-$), 3.09 (br, 6H, $-CH_2-$), 2.88 (br, 9H, $-CH_2-$), 2.62 (br, 3H, $-CH_2-$); ^{13}C NMR (125 MHz, D_2O): δ 171.3 (imine), 169.2, 158.9, 157.4, 137.1, 136.4, 131.6, 125.3, 124.7, 62.8, 60.5, 57.6, 56.5, 54.0, 53.9, 48.1. CSI-MS *m/z* calcd for $[\mathbf{M}-(Cl^-)_5]^{5+}$ 295.1, found: 295.6; calcd for $[\mathbf{M}-(Cl^-)_4]^{4+}$ 377.6, found: 377.1; calcd for $[\mathbf{M}-(Cl^-)_3]^{3+}$ 515.1, found 515.5; calcd for $[\mathbf{M}-(Cl^-)_2]^{2+}$ 790.1, found: 790.7.

- **CSI-MS and NMR spectrum of Ru_6L_4 molecular capsule**

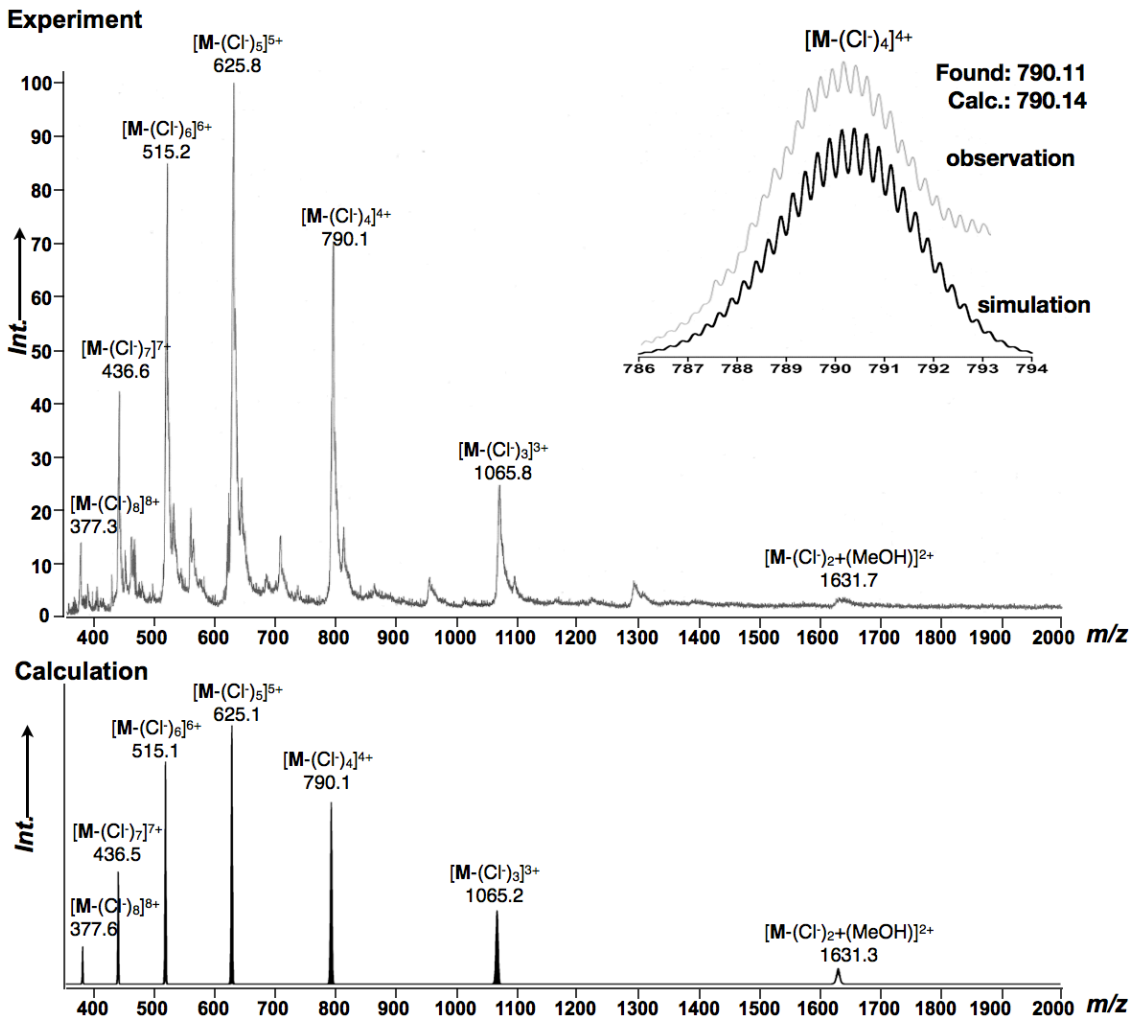

Figure S2.1. CSI-MS spectrum (top: observation, bottom: simulation) of a Ru_6L_4 capsule **1**. (Form SI of *Chem. Asian J.* **2013**, *8*, 2596. Reprinted with permission of Wiley-VCH)

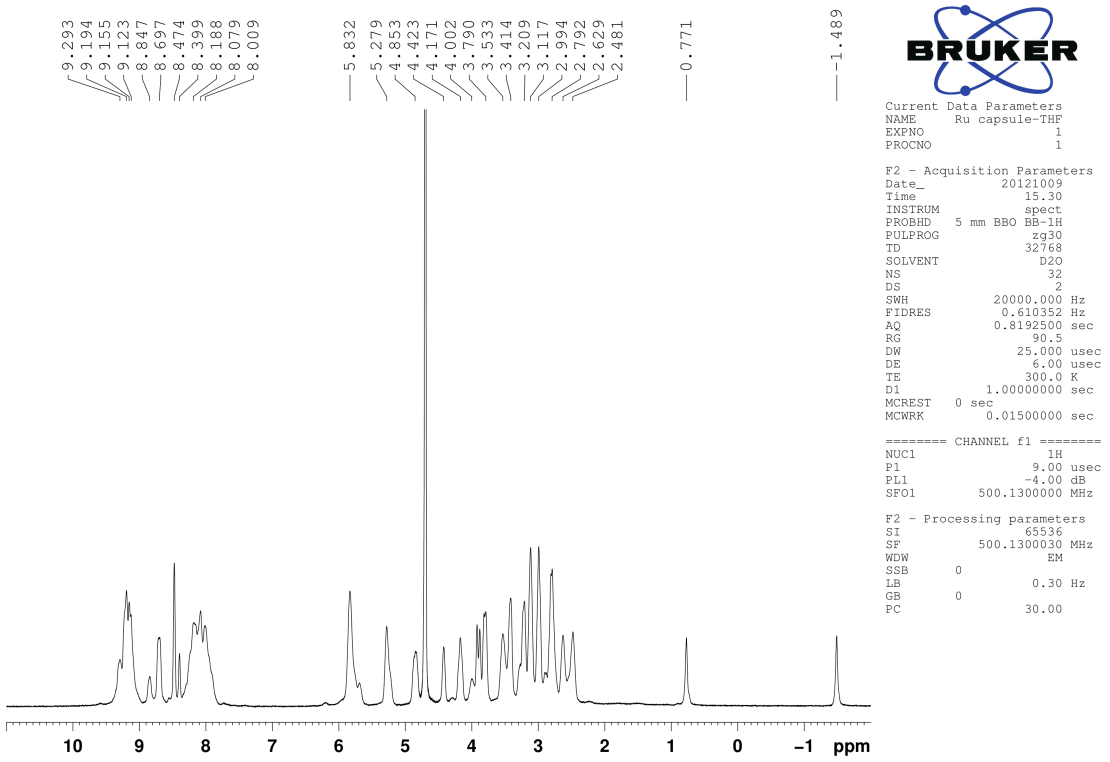

Figure S2.2. ^{1}H NMR spectrum (500 MHz, D_2O, 300 K) of inclusion complex **1⊃4**.

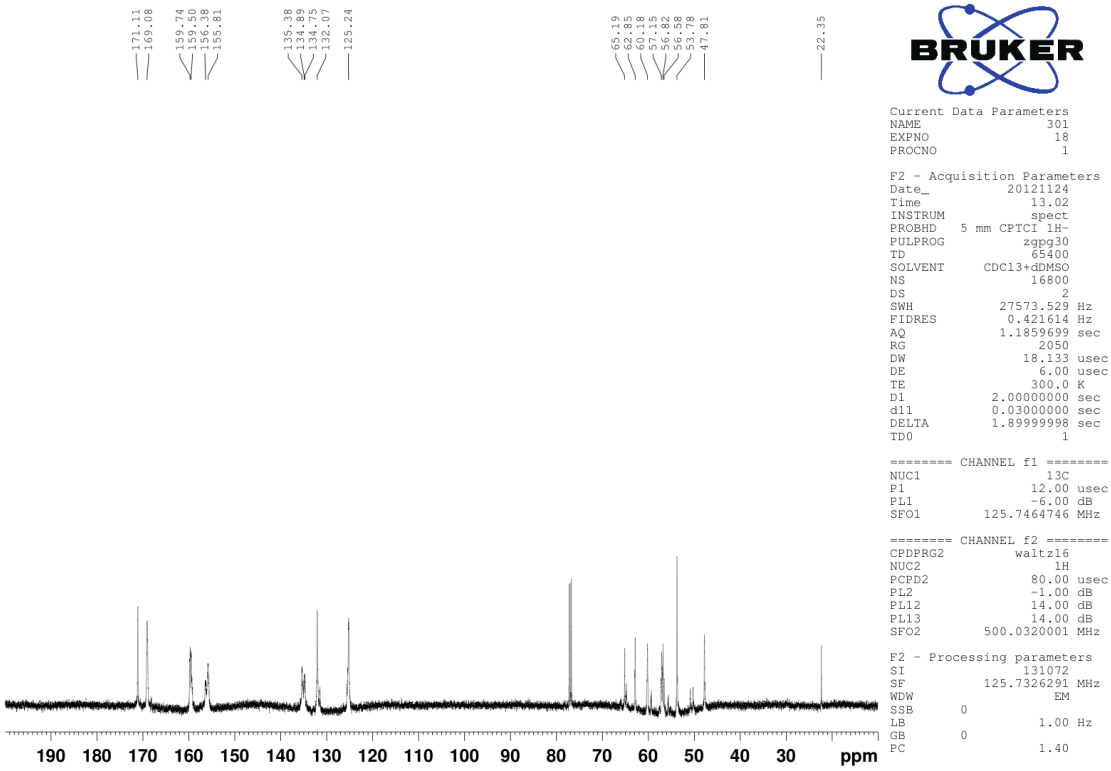

Figure S2.3. ^{13}C NMR spectrum (125 MHz, D_2O, 300 K) of inclusion complex **1⊃4**.

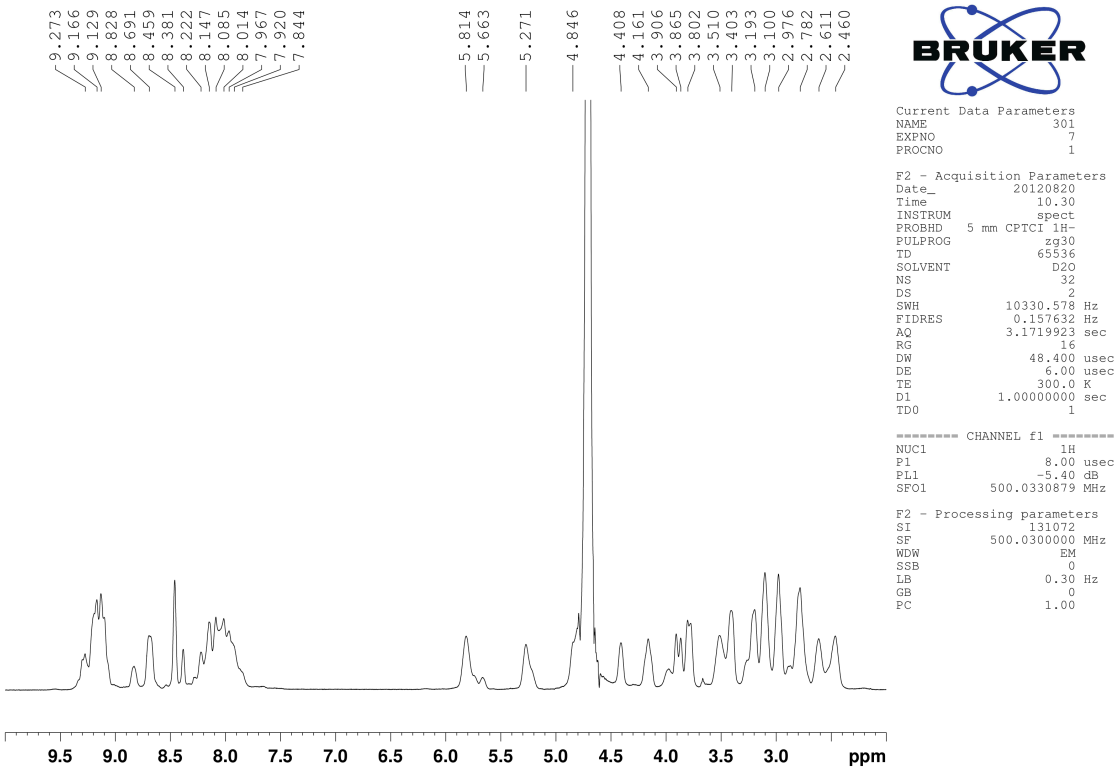

Figure S2.4. ^{1}H NMR spectrum (500 MHz, D_2O, 300 K) of Ru_6L_4 capsule **1**.

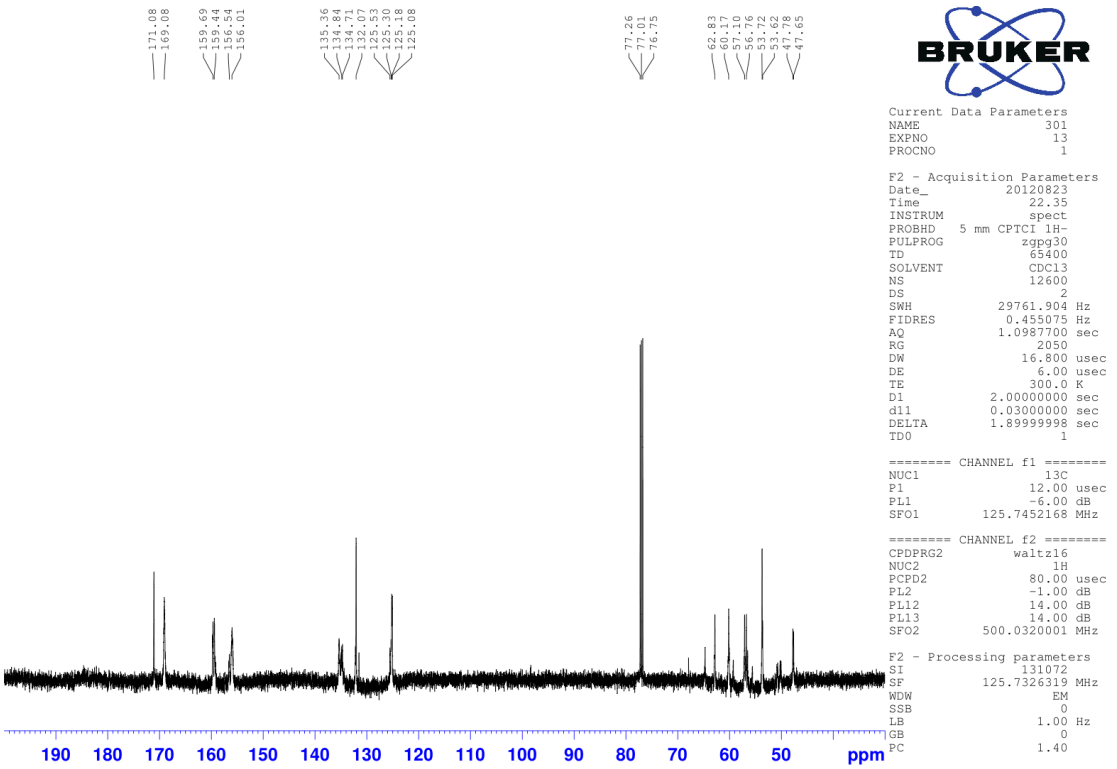

Figure S2.5. ^{13}C NMR spectrum (125 MHz, D_2O, 300 K) of Ru_6L_4 capsule **1**.

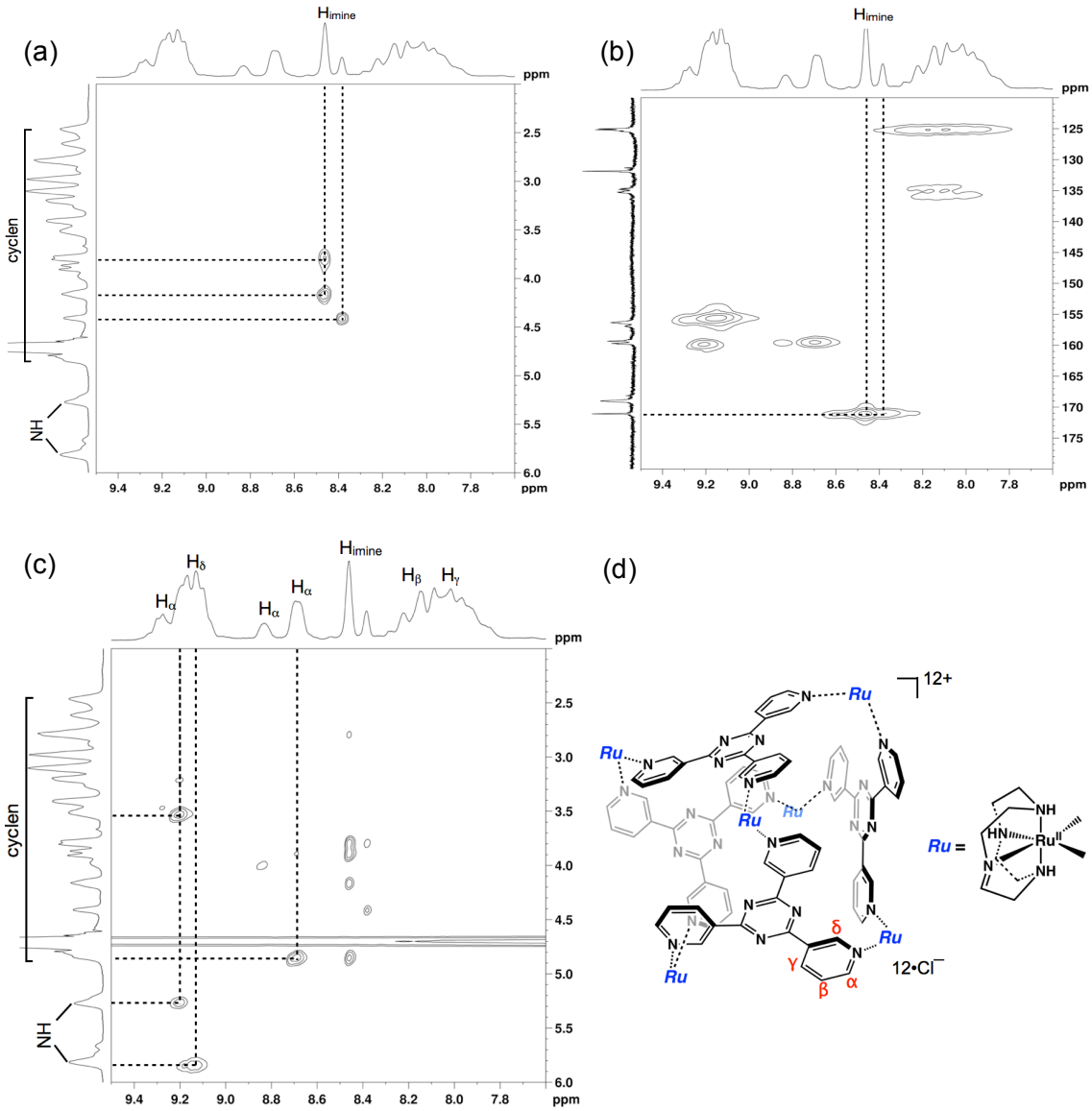

Figure S2.6. 2D NMR spectra (D_2O, 300K) of as-synthesized Ru_6L_4 capsule **1**. a) COSY and b) HMQC NMR spectra (only the correlation at N=C−H region was shown); c) NOESY NMR spectra (only the correlation between cyclen ligand and triazine ligand **3** was shown); d) the molecular structure of **1** showing numbering of triazine ligand.

- **CSI-MS and NMR spectrum of Ru_3L_2 clam-like complex**

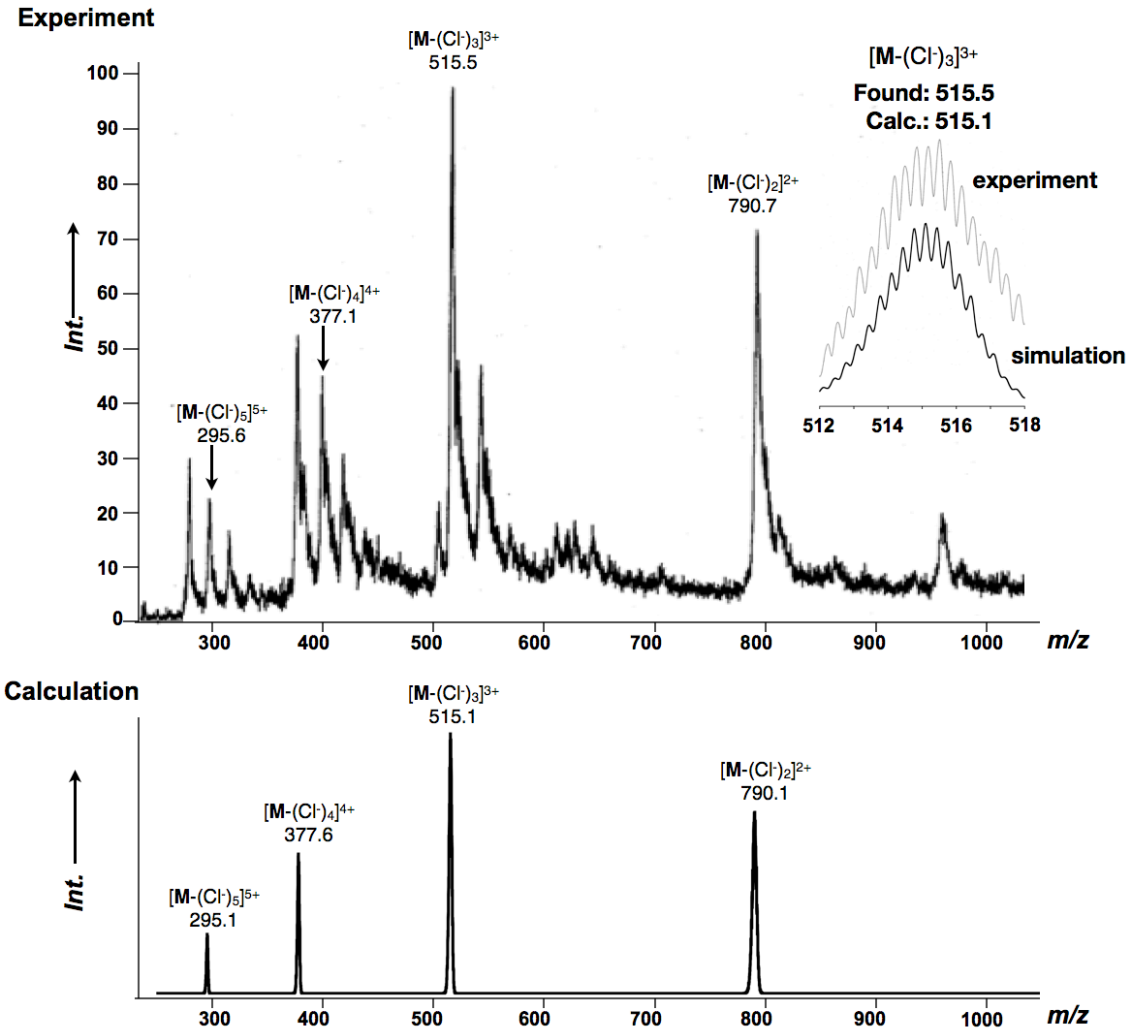

Figure S2.7. CSI-MS spectrum (top: observation, bottom: simulation) of a Ru_2L_3 clam-like structure.

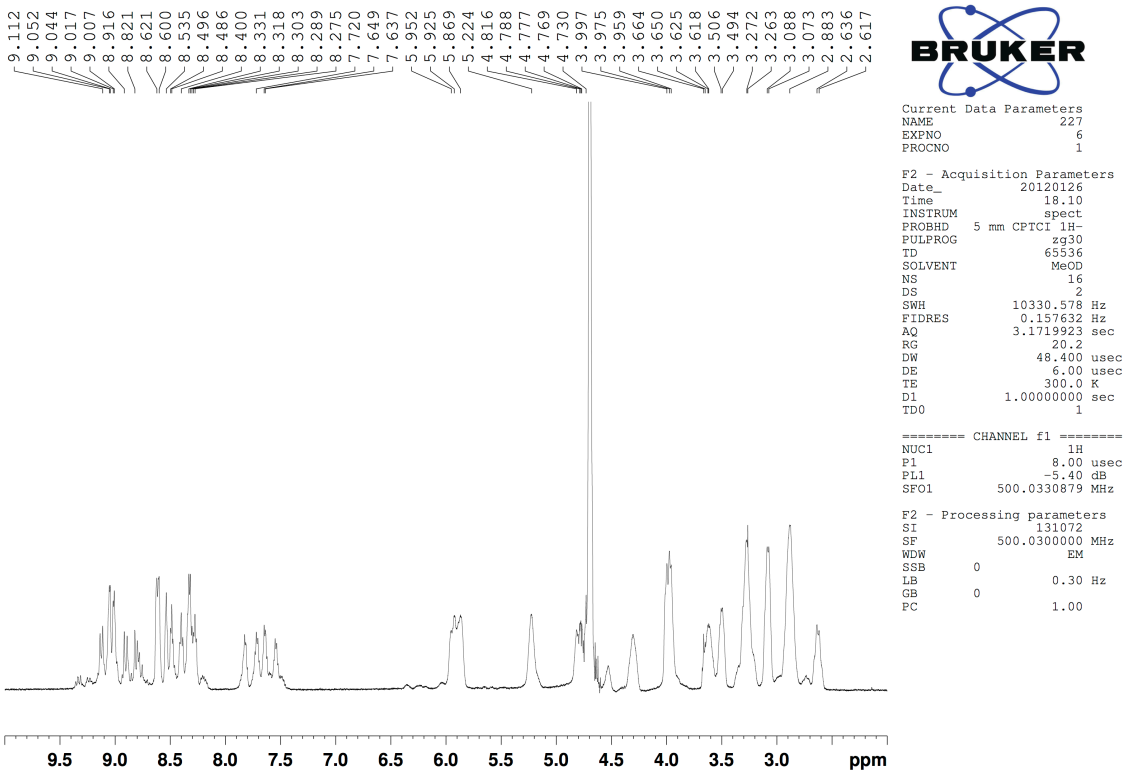

Figure S2.8. ^{1}H NMR spectrum (500 MHz, D_2O, 300 K) of Ru_3L_2 clam-like structure.

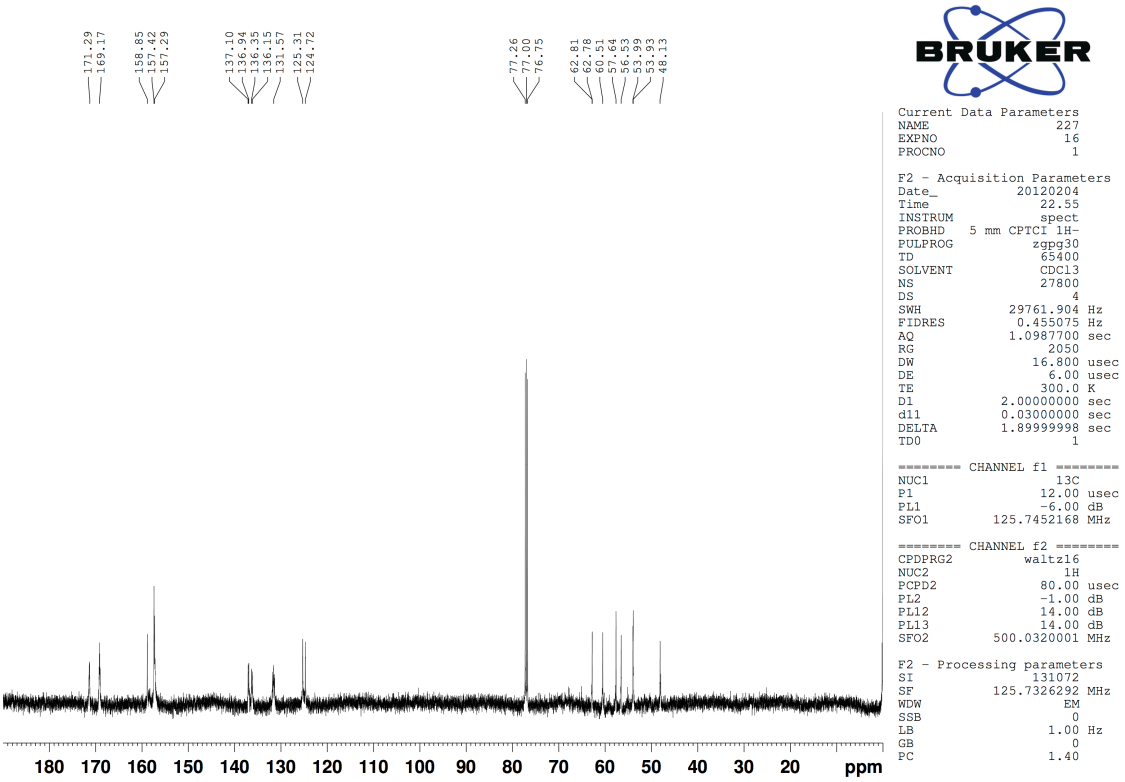

Figure S2.9. ^{13}C NMR spectrum (125 MHz, D_2O, 300 K) of Ru_3L_2 clam-like structure.

- **General procedures for guest encapsulation**

To a 6 mM D_2O solution of **1** (500 μL), 10 μl of liquid guest was added. After stirring for 30 min, surplus of the guest was evaporated at 60 ºC. The host-guest complex was directly analysed by NMR spectroscopy.

- **DOSY NMR experiment**

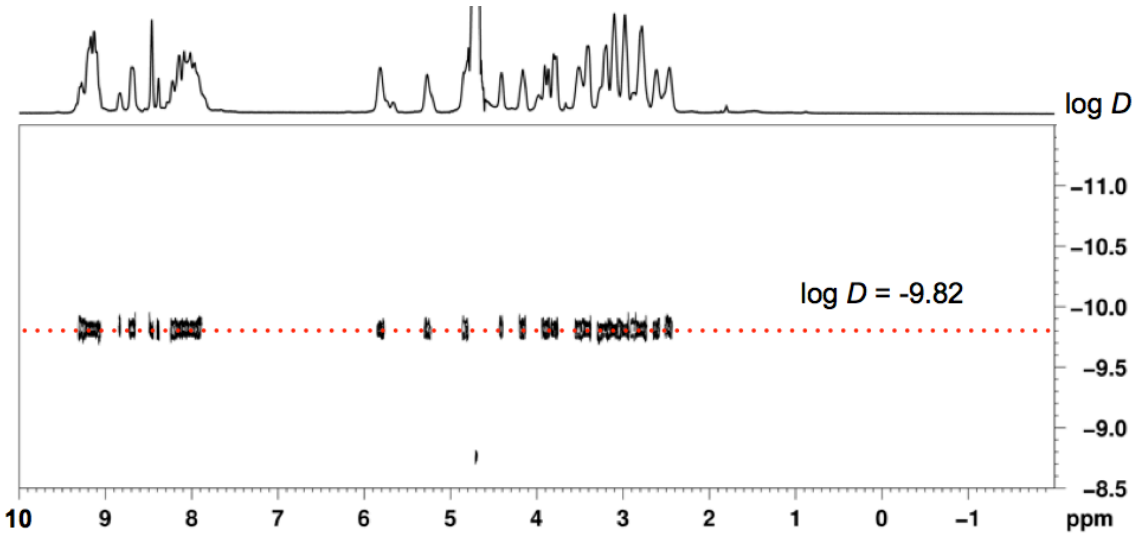

Figure S2.10. DOSY spectrum of Ru_6L_4 capsule **1**. (Form SI of *Chem. Asian J.* **2013**, *8*, 2596. Reprinted with permission of Wiley-VCH)

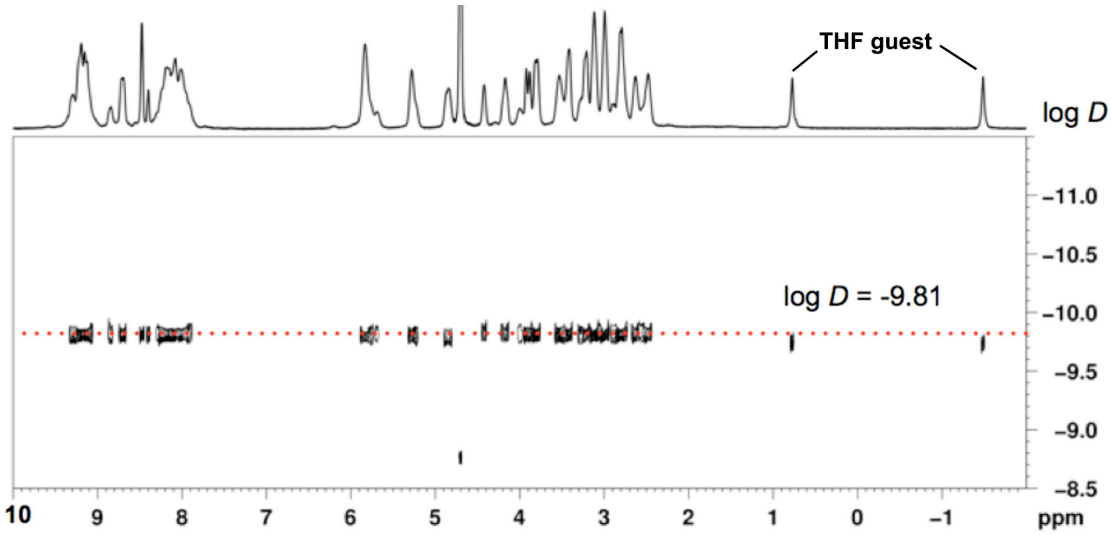

Figure S2.11. DOSY spectrum of Ru_6L_4 capsule–THF complex **1⊃4**. (Form SI of *Chem. Asian J.* **2013**, *8*, 2596. Reprinted with permission of Wiley-VCH)

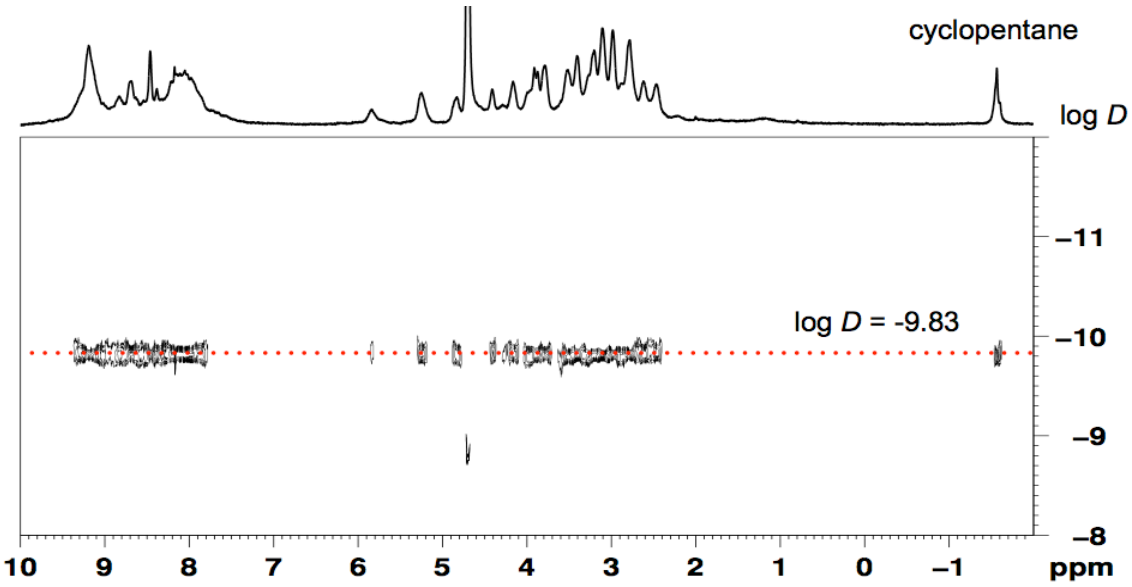

Figure S2.12. DOSY spectrum of Ru_6L_4 capsule–cyclopentane complex **1⊃5**.

- **Brief introduction of VOIDOO program[44]**

VOIDOO can be employed in the study of cavities such as they occur in the supramolecular host and generate a solvent-assessable surface using van der Waals radii of atoms corresponding to the cavity of the host molecules. There are two types of cavity can be detected by *VOIDOO* program: (i) A void that the cavity is isolated from external environment; (ii) invagination that the cavity connected with external environment through small pore or aperture (Figure S2.13). In this thesis, all the structure can be classified as second type.

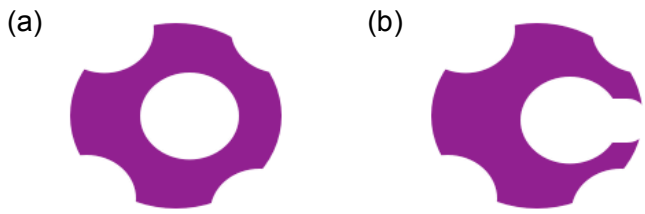

Figure S2.13. VOIDOO suitable for two types of cavity (a) Void; (b) Invagination

Normally, the VOIDOO worked in three steps: (i) Detections of all cavities that exist in the host structure, the number of cavities depends on the probe radius parameter (default setting is 1.4 Å). (ii) Volume calculation, it is worthy to note that the different between calculated volume and true volume is less than ~5% when the grid spacing is less than 0.3 Å. (iii) Visualization of cavity with mesh that allowed to confirm the calculated cavity did not falling out of the inner space.

- **Cavity calculation**

The inner cavity volumes of **1** with different guests were determined using VOIDOO calculations. The calculations were based on the crystal structure of **1⊃4** and molecular modelling of **1⊃5** and **1⊃6**. A virtual probe with a radius of a radius of 1.4 Å (set by default, water-sized) was employed for all cases and the following parameters were changed from their default settings:

Maximum number of volume-refinement cycles: 30
Minimum size of secondary grid: 3
Grid for plot files: 0.1
Primary grid spacing: 0.1
Plot grid spacing: 0.1

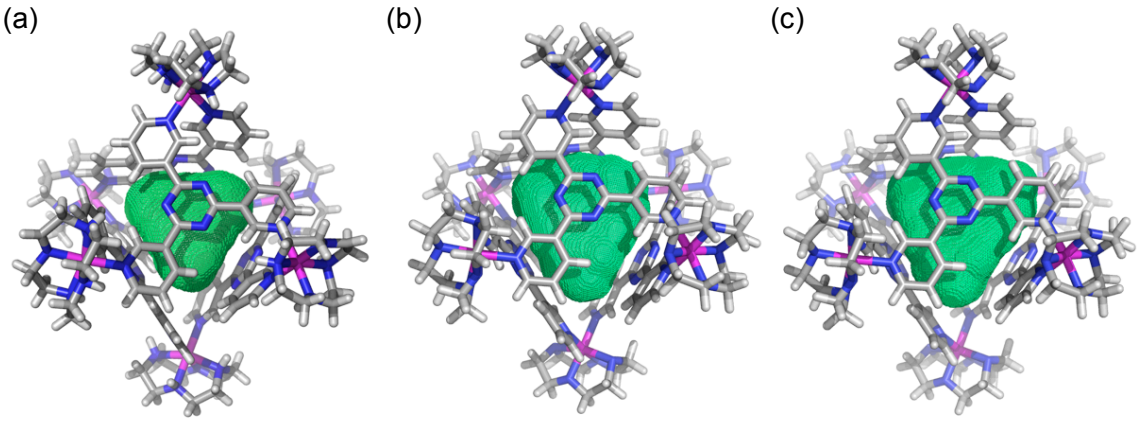

Figure S2.14. Crystal and molecular modelling structure of the (a) **1⊃4**; (b) **1⊃5**; (c) **1⊃6** with their void volumes given and shown in green mash that calculation by VOIDOO (the guest molecules are omitted for clarity).

- **Selected bond length and angle in the intermediate structures for guest encapsulation**

Table S2.1. Selected bond length and angle

Intermediate structure[a]	C_{THF}-C_{TPTopp} (Å)[b]	Ru-Ru (Å)[c]	∠ Ru-N_{py}-Ru (°)	aperture size (Å^3)
a	3.60	11.27	86.07	3.22 × 3.16 × 3.42
b	4.60	11.62	88.18	3.20 × 3.85 × 3.54
c	5.60	11.65	88.61	3.40 × 4.33 × 4.03
d	6.60	11.67	88.64	3.93 × 4.34 × 4.65
e	7.60	11.65	88.80	5.07 × 5.84 × 6.01
f	8.60	11.64	88.82	6.32 × 6.66 × 6.64
g	9.60	11.69	89.23	6.86 × 7.03 × 7.38
h	10.60	11.72	89.37	6.86 × 7.14 × 7.54
i	11.60	11.68	89.06	6.76 × 6.87 × 7.26
j	12.60	11.73	89.57	5.87 × 6.56 × 5.87
k	13.60	11.55	88.14	3.22 × 3.81 × 3.55

[a]the 11 intermediate structures in Figure 2.5; [b]the distance between the centre of THF guest and the centre of **3-TPT** opposite to the active aperture; [c]the average value of bond length; [d]the average value of bond angle; [e]the aperture was define as distance between distance between hydrogen as shown as yellow triangle in Figure 2.4b.

- **X-ray crystallographic data**

Compound code	**1⊃4**[a]	
Empirical formula	$C_{240}H_{312}N_{96}Ru_{12}Cl_{15}$•1.14($C_4H_4O$)	
Formula weight	6368.95	
Temperature	90(2) K	
Wavelength	0.71073 Å	
Crystal system	Monoclinic	
Space group	*C2/c*	
Unit cell dimensions	a = 47.189(9) Å	α = 90°
	b = 27.418(5) Å	β = 110.347(2)°
	c = 40.663(8) Å	γ = 90°
Volume	49328(14) $Å^3$	
Z	4	
Density (calculated)	0.858 g/cm^3	
Absorption coefficient	0.477 cm^{-1}	
F(000)	13011	
Crystal size	0.38 × 0.30 × 0.13 mm^3	
Theta range for data collection	1.25 to 26.66°	
Index ranges	-59≦ h ≦59, -34≦ k ≦34, -50≦ l ≦51	
Reflection collected	260830	
Independent reflections	51992	
Completeness to theta = 26.66	99.5 %	
Data / restraints / parameters	51992 / 1651 / 1105	
Goodness-of-fit on F2	1.129	
Final R indices [I > 2sigma(I)]	R_1 = 0.0565, wR_2 = 0.1791	
R indices (all data)	R_1 = 0.0744, wR_2 = 0.1908	
Largest diff. peak and hole	1.502 and -1.243 e. $Å^3$	

[a]Note that the disordered Cl^- and solvent was removed by SQZEEZE routine in PLATON according to the reported procedure.[45]

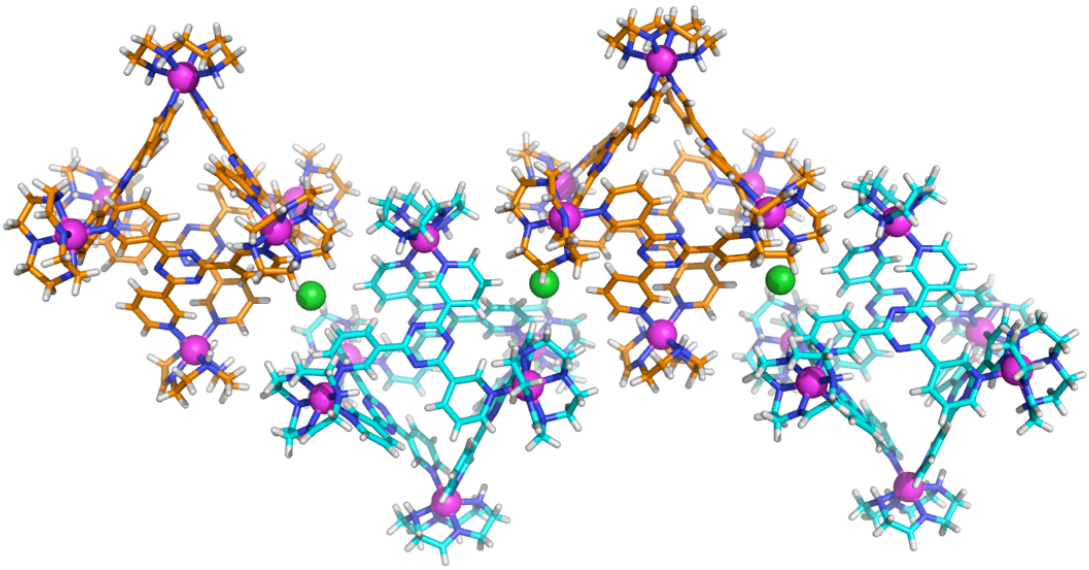

Figure S2.15. Crystal packing of **1⊃4** through the CH-Cl interactions (the THF guests was omitted for clarity, Green; Cl anion)

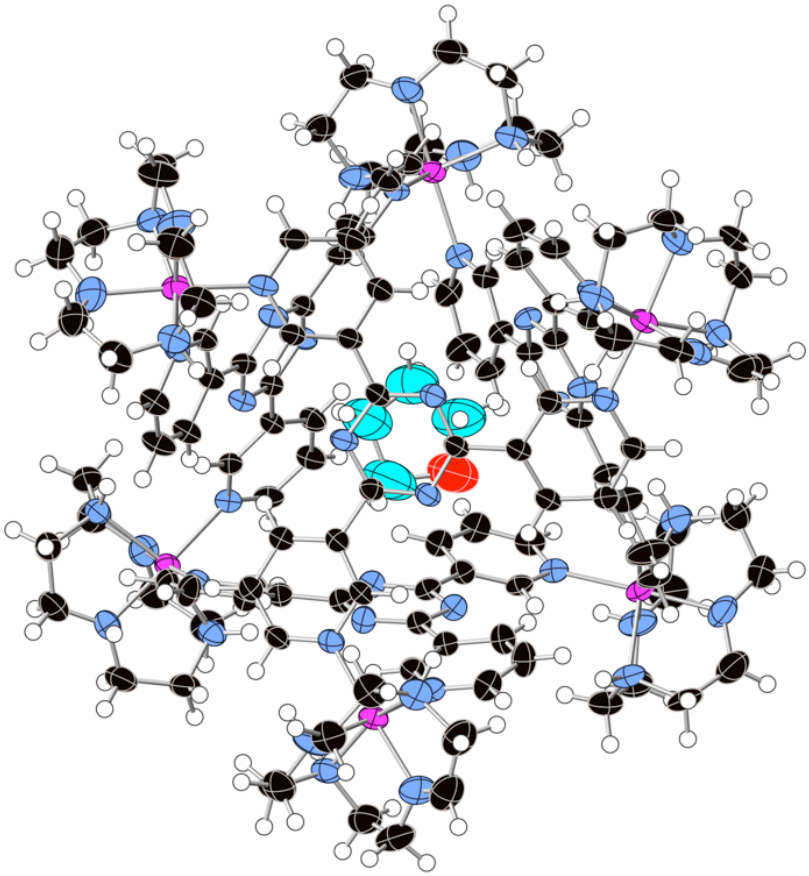

Figure S2.16. ORTEP of **1⊃4** at 50% level.

Compound code	**Ru_3L_2 clam-like structure**[a]	
Empirical formula	$C_{60}H_{76}N_{24}Ru_3O_2$•6.07($BF_4$)	
Formula weight	1995.94	
Temperature	90(2) K	
Wavelength	0.71073 Å	
Crystal system	Monoclinic	
Space group	*C2/c*	
Unit cell dimensions	a = 31.354(5) Å	α = 90°
	b = 16.612(3) Å	β = 121.224(2)°
	c = 16.856(3) Å	γ = 90°
Volume	7508(2) $Å^3$	
Z	4	
Density (calculated)	1.766 g/cm^3	
Absorption coefficient	0.718 cm^{-1}	
F(000)	4004.3	
Crystal size	0.16 × 0.12 × 0.10 mm^3	
Theta range for data collection	1.44 to 24.63°	
Index ranges	-36≦ h ≦36, -19≦ k ≦19, -19≦ l ≦19	
Reflection collected	33960	
Independent reflections	6302	
Completeness to theta = 24.63	99.4 %	
Data / restraints / parameters	6341 / 572 / 129	
Goodness-of-fit on F2	1.062	
Final R indices [I > 2sigma(I)]	R_1 = 0.0484, wR_2 = 0.1238	
R indices (all data)	R_1 = 0.0759, wR_2 = 0.1396	
Largest diff. peak and hole	1.154 and -0.908 e. $Å^3$	

[a]The crystals suitable for X-ray crystallographic analysis was obtained after anion exchange with BF_4^-.

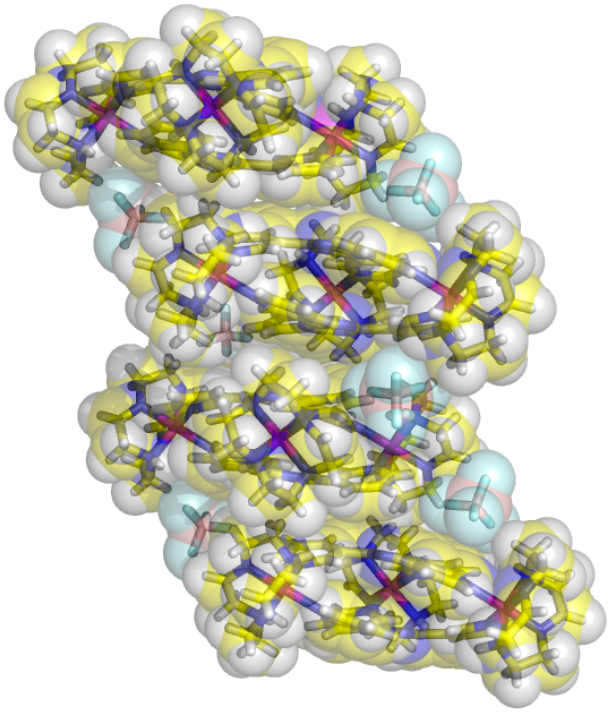

Figure S2.17. Crystal packing of Ru_3L_2 clam-like structure

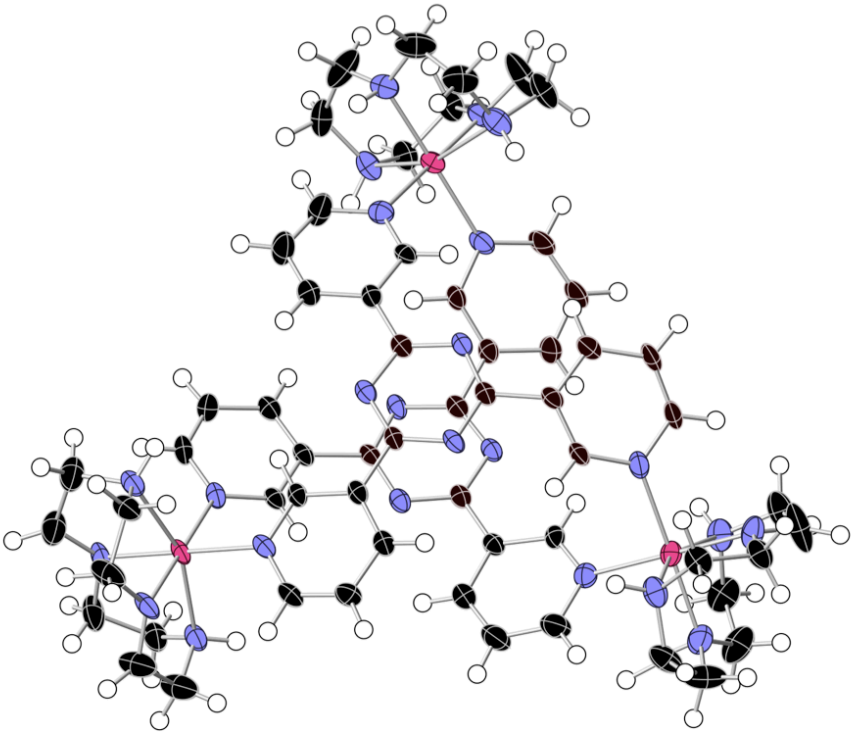

Figure S2.18. ORTEP of at Ru_3L_2 clam-like structure 50% level.

Chapter 3

Construction of Dynamic Capsule Cavity in Crystals

In this chapter I have prepared networked Co_6L_4 capsules **2** in solid-state that consist of an infinite network of Co_6L_4 capsules and solvent accessible pores (two environments for guests). The dynamic nature of networked capsules **2** was revealed by single-crystal-to-single-crystal guest exchange experiments. In addition, molecular modeling studies were also conducted to probe the flexibility of **2**, and the cavity calculation revealed the dynamic cavity change of networked capsules **2** upon guest accommodation even in the solid-state.

3.1 *Introduction*

Dynamic solution capsules are able to isolate the guests from external environment and mediate the physical and chemical properties of encapsulated guests, such as stabilization of reactive intermediates and the acceleration of reaction rates (see the general introduction in Chapter 1). Such chemistries have rarely developed in the solid (crystalline) state, compared with great attentions have been paid to pore structure (e.g. porosity, pore size and shape or pore-surface functionalization) in the MOFs or PCPs field,[21] because the incorporation of confined host cavities into MOFs or PCPs is rather difficult. Recently the Fujita group has ingeniously developed a 'networking strategy', which allows us to construct networked structure, composed of well-defined discrete host cavities and interstitial pores, based on solution hosts.[30]

Herein, I have synthesized networked Co_6L_4 capsules **2** composed of two distinct void spaces (capsule cavities and interstitial pores). In addition, unique dynamic guest exchange and cavity change properties of networked capsules **2** are descried.

3.2 *Synthesis and Characterization*

Networked capsules **2** was synthesized by slowly layering a methanol solution of $Co(NCS)_2$ onto a thiophene (**7**)/methanol solution of **3-TPT**. Pale red crystals were obtained after one week in 60% yield.[46] X-ray crystallographic analysis revealed that networked capsules **2** were composed of an infinite array of Co_6L_4 capsules and solvent accessible pores. During the crystallization process four thiophene (**7**) guest molecules were tightly encapsulated within capsule units (Figure 3.1).

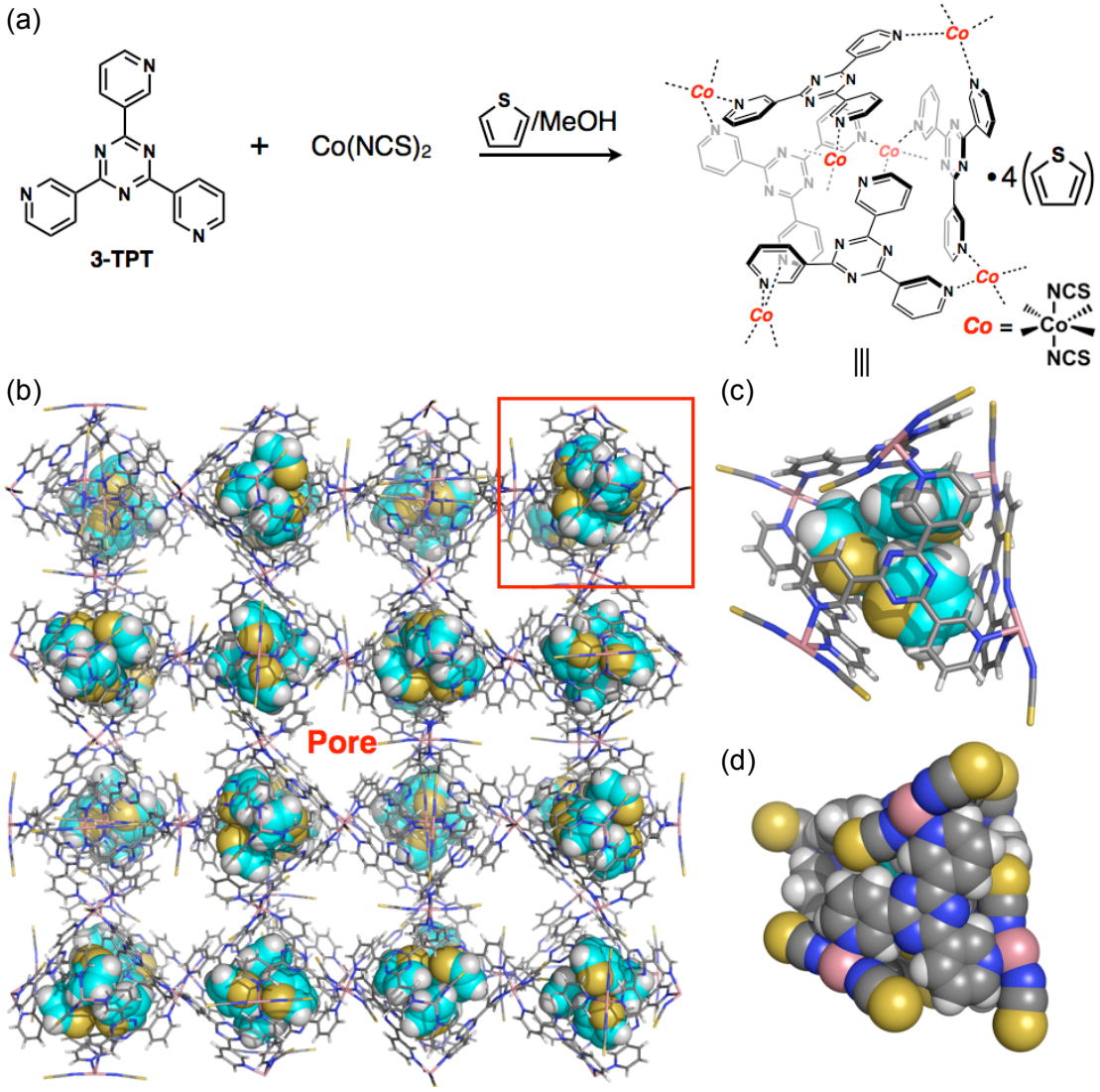

Figure 3.1. (a) Synthesis of networked capsules **2** accommodating four thiophene guests; X-ray structure of (b) networked structure of **2⊃(7)$_4$** and one capsule was marked with a red square; (c) stick models of one M_6L_4 capsule where thiophene guests were shown in CPK models; (d) CPK model of one capsule.

Networked capsules **2** have two distinct void spaces. One is the well-defined Co_6L_4 capsule cavity that is similar to Ru_6L_4 solution capsule **1**. Within the cavity of capsules, the guest molecules are tightly packed and their orientation are constrained (Figure 3.1c). Importantly, they are surrounded by aromatic walls and isolated from the external environment (pores) as shown in Figure 3.1d. Another is the interstitial pores that provide a solution-like fluidity, and the mobility and volatility of guest molecules in the pores is similar to their bulk solution phase.[46] Therefore, sometimes the highly mobile or disorder guests in the pores could not be determined by X-ray crystallography (Figure 3.1b).

It is worthy to emphasize that small openings in the host shell allow the internal cavity of capsules to communicate with the external environment (pores). Thus, unlike the example described in Figure 1.9, the guest uptake, release or exchange can occur by the passage of guests through the apertures of Co_6L_4 capsules.

3.3 *Dynamic Guest Exchange*

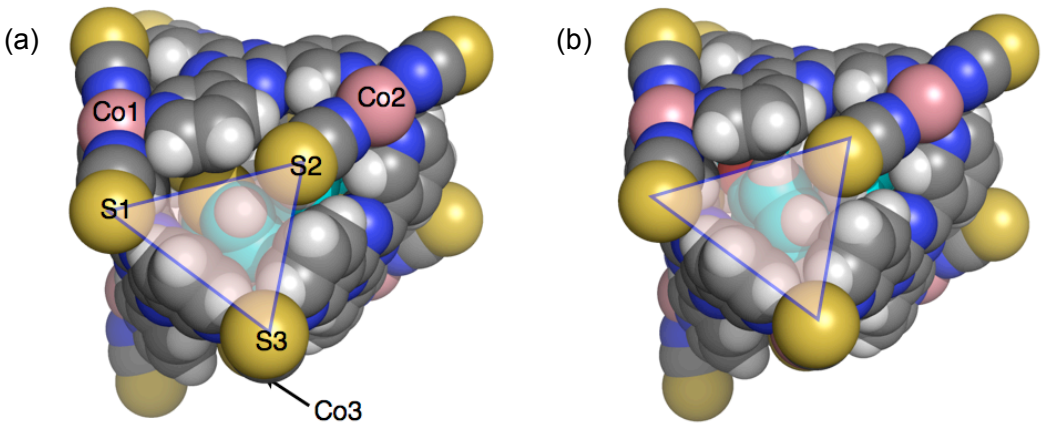

Figure 3.2. X-ray structure of one capsule unit in (a) **2⊃(7)$_4$** and in (b) **2⊃(8)$_2$** (shown in CPK model). (blue triangle represent the aperture of capsule)

Examination of the crystal structure of **2⊃(7)$_4$** (where ⊃ denoted encapsulation) (Figure 3.2a) leads to the conclusion that the encapsulated thiophene guests are well surrounded by the aromatic backbones of the networked capsules **2** and the only small openings that are narrower than size of guests **7** exist in the host shell. In addition, to probe the flexibility of networked capsules **2**, bulky guest molecules, diphenyl ether (**8**),

were introduced into **2** through a single-crystal-to-single-crystal (SCSC) guest exchange reaction. The X-ray structure of inclusion complex **2⊃(8)$_2$** also revealed that the apertures of capsule is much narrower than the size of guests **8** (Figure 3.2b).

These structural evidences strongly suggested the dynamic guest exchange occurred. Considering the suppression of liability of Co-N_{py} bond in the crystalline state, one most possible guest exchange mechanism is assumed: Guest exchange occurs without any ligand dissociation and the Co_6L_4 capsules need to expand their apertures to release the former guests and accommodate the later guests, and then squeeze their apertures to make tight packing of guests within the cavity of networked capsules **2**. The dynamic behavior of networked capsules **2**, expansion and squeezing apertures, is very similar to the Ru_6L_4 capsule **1** in solution.

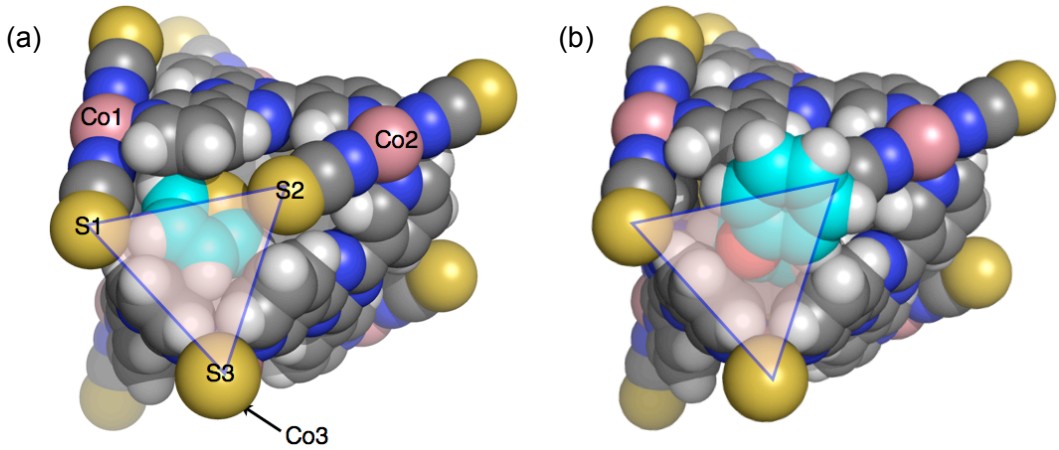

Figure 3.3. Molecular modeling structures of the largest expansion of aperture in (a) **I2⊃(7)$_4$** and (b) **I2⊃(8)$_2$** (shown as CPK model). (blue triangle represent the aperture of capsule).

To probe the host deformation during the guest exchange, molecular modeling studies were employed to investigate the intermediate deformed structures that did not observed experimentally. There are two important intermediate deformed structures: (1) Thiophene guests just released from the capsule (**I2⊃(7)$_4$** where **I** means intermediate structure) (the largest expansion of capsule aperture for thiophene guests) (Figure 3.3a); (2) Diphenyl ether guests just accommodated in the capsules (**I2⊃(8)$_2$**) (the largest expansion of capsule aperture for diphenyl ether guests) (Figure 3.3b). To remove guests **7** and accommodate guests **8**, the networked capsules **2** deforms by rotation of **3-TPT** as mentioned in Chapter 1 (Scheme 1.3) and the enlargement or

shrinking of the active aperture can be measured by the two factors (Table 3.1): (1) The blue triangle created by three sulfur atoms, S1, S2 and S3, as shown in the Figure 3.2. (2) The distances among three cobalt atoms located in the active aperture, Co1, Co2 and Co3, as shown in Figure 3.2, indicating the movement of metal center during deformation of capsule host.

The detailed analysis of two crystals structures of **2⊃(7)$_4$** and **2⊃(8)$_2$** and two molecular modeling structures of **I2⊃(7)$_4$** and **I2⊃(8)$_2$** revealed that the expansion and shrinking of capsule indeed occur with the increase of guests size (from thiophene to diphenyl ether). Firstly, the distances among three sulfur atoms expanded from 8.19 × 8.42 × 8.28 Å^3 in **2⊃(7)$_4$** to 8.87 × 9.25 × 9.60 Å^3 in **I2⊃(7)$_4$** and then further expanded to 8.64 × 9.51 × 10.01 Å^3 in **I2⊃(8)$_2$**, at last squeezed to 8.35 × 8.84 × 8.64 Å^3 in **2⊃(8)$_2$**. Same dynamic behaviors were observed for the distances among the cobalt atoms, located in the active aperture, indicating the apertures of capsules were firstly expanded for removal of guests **7** and further enlarged to allow ingress of bulky guests **8**, at last shrunk to make tight packing of guests **8**. These structure evidences unambiguously proved that the dynamic nature of networked capsules **2** during the guest exchange and well supported the non-dissociative guest exchange mechanism.

Table 3.1. The expansion and squeezing of capsule aperture

compound	S1-S2-S3 (Å^3)^a	Co1-Co2-Co3 (Å^3)^b
2⊃(7)$_4$	8.19 × 8.42 × 8.28	11.32 × 11.02 × 11.28
I2⊃(7)$_4$	8.87 × 9.25 × 9.60	12.69 × 11.89 × 12.47
I2⊃(8)$_2$	8.64 × 9.51 × 10.01	12.55 × 12.07 × 12.47
2⊃(8)$_2$	8.35 × 8.84 × 8.64	11.53 × 11.16 × 11.43

^{a}the triangle size, created by S1, S2 and S3, in Figure 3.2 and ordered as D_{S1-S2}, D_{S1-S3} and D_{S2-S3}; ^{b} the triangle size, created by Co1, Co2 and Co3, in Figure 3.2 and ordered as $D_{Co1-Co2}$, $D_{Co1-Co3}$ and $D_{Co2-Co3}$.

3.4 *Dynamic Cavity Change*

The analysis of crystal structures of **2⊃(7)$_4$** and **2⊃(8)$_2$** also reveals 'induce fit' phenomena that the networked capsules **2**, like solution Ru_6L_4 capsule **1**, varied its cavity volume to fit encapsulated guests with different size. To test this theory, other guest molecules, such as furan, pyrrole and cyclopentadiene (**9**), were introduced into the networked capsules **2**.[46] The cavity volume of crystalline host **2** was calculated by VOIDOO program,[44] based on the crystal structure of inclusion complexes of **2⊃(furan)$_4$**, **2⊃(pyrrole)$_4$**, **2⊃(7)$_4$**, **2⊃(9)$_4$** and **2⊃(8)$_2$**.

The results clearly showed that the cavity volume of **2** were able to expand by ~ 13% from 472 Å^3 for **2⊃(furan)$_4$** to 535 Å^3 for **2⊃(8)$_2$** (Table 3.2 and Figure S3.1). The average edge length between two adjacent cobalt atoms lengthened from 11.21 to 11.40 Å (**2⊃(furan)$_4$** to **2⊃(8)$_2$**), the average bond angle of Co-N_{py}-Co increased from 90.15 to 91.70° (**2⊃(furan)$_4$** to **2⊃(8)$_2$**) and the vectors in unit cell parameters also lengthened from 63.724(7) to 64.412(10) Å ($a = b = c$) (**2⊃(furan)$_4$** to **2⊃(8)$_2$**) (Table S3.1). All these structural evidences are indicative of the expansion of host cavity with the increase of guest volumes (from furan to diphenyl ether) that agreed with the calculation results from VOIDOO program.

Table 3.2. Cavity volumes of Co_6L_4 capsules **2** with various guests

Guest	Guest volume (Å^3)^a	Host cavity (Å^3)^b
Furan ^{a}	311.76	472.16
Pyrrole ^{a}	324.12	482.54
Thiophene ^{a}	346.40	493.51
Cyclopentadiene ^{a}	349.44	492.20
Diphenyl ether ^{b}	383.98	535.21

^{a}Host/Guest = 1/4. ^{b}Host/Guest = 1/2. ^{c}van der Waals volumes calculated from structure optimized using SPARTAN'10 with MP2 using both a 6-311+G** basis set. ^{d}The cavity volumes calculated from VOIDOO program (probe radius =1.40 Å) based on the X-ray structures.

3.5 *Conclusion*

In summary, networked Co_6L_4 capsules **2** was prepared by inspiration from the discrete Ru_6L_4 capsule **1**. The X-ray crystallographic analysis confirmed that complex **2** was composed of infinite capsule units and solvent accessible pores. Through the X-ray structure analysis and molecular modeling studies, a non-dissociative mechanism was proposed and revealed that the networked capsules **2** exhibited flexible or dynamic guest encapsulation and exchange process via aperture expansion and shrinking. In addition, the cavity volume of the networked capsules **2** enlarged by ~ 13% upon the accommodation of guests with size increase, leading to induced-fit binding of guests.

3.6 *Experimental Section*

- **General procedures**

Solvent and reagents were purchased from TCI, WAKO Pure Chemical Industries, Furuya metal Co., Ltd. or Sigma-Aldrich. All chemicals were used without any further purification except where noted. Thermo gravimetric analysis was performed on a STA 409 PG/T equipped with a QMS 403C/T (NETZSCH). Elemental analysis was performed on a YANACO MT-6. Single crystal X-ray diffraction data were made using a BRUKER APEX-II/CCD diffractometer equipped with a focusing mirror (MoK_{α} radiation λ= 0.71073 Å) and a N_2 generator (Japan Thermal Eng. Co., Ltd.).

- **Preparation of networked capsules**

The networked capsules **2⊃(furan)$_4$**, **2⊃(pyrrole)$_4$**, **2⊃(7)$_4$**, **2⊃(8)$_4$**, and **2⊃(9)$_4$** were prepared and characterized according to the reported procedure.[46] Here I would like to describe the synthesis of **2⊃(7)$_4$** as general procedure.

A solution of 2,4,6-tris(3- pyridyl)-1,3,5-triazine (**3-TPT**; 6.3 mg, 20 mmol) in a mixture of thiophene (**7**; 4.0 mL) and methanol (1.0 mL) was placed in a test tube (inner diameter 1cm, height 10 cm). Absolute methanol (0.2 mL) was layered onto the top of the solution as a buffer. Then, a solution of $Co(NCS)_2$ (10.5 mg, 60 mmol) in methanol (1.0 mL) was carefully layered on the top of the resultant solution, and the test tube was allowed to stand at room temperature for one week in 60 % yield .

- **Selected bond length and angle in the X-ray structures of inclusion complexes**

Table S3.1. Selected bond length and angle

Complex	Co-Co (Å)[a]	∠ Co-N_{py}-Co (°)[c]	Unit cell ($a = b = c$ Å)[d]
2⊃(furan)$_4$	11.21	90.15	63.724(7)
2⊃(pyrrole)$_4$	11.24	90.41	63.890(2)
2⊃(7)$_4$	11.21	91.63	63.628(9)
2⊃(9)$_4$	11.31	89.23	63.920(3)
2⊃(8)$_4$	11.40	91.70	64.412(10)

[a]the average edge length between two adjacent cobalt atoms; [b] the average value of bond angle; [d]the space group is Cubic, *Fd-3c*.

- **Cavity calculation**

The inner cavity volumes of networked capsules **2** with different guests were determined using VOIDOO calculations. The calculations were based on the crystal structure of **2⊃(furan)$_4$**, **2⊃(pyrrole)$_4$**, **2⊃(7)$_4$**, **2⊃(8)$_4$**, and **2⊃(9)$_4$**. A virtual probe with a radius of a radius of 1.4 Å (set by default, water-sized) was employed for all cases (Due to the large pore size of networked capsules **2**, four benzene molecules were used to block the pores and prevent the probe from "falling out" of the inner sphere),[47] and the following parameters were changed from their default settings:

Maximum number of volume-refinement cycles: 30
Minimum size of secondary grid: 3
Grid for plot files: 0.1
Primary grid spacing: 0.1
Plot grid spacing: 0.1

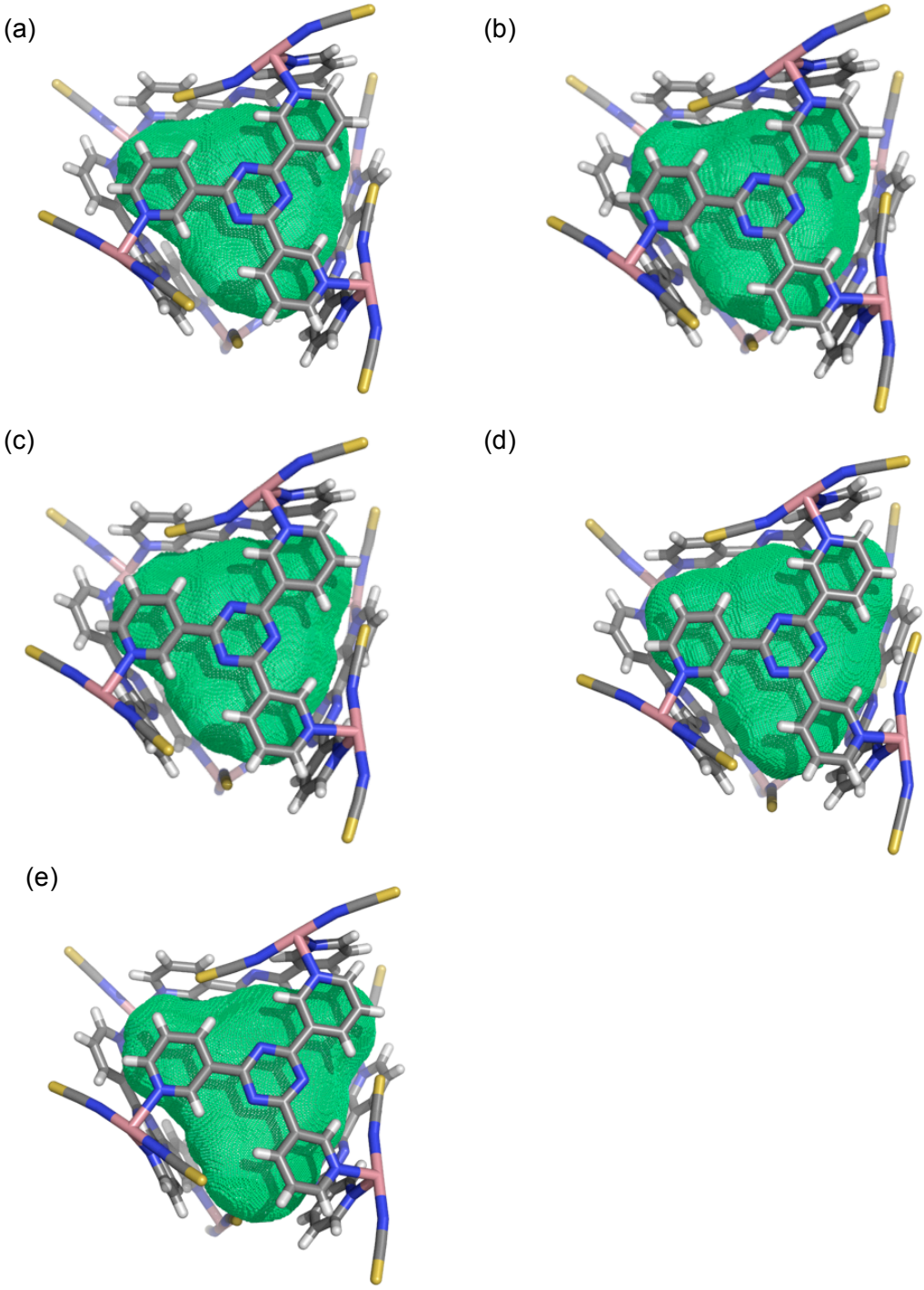

Figure S3.1. Crystal structure of the (a) **2⊃(furan)$_4$**; (b) **2⊃(pyrrole)$_4$**; (c) **2⊃(7)$_4$**; (d) **2⊃(9)$_4$**; **(e) 2⊃(8)$_4$** with their void volumes given and shown in green mash that calculation by VOIDOO (the guest molecules are omitted for clarity).

Chapter 4

Bridge of Solution and the Solid-State Chemistry

In this chapter I have compared the crystal structures of discrete Ru_6L_4 capsule **1⊃4** and networked Co_6L_4 capsules **2⊃(4)$_4$** (where ⊃ denotes encapsulation) and X-ray analysis confirmed that solution and crystalline capsules both have common M_6L_4 capsule unit. In both crystal structures, the THF (**4**) guest molecules are accommodated within the M_6L_4 capsule and the detailed structural analysis reveals that the THF guests have similar interactions with the host frameworks in discrete and networked capsules, indicating the qualitatively same host-guest chemistry have been achieved. Due to the cavity equivalency, the common host-guest properties have been found in solution and in crystals.

4.1 *Introduction*

Bridge of solution and the solid (crystalline) state chemistry with a complementary pair of solution and crystalline host allows us to combine the advantages of solution and the solid-state chemistry, such as the transformation of rich and dynamic solution chemistry into solid-state, and visualization of solution host-guest chemistry by X-ray analysis with solid-state host. The Fujita group has recently developed the 'networking strategy' for constructing the complementary pair of solution and crystalline cages.[30] There are two essential structure features for bridging solution and the solid-state chemistry: (1) Equivalent host cavities in two states offer the same guest binding environment and host-guest interactions; (2) For the solid (crystalline) hosts, the aperture of host units cannot be blocked by adjacent host units during the crystal packing. Based on this approach, I have successfully prepared a complementary pair of solution (Chapter 2) and crystalline capsules (Chapter 3). The solution and crystalline capsules have exhibited similar dynamic behavior upon guest binding in solution and in the solid-state.

In this chapter, to confirm whether solution and solid-state capsules have equivalent host cavity, the detailed crystallographic analysis is discussed. In addition, based on the X-ray structures, the interactions between host (solution or crystalline capsules) and guests (THF) are described. Finally, the common host-guest properties have been found in solution and in crystals due to the cavity equivalency and similar dynamic behavior.

4.2 *Cavity Equivalency and Common Guest Encapsulation*

To compare the X-ray structure of two capsules, the common guest molecules, THF (**4**), were introduced into networked capsules **2** via a *SCSC* guest exchange reaction (see experimental section for details). The X-ray crystallographic analysis of **1⊃4** (prepared according to procedures described in Chapter 2) and **2⊃(4)$_4$** (where ⊃ denoted encapsulation) confirmed that discrete Ru_6L_4 capsule adopt octahedral M_6L_4 capsule topology, which is similar to the capsule units in the networked Co_6L_4 capsules (Figure 4.1 and Figure S4.11). In addition, the edge lengths of discrete Ru_6L_4 capsule (two adjacent Ru atoms) were ranging from 11.13 to 11.42 Å (avg. 11.27 Å) that was

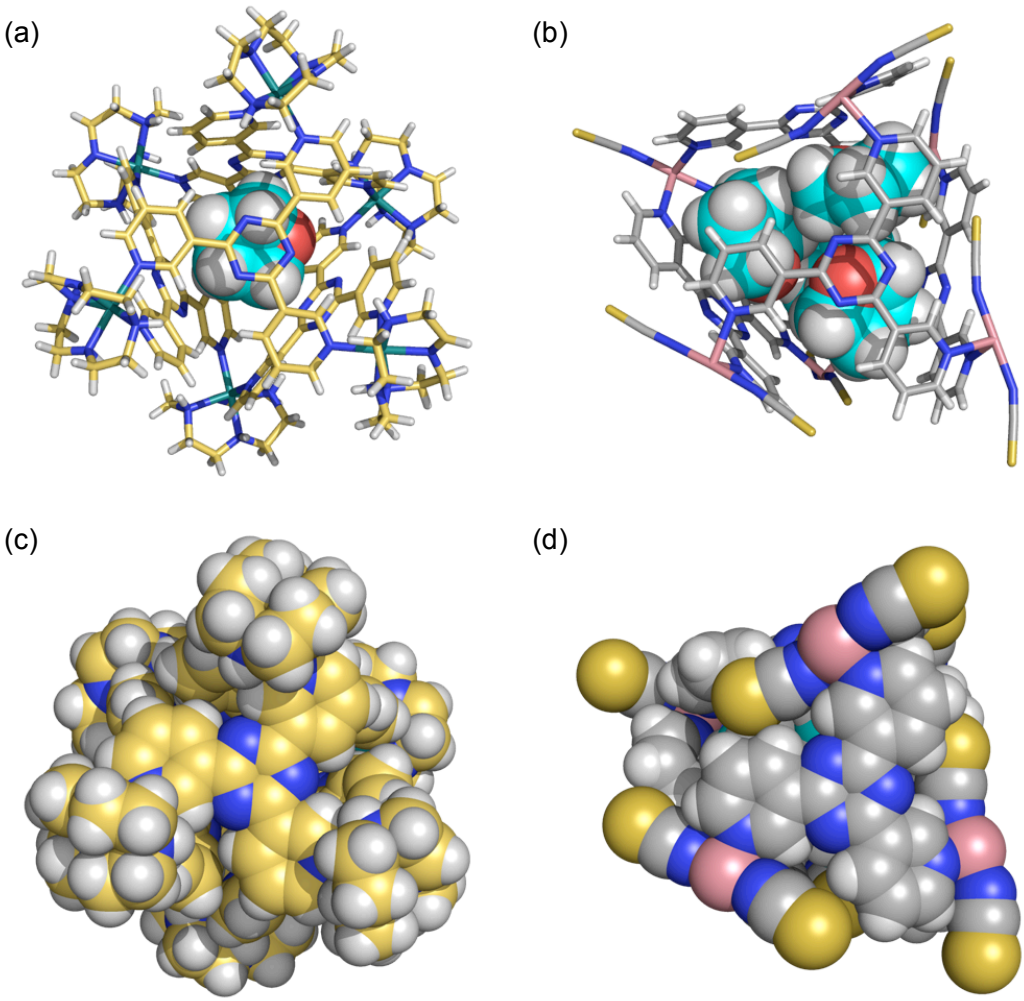

Figure 4.1. Comparison of X-ray structures of (a) discrete Ru_6L_4 capsules **1** accommodating one THF guest and (b) one capsule unit in networked Co_6L_4 capsules **2** accommodating four THF guests (stick models of capsule where THF guest is shown in CPK model); (c), (d) CPK model.

similar with Co–Co distance in networked capsules (avg. 11.25 Å) (Table S4.1).

It is worthy noting that the observed host-guest ratios (1:1 for **1** and 1:4 for **2**) and cavity volumes, calculated by VOIDOO program, (141 and 519 $Å^3$ for **1** and **2**) are different (Figure 4.2). The shrinking of cavity volume in solution capsule can be explained by the structural evidences. The bond lengths of M-N_{py} in Ru_6L_4 capsule **1** were ranged from 2.09–2.11 Å (avg. 2.10 Å) that was shorter than that in Co_6L_4 capsules **2** (avg. 2.19 Å), and the bond angles of N_{py}-M-N_{py} in Ru_6L_4 capsule **1** were ranged from 85.63–86.51° (avg. 86.08°) that was also smaller than that in Co_6L_4 capsules **2** (avg. 91.27 Å) (Table S4.1). Thus the cavity volume of discrete capsule **1** is much smaller than that of networked capsule **2**.

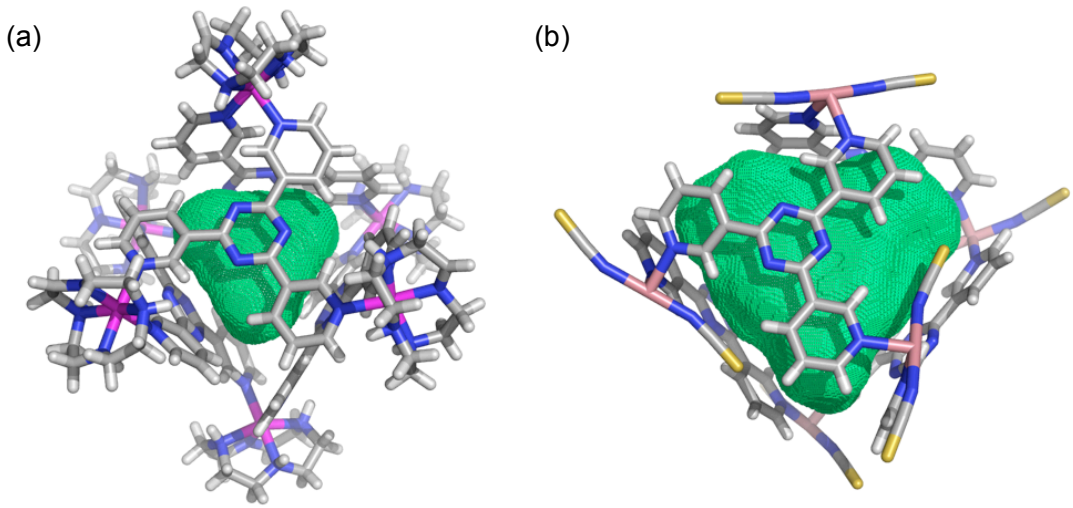

Figure 4.2. Crystal structures of (a) **1⊃4**; (b) **2⊃(4)$_4$** with their void volumes given and shown in green mash that calculation by VOIDOO (the guest molecules are omitted for clarity). (Form SI of *Chem. Asian J.* **2013**, *8*, 2596. Reprinted with permission of Wiley-VCH)

Although the cavity volume and host-guest ratios are different, the aperture of both capsules have been squeezed to constrain the guests and isolate the guests from external environment, indicating two capsules show similar dynamic behavior upon encapsulation of common guest **4**.

In addition, the detailed structure information also revealed that the similar host-guest interactions were observed in **1⊃4** and **2⊃(4)$_4$**. The encapsulated THF guest interacted with the interior walls of the discrete capsule **1** by CH-π interactions, van der Waals interactions and hydrophobic interactions. [48] The hydrogen atoms of

encapsulated THF guests have close contact with the center of triazine rings in the **3-TPT** walls of 2.51 and 2.68 Å (Figure 4.3a). Similar interactions were observed in the networked capsule **2** with close contact of 2.96 and 2.86 Å (Figure 4.3b).

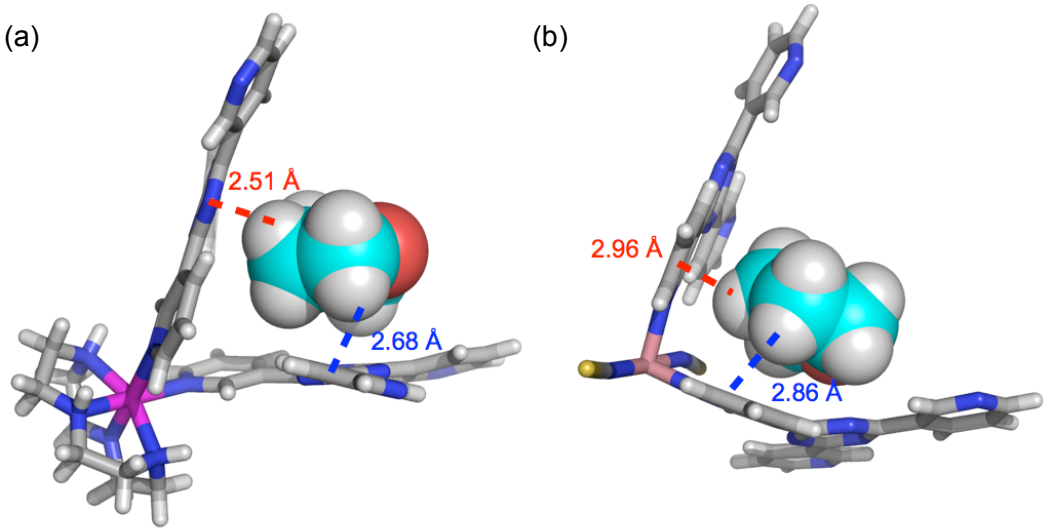

Figure 4.3. The CH-π interactions in (a) discrete Ru_6L_4 capsule **1** and (b) networked Co_6L_4 capsules **2** accommodating THF guest molecule.

These structural evidences demonstrated that the common dynamic capsule cavity could lead to qualitatively same host-guest chemistry in solution and in crystals. With a pair of dynamic capsules, the solution and solid-state chemistry can be bridged. In the following section, I would like to discovery the common host-guest properties in solution and in crystals with a pair of dynamic capsules.

4.3 *Guest Screening and Suppression of Volatility*

One of the advantages of solution host-guest chemistry is fast screening of suitable guests by solution NMR analysis. With a pair of capsules, I expected that I can quick test the suitable guest for crystalline capsules through the solution studies.

To test this idea, cyclic and acyclic hydrocarbons were tested with solution capsule **1**. To an aqueous solution of **1**, volatile hydrocarbons were added in excess to give biphasic system. Formation of the host-guest complex was easily checked by ^{1}H NMR spectroscopy after evaporation of the surplus guest under reduced pressure. I found that volatile cyclic compounds, such as cyclopentane (**5**; b.p. 50 ºC) and cyclohexane (**6**; b.p. 81 ºC), were predominantly encapsulated over acylic ones by capsule **1** even after

heating at 60 ℃ (Figure S4.3 to S4.6) (Encapsulation of guest **5** and **6** with solution capsule **1** was confirmed by the highly up-filed shifted signals of guests in ^{1}H NMR as described in Chapter 2.). Given this result, I anticipated that crystalline host **2** would also bind guest **5** and **6** to give a non-volatile cyclopentane and cyclohexane–clathrate.

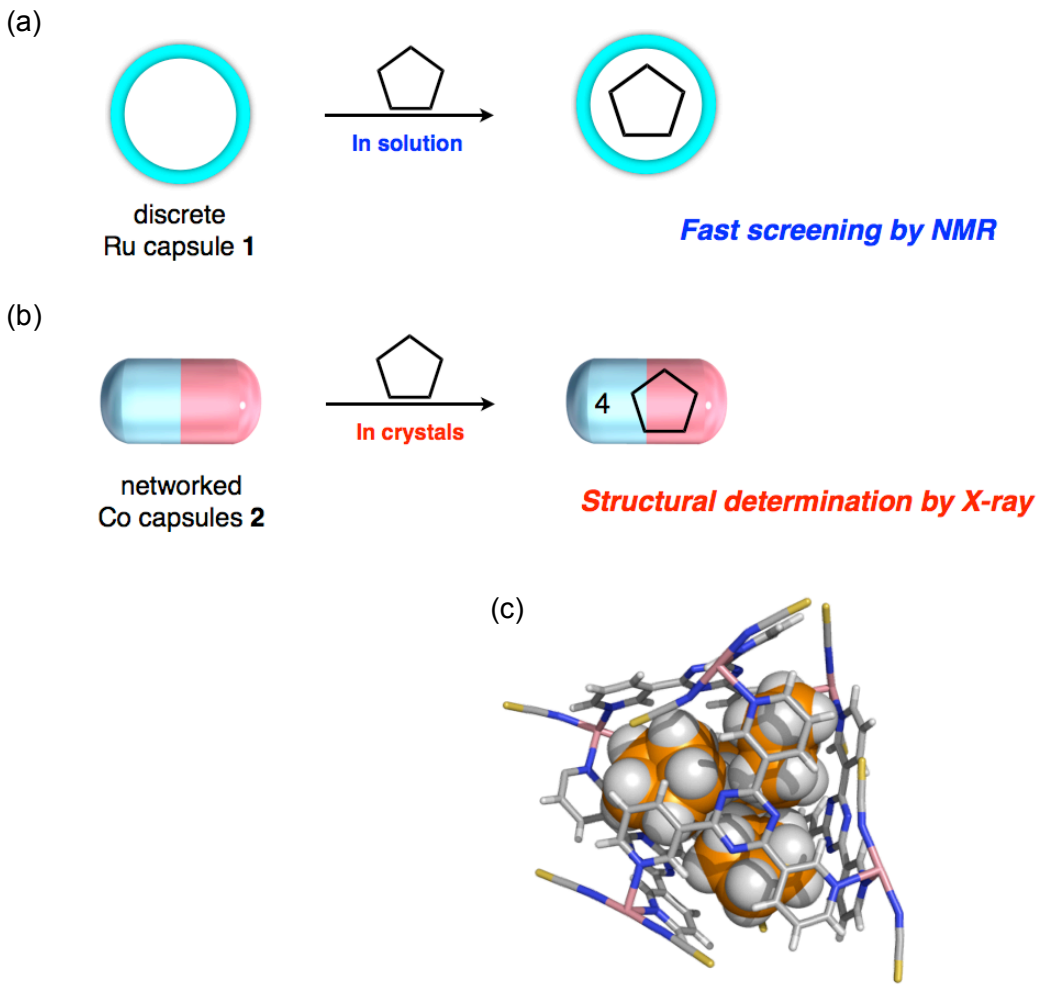

Figure 4.4. Schematic presentation for inclusion of cyclopentane (**5**) into (a) solution capsule **1** and (b) crystalline capsules **2**; The X-ray structures of (c) **2⊃(5)**$_4$ (only one M_6L_4 capsule unit is shown in stick models where guests **5** are shown in CPK models). (Form *Chem. Asian J.* **2013**, *8*, 2596. Reprinted with permission of Wiley-VCH)

The inclusion complexes, **2⊃(5)**$_4$ or **2⊃(6)**$_4$, were prepared by immersion of crystals of as-synthesized capsules **2⊃(7)**$_4$ under neat conditions and the tight packing of **5** in the capsule cavity was confirmed by the X-ray crystal structures (the guests **6**

were highly disorder in the symmetric position, I can not fully solve the X-ray structure) (Figure 4.4). The thermogravimetric (TG) analysis revealed the strong binding of encapsulated guests (Figure S4.7 and 4.8). Take **2⊃(5)$_4$** as an example, upon heating crystals of **2⊃(5)$_4$**, a distinct weight loss (*ca*. 10 wt%) attributable to the release of guests **5** from the capsule was observed at 190-210 ºC with a sharp endothermic peak in the DSC curve (Figure S4.7 and 4.8). Moreover, even after heating crystals of **2⊃(5)$_4$** at 100 ºC for 1 d under open-air conditions, cyclopentane **5** could still be extracted from the crystals with $CDCl_3$ (after digestion). These results clearly indicate the suppression of volatility caused by the confinement effect of capsules as observed in solution capsule **1**.

These results demonstrated that 'cream skimming' (combination of advantages) of solution and solid-state host-guest chemistry can be achieved through solution and crystalline capsules with similar dynamic capsule cavity.

4.4 *Suppression of D-A Dimerization*

Due to the well isolation of guest molecules from outside environment, the motion and volatility is restrained within the cavity of capsules. Given this property, I expected that the capsules could control the reactivity of encapsulated guests. To test this, a reactive cyclic chemical, cyclopentadiene (**9**), was tested with the solution

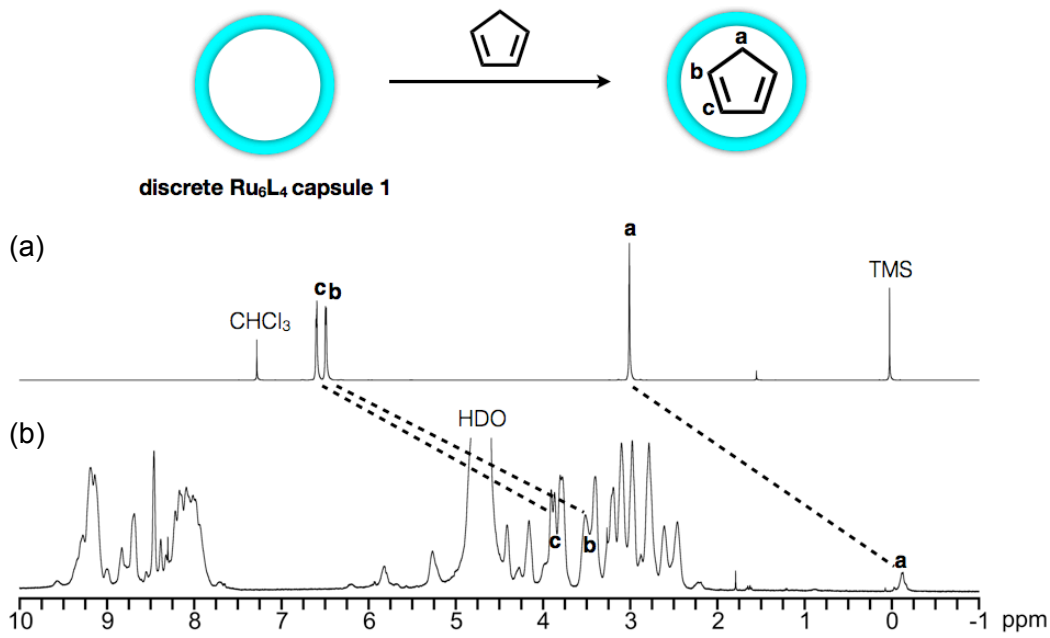

Figure 4.5. The ^{1}H NMR (500 Mz, 300 K) of (a) free cyclopentadiene in $CDCl_3$; (b) inclusion complex **1⊃9** in D_2O.

capsules.

Cyclopentadiene accommodation in solution was confirmed by upfield-shifted signals of **9** at 3.75, 3.46 and –0.12 ppm in ^{1}H NMR (Figure 4.5). The guest **9** was stable within the cavity of solution host **1** even after heating **1⊃9** at 40 ºC for 3 d and the Diels–Alder dimerization products were not observed (Figure 4.6a).

As in the case of solution host **1**, The as-synthesized cyclopentadiene inclusion crystals were heated at 40 for 24 h, the X-ray analysis confirmed that the Diels-Alder dimerization of installed guests **9** were completely suppressed due to the constraint of guests' conformation by M_6L_4 capsules (Figure 4.6b).[46]

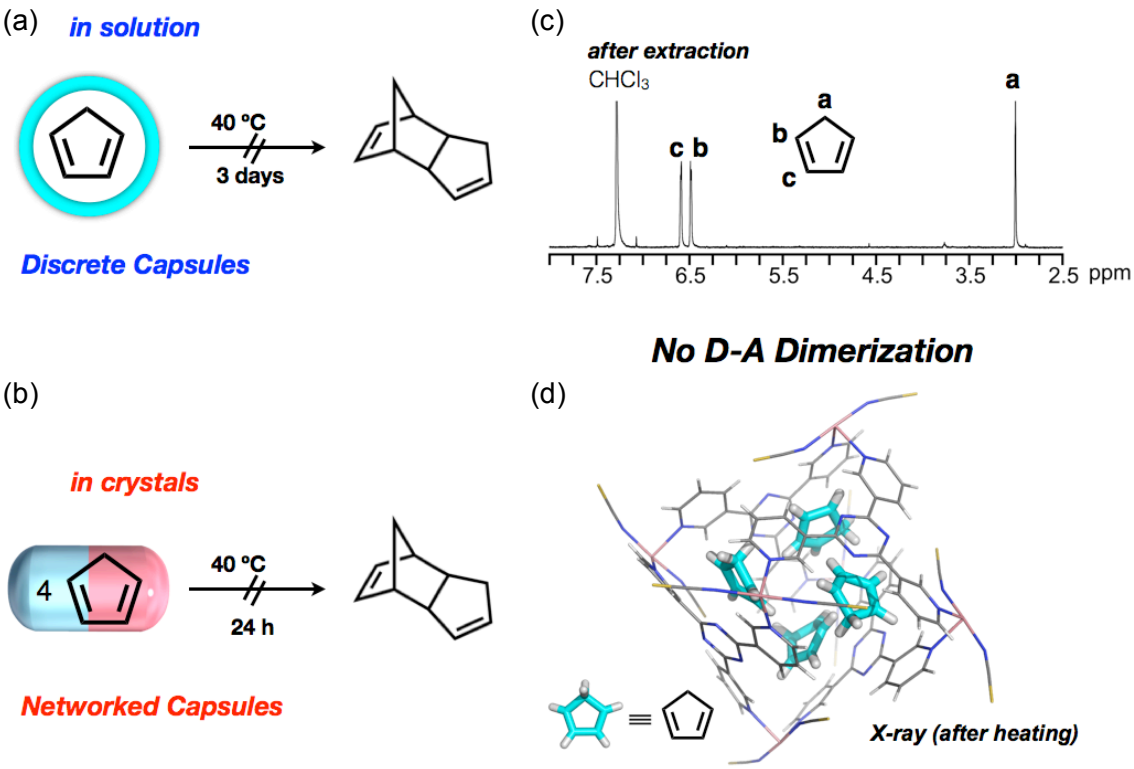

Figure 4.6. Schematic presentation for suppression of D-A dimerization in (a) solution capsule **1⊃9** and (b) crystalline capsules **2⊃(9)$_4$**; (c) the ^{1}H NMR (500 Mz, 300 K, $CDCl_3$) of **9** extracted from after inclusion complex **1⊃9** after heating for 3 days; (d) the X-ray structures of **2⊃(9)$_4$** after heating at 40 °C for 1 day (only one M_6L_4 capsule unit is shown in line models where guests **9** are shown in stick models).

4.5 *Control of Guest Delivery*

The *SCSC* guest exchange reaction as described in chapter 3 revealed that although the encapsulated guest molecules were strongly held within the cavity of capsule, the suitable guests triggered the replacement of former guests. Given this property, I expected that the solution and crystalline capsules could control the guest delivery. To my delight, the dynamic nature of hosts **1** and **2** are advantageous for controlled release of encapsulated guest molecules. When an aqueous solution of inclusion complex **1⊃9** was washed with chloroform, cyclopentadiene (**9**) was completely extracted into the organic phase. While guest **9** was not extracted with hexadecane, a poor guest for capsule. In a similar way, inclusion crystals **1⊃(9)**$_4$ also released guest **9** upon washing crystals with chloroform, although no guest elusion into the supernatant was observed by soaking crystals in hexadecane (Figure 4.7).

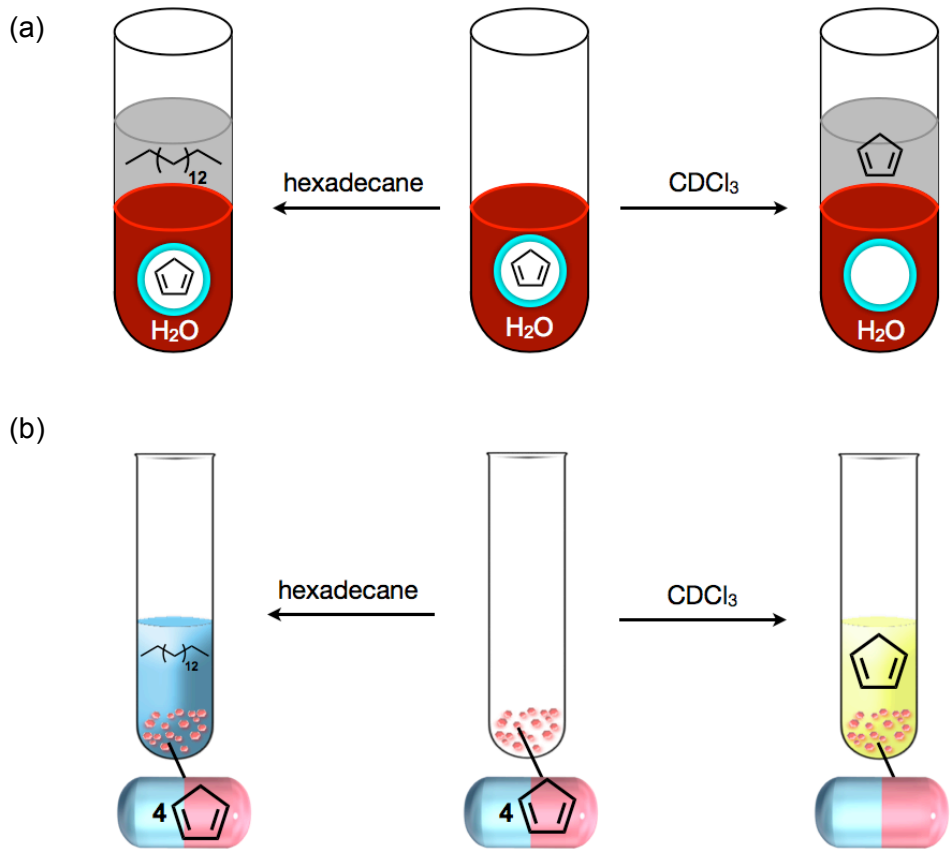

Figure 4.7. Schematic presentation for controlled release of cyclopentadiene (**9**) guests (a) solution capsule **1⊃9**; (b) crystalline capsule **2⊃(9)**$_4$.

4.7 *Suppression of Polymerization*

Acrylic acid and its ethers which are also known as acrylates, are volatile, reactive, toxic and odorous chemicals and widely used in surface coatings, textiles, fibers and adhesives.[49] The acrylates polymerize very easily under light or air condition, therefore the stabilizer (e.g. hydroquinone, or its monomethyl ether) is added to the commercial acrylates to prevent the undesired polymerization during the storage and transportation.

I have described above that the reactive guest, cyclopentadiene, is stabilized with the solution capsule **1** even after heating. Given this property of capsules, I envisioned that the light sensitive acrylates could be stable encapsulated within the capsule to give light-stable acrylates.

To test this, *tetr*-butyl acrylate (**10**) was tested with the solution capsules. Encapsulation of acrylates in solution was confirmed by upfield-shifted signals of *t*-butyl group in **10** at –1.33 ppm in ^{1}H NMR (Figure 4.8) (the olefin signals of encapsulated **10** were too broad to distinguish from the broad host signals). The guest **10** was stable within the cavity of solution host **1** even after UV light irradiation for 3 hours and polymer were not formed.

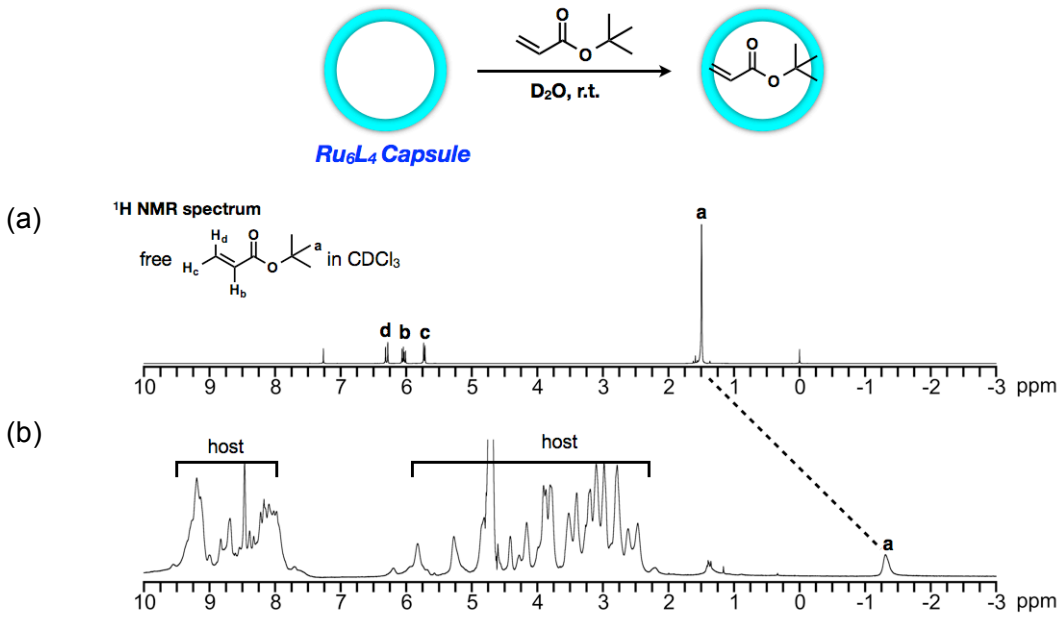

Figure 4.8. The ^{1}H NMR (500 Mz, 300 K) of (a) free t-butyl acrylate in $CDCl_3$; (b) inclusion complex **1⊃10** in D_2O.

The *tetr*-butyl acrylates (**10**) was introduced into the networked capsules **2** by soaking the as-synthesized crystals of **2⊃(7)$_4$** under neat conditions at r.t. for 1 week. During this process, the supernatant was replaced four times with a fresh guest solution, resulting in the acrylate-installed capsule network **2⊃(10)$_2$**.

The acrylates installation proceeded in a SCSC fashion, the penetration of acrylates guests into crystals were clearly confirmed by IR analysis, the stretching of C=O appeared as intense peak at 1719 for **10** (Figure 4.9).

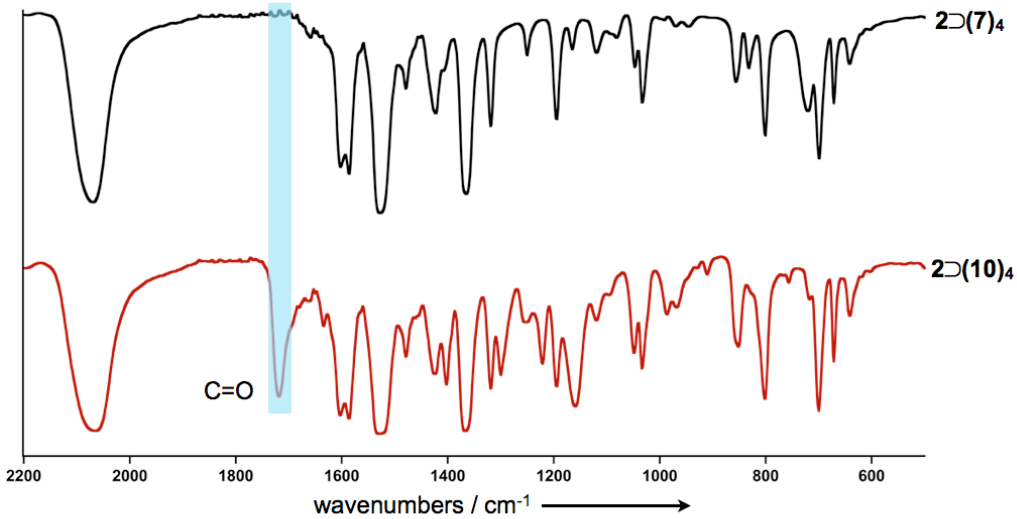

Figure 4.9. IR analysis of black, **2⊃(7)$_4$**; red, **2⊃(10)$_2$**.

The existence of acrylates guest in capsules was confirmed by the X-ray crystallographic analysis and it clearly revealed that four molecules of **10** are tightly packed via CH–π and Van de Waals interactions with **3-TPT** walls, and π–π interaction with N=C=S ligand in each capsule unit (Figure 4.10). In addition, the adjacent vinyl groups are well-separated with a center-to-center distance of 4.76 Å suggesting the suppression of polymerization within the capsule.

To my delight, the acrylates **10** within the networked capsules are stable toward UV light and do not undergo the photo-induced polymerization. After washing the as-synthesized crystals **2⊃(10)$_2$** with hexadecane to remove the surplus amount of guests **10** in the pores (see experimental section for details), I exposed the crystals **2⊃(10)$_2$** to UV light for 3 h. The ^{1}H NMR analysis of the guests, which are digested with HCl aq., and extracted with $CDCl_3$ indicated polymerization of **10** did not proceeded within crystals and monomer of **10** were recovered (Figure S4.9c).

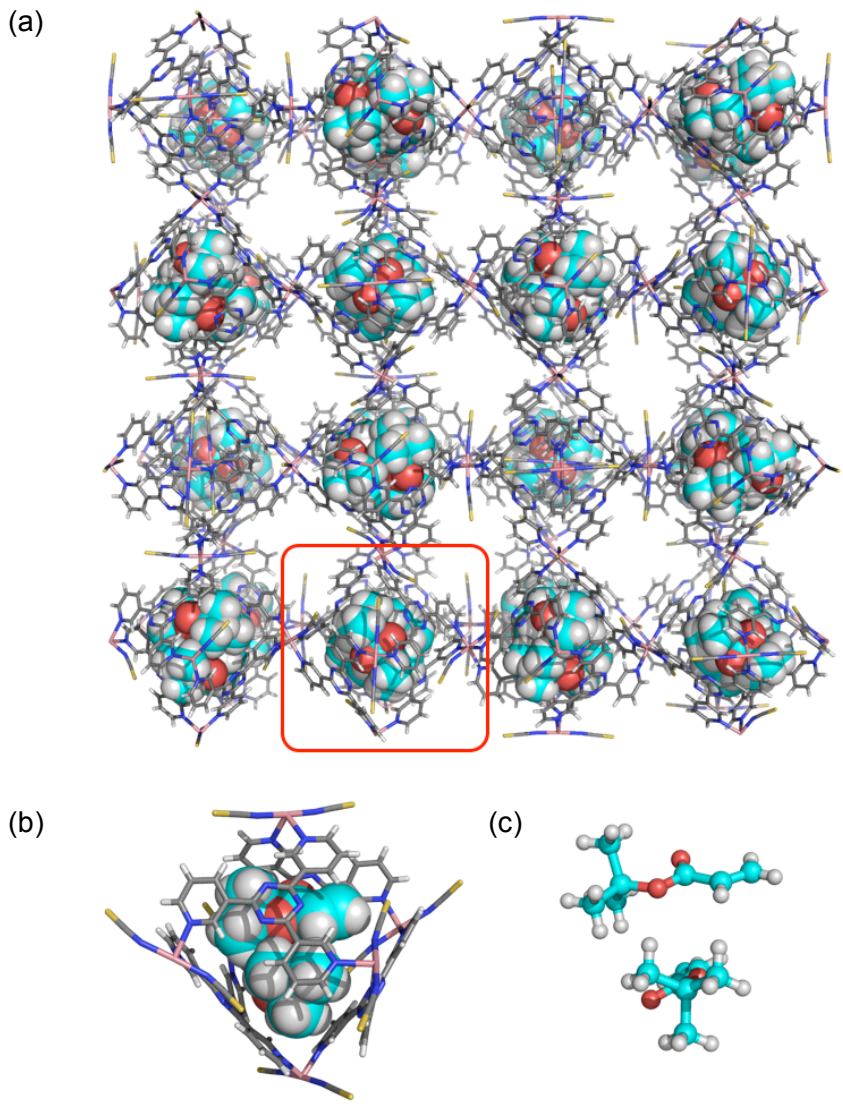

Figure 4.10. X-ray structures of **2⊃(10)$_2$** (a) networked structure; (b) stick models of one M_6L_4 capsule unit where *t*-butyl acrylate guests are shown in CPK models; (c) the orientation of *t*-butyl acrylate guests are shown in ball-stick models.

In control experiment, the acrylates are readily polymerized by the UV irradiation. When a solution of **10** in toluene ([**10**] = 0.5 M, it is worthy noting that the concentration of acrylates in solution are both lower than that (0.66 M) in crystal) exposure to UV light for 3 h, the polymer-**10** were formed in 67 % conversion with a average molecular weight (determinated from HPLC analysis) $M_n = 1.00 \times 10^4$ (Figure S4.9b and 4.10).

4.7 *Conclusion and Limitation*

In summary, the detailed X-ray crystallographic analysis revealed that discrete Ru_6L_4 capsule **1** (solution host) was isostructural with repeated subunit in the networked Co_6L_4 capsules **2** (crystalline host) and similar host-guest interaction was observed including CH-π interactions, van der Waals interactions and hydrophobic effects. With a complementary pair of solution and solid capsules, the bridge of solution and solid-state chemistry was achieved: (1) Common guest encapsulation; (2) Guest screening (cyclic compound over acyclic ones) and suppression of volatility; (3) Suppression of D-A dimerization; (4) Control of guest delivery; (5) Suppression of polymerization.

In this thesis, I have expand the 'networking strategy' to dynamic capsule hosts, however, due to the intrinsic different between two capsules, especially cavity volume, there are some limitations or defects for bridging solution and the solid-state chemistry with these two dynamic capsules: (1) the inclusion number of guest is different, therefore the X-ray structure of host-guest complexes with crystalline capsule could not be quantitatively and precisely reflected back the host-guest complexes in solution. For instance, the guests are larger than the cavity of solution capsule **1** (not suitable for solution capsule) and smaller than that of crystalline capsules might be accommodated within the networked capsules **2**. (2) The mechanism of reactivity control of cyclopentadiene is different, for networked capsules, the restrict orientation of cyclopentadiene guests is the reason for suppression of dimerization while for discrete capsule, only one cyclopentadiene guest is isolated so that the dimerization could not happen.

Although these limitations exist, I would like to emphasize this research is still important and valuable: (1) it proves that the 'networking strategy' is an effective and universal approach for constructing either rigid or flexible (dynamic) a pair of solution and crystalline metallo-organic hosts. (2) it allows us to design and transfer novel properties of solution hosts into the solid-state, and vice versa. (3) it open another way for developing the MOFs or PCPs chemistry, the incorporation of host cavity into pores structure would bring new functions into MOFs or PCPs.

4.8 *Experimental Section*

- **General procedures**

Solvent and reagents were purchased from TCI, WAKO Pure Chemical Industries, Furuya metal Co., Ltd. or Sigma-Aldrich. All chemicals were used without any further purification except where noted. ^{1}H, ^{13}C and 2D NMR spectra were recorded on Bruker DRX-500 (500 MHz) spectrometers. All the NMR spectra were collected at 300 K, and chemical shifts were reported as the delta scale in parts per million (ppm) relative to an internal standard, tetramethylsilane (δ = 0.00 ppm for ^{1}H and ^{13}C NMR). IR measurements were carried out as KBr pellets using a DIGILAB FTS7000 instrument. Thermo gravimetric analysis was performed on a STA 409 PG/T equipped with a QMS 403C/T (NETZSCH). Elemental analysis was performed on a YANACO MT-6. Single crystal X-ray diffraction data were made using a BRUKER APEX-Ⅱ /CCD diffractometer equipped with a focusing mirror (MoK_{α} radiation λ = 0.71073 Å) and a N_2 generator (Japan Thermal Eng. Co., Ltd.). UV irradiation was performed with an HB400X-23 450-W high-pressure mercury lamp (SEN LIGHTS CORP) and SUPERCURE-203S UV light source (SAN-EI ELECTRIC). Analytical HPLC–GPC chromatograms were recorded on a JASCO UV-970 spectrometer equipped with a JASCO PU-980 pump using a TSKgel G2500Hxl column (eluent: tetrahydrofuran (HPLC grade, WAKO)).

- **Synthesis and characterization**

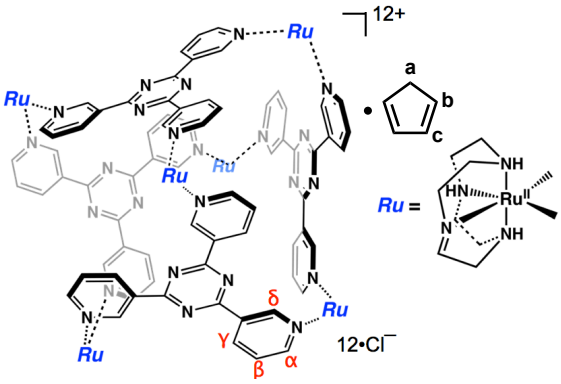

Preparation of cyclopentadiene inclusion complex 1⊃9: To a 6 mM D_2O solution of **1** (500 μL), 10 μl of liquid cyclopentadiene (**9**) was added. After stirring for 30 min, surplus of the guest was evaporated at 60 ºC. The host-guest complex **1⊃9** was directly analysed by NMR spectroscopy.

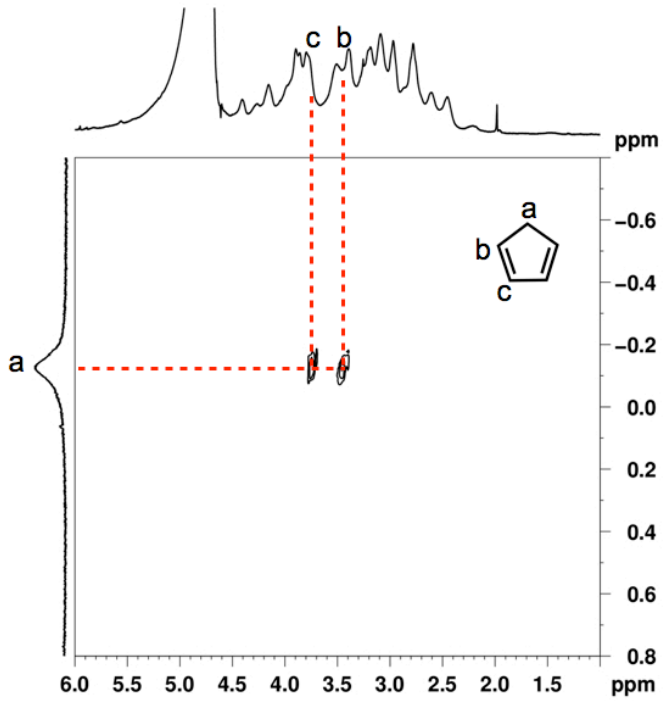

Figure S4.1. COSY NMR spectra (D_2O, 300K) of **1⊃9** spectra (only the correlation of encapsulated cyclopentadiene was shown) (Form SI of *Chem. Asian J.* **2013**, *8*, 2596. Reprinted with permission of Wiley-VCH)

Encapsulation of cyclopentane within networked capsule 2: As-synthesized **2⊃(7)$_4$** (60 mg) was immersed in 2 ml of cyclopentane at 60 ºC for 4 d, during that time the supernatant was replaced with fresh guests three times. After filtration, crystals were directly analysed by X-ray diffraction and elemental analysis.

Encapsulation of *tetr*-butyl acrylate with networked capsules 2: As-synthesized **2⊃(7)$_4$** (40 mg) was immersed in *t*-butyl acrylate (**10**) (1 mL) and allowed to stand at room temperature for 1 week during which the supernatant was replaced four times with a freshly acrylates by decantation. The crystals were collected by filtration to give inclusion complex **2⊃(10)$_2$** quantitatively.

THF inclusion complex 2⊃(4)$_4$: Elemental analysis (%): calculated for $\{[(Co(NCS)_2)_3(m\text{-TPT})_4]\bullet 11.0(\mathbf{4})\}_n$: C 57.07, H 5.34, N 16.36; found: C 57.36, H 5.25, N 16.52.

Cyclopentane inclusion complex 2⊃(5)$_4$: Elemental analysis (%): calculated for $\{[(Co(NCS)_2)_3(m\text{-TPT})_4]\bullet 7.0(\mathbf{5})\}_n$: C 59.91 H 5.25, N 18.55; found: C 59.86, H 5.43, N 18.32.

Cyclopentane inclusion complex 2⊃(6)$_4$: Elemental analysis (%): calculated for $\{[(Co(NCS)_2)_3(m\text{-TPT})_4]\bullet 7.0(\mathbf{6})\}_n$: C 60.98 H 5.63, N 17.78; found: C 61.32, H 5.92, N 17.61.

***Tetr*-butyl acrylate-installed networked capsules 2⊃(10)$_2$:** Elemental analysis: calculated for $\{[(Co(NCS)_2)_3(\mathbf{3\text{-}TPT})_4]\bullet 5.0(\mathbf{10})\}_n$: C 56.19, H 4.51, N, 17.40; found: C 56.39, H 4.67, N 17.29. IR (KBr): 3391 (m), 3063 (m), 2978 (m, C-H), 2065 (s, SCN), 1719 (s, C=O), 1587 (s), 1526 (s), 1479 (m), 1424 (m), 1366 (s), 1317 (m), 1195 (m), 1159 (s), 1031 cm^{-1} (m).

Remove guests in the pores: As-synthesized networked capsules crystals **2⊃(10)$_2$** (40 mg) were soaked in 1 mL hexadecane and the supernatant was replaced four times with pure hexadecane at 30 min interval. The crystals were collected by filtration to give after washed crystals sample. Elemental analysis: calculated for

$\{[(Co(NCS)_2)_3(\mathbf{3\text{-}TPT})_4]\bullet 1.5(\mathbf{10})(C_{16}H_{34})_5\}_n$: C 65.30, H 7.68, N, 13.56; found: C 65.39, H 7.88, N 13.42.

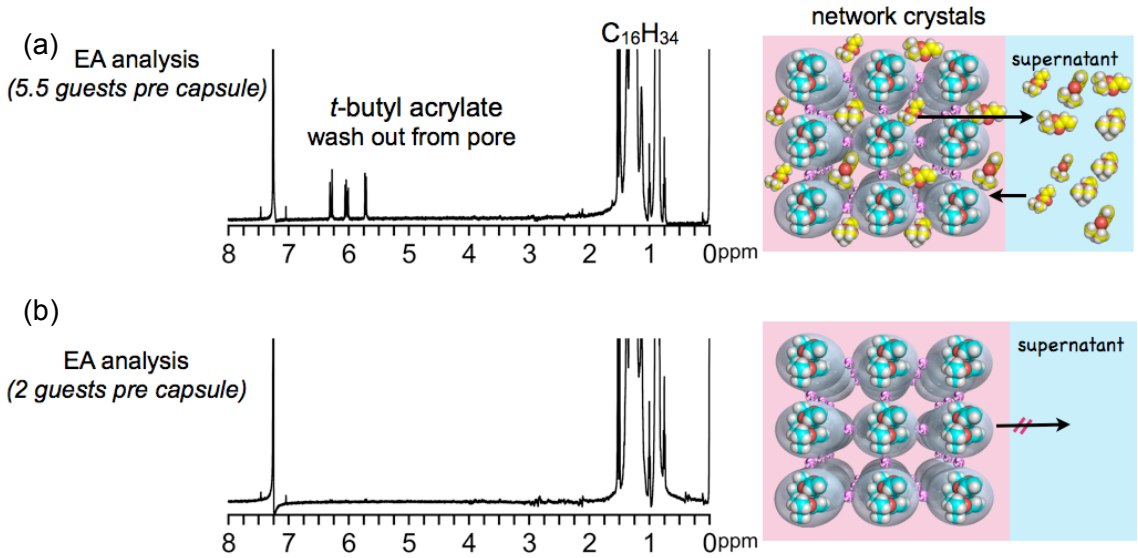

Figure S4.2. (left) ^{1}H NMR spectra ($CDCl_3$, 300 K) of aliquots of the supernatants in contact with (a) **2⊃(10)$_2$** and (b) after washed sample **2⊃(10)$_2$** (see above procedure). (right) Two cartoons showing that guests **10** in the pore readily washed out, but those in the capsules are not extracted by washing with hexadecane

- **Controlled release of cyclopentadiene in solution and crystalline capsule**

For the solution capsule: To a 6 mM D_2O solution of inclusion complex **1⊃9** (500 μL), 500 μL of $CDCl_3$ or hexadecane was added to form biphasic system. After stirring for 1 min, the water layer was directly analysed by ^{1}H NMR spectroscopy.

For the crystalline capsules: The crystals of inclusion complex **2⊃(9)$_4$** (20 mg) was immersed into 1 mL of $CDCl_3$ or hexadecane for 4 hours. After filtration, the crystals were digested by 5 M HCl and organic residuals were extracted with $CDCl_3$. The $CDCl_3$ layer was directly analyzed by ^{1}H NMR spectroscopy

- **Accommodation of linear and cyclic hydrocarbons**

According to the experimental procedure for cyclopentadiene encapsulation, linear (*n*-pentane and *n*-hexane) and cyclic (cyclopentane (**5**) and cyclohexane (**6**)) hydrocarbons were accommodated into capsule **1**.

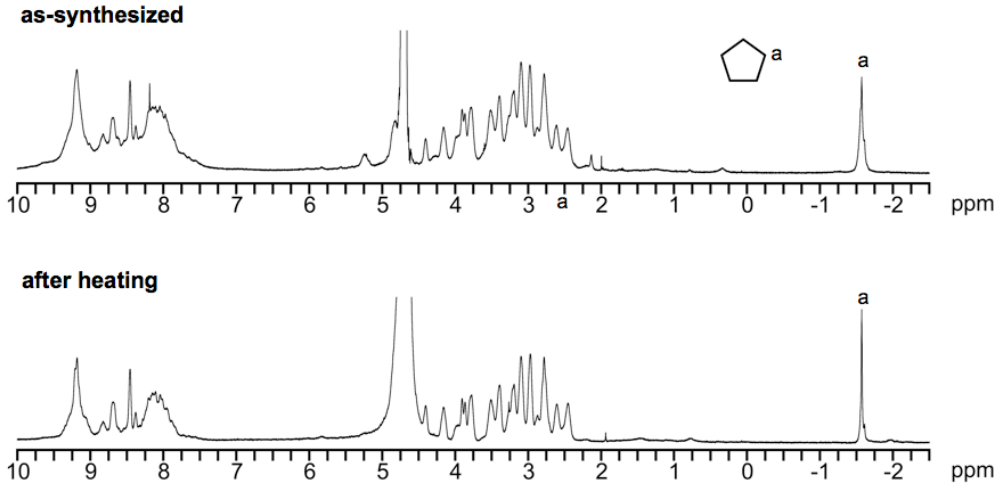

Figure S4.3. ^{1}H NMR (500 MHz, D_2O, 300 K) spectra of cyclopentane inclusion complex **1⊃5** (top: as-synthesized, bottom: after heating at 60 ºC for 1 h) (Form SI of *Chem. Asian J.* **2013**, *8*, 2596. Reprinted with permission of Wiley-VCH.)

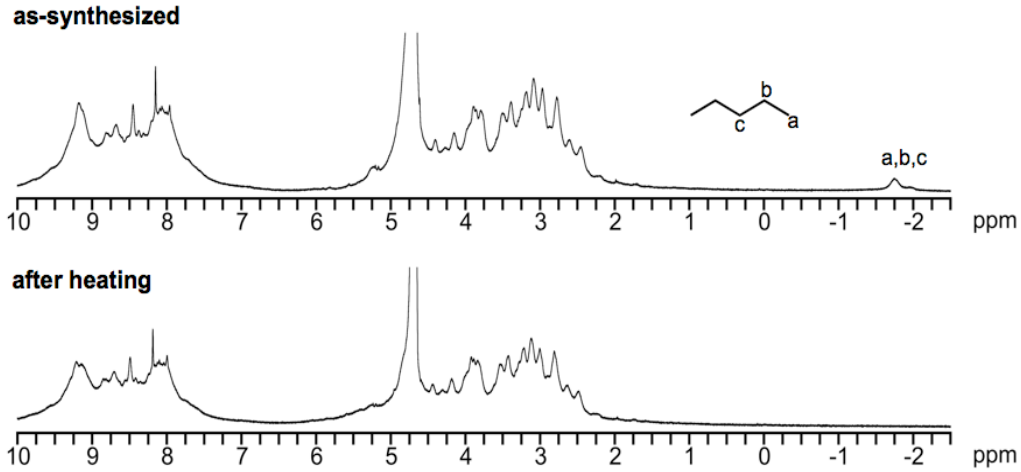

Figure S4.4. ^{1}H NMR (500 MHz, D_2O, 300 K) spectra of *n*-pentane inclusion complex **1⊃*n*-pentane** (top: as-synthesized, bottom: after heating at 60 ºC for 1 h) (Form SI of *Chem. Asian J.* **2013**, *8*, 2596. Reprinted with permission of Wiley-VCH)

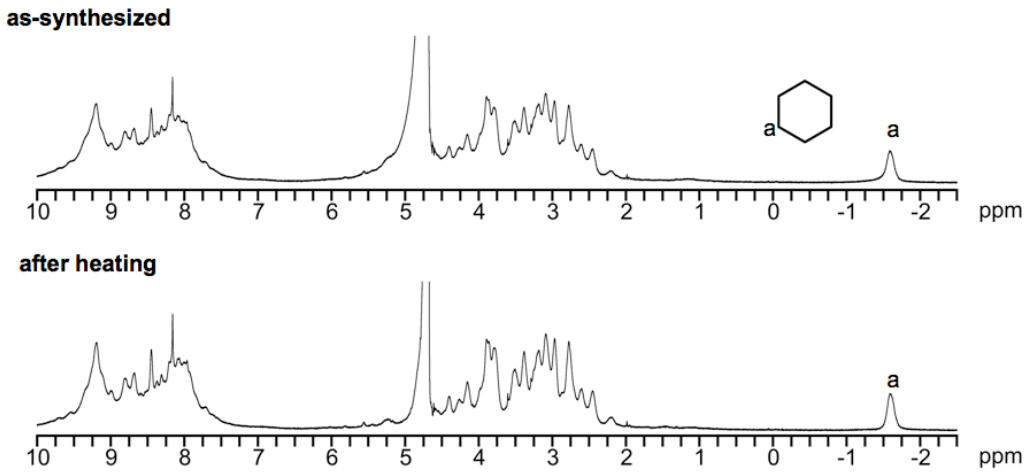

Figure S4.5. ^{1}H NMR (500 MHz, D_2O, 300 K) spectra of cyclohexane inclusion complex **1⊃6** (top: as-synthesized, bottom: after heating at 60 ºC for 1 h) (Form SI of *Chem. Asian J.* **2013**, *8*, 2596. Reprinted with permission of Wiley-VCH)

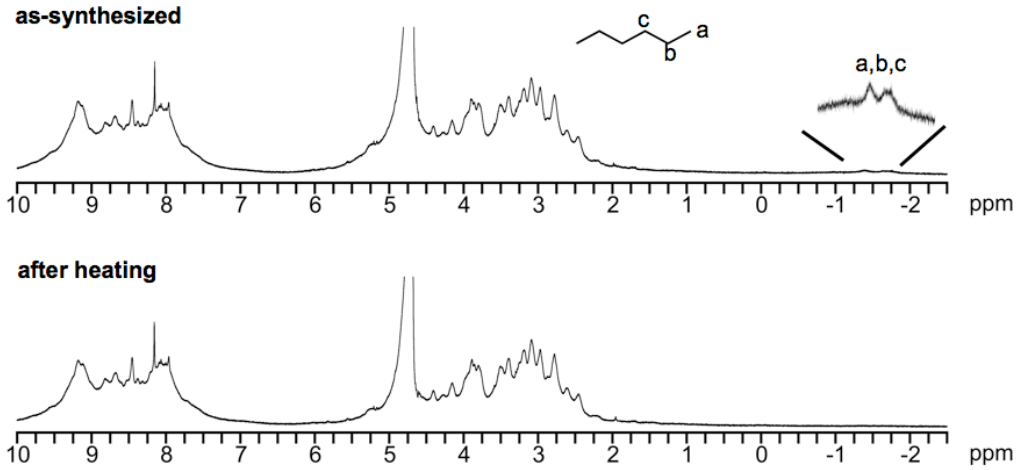

Figure S4.6. ^{1}H NMR (500 MHz, D_2O, 300 K) spectra of *n*-hexane inclusion complex **1⊃*n*-hexane** (top: as-synthesized, bottom: after heating at 60 ºC for 1 h) (Form SI of *Chem. Asian J.* **2013**, *8*, 2596. Reprinted with permission of Wiley-VCH)

- **Suppression of volatility of guests in networked capsule crystal**

The crystals of **2⊃(5)**$_4$ or **2⊃(6)**$_4$ was heated at 100 ºC for 1 d under open-air condition, and then the crystals were digested with HCl aq. (5 M) and extracted with $CDCl_3$. The organic layer was directly analysed by NMR spectroscopy. For TG-DSC measurement the crystals of **2⊃(5)**$_4$ or **2⊃(6)**$_4$was heated at 100 ºC for 6 h under reduced pressure using oil pump.

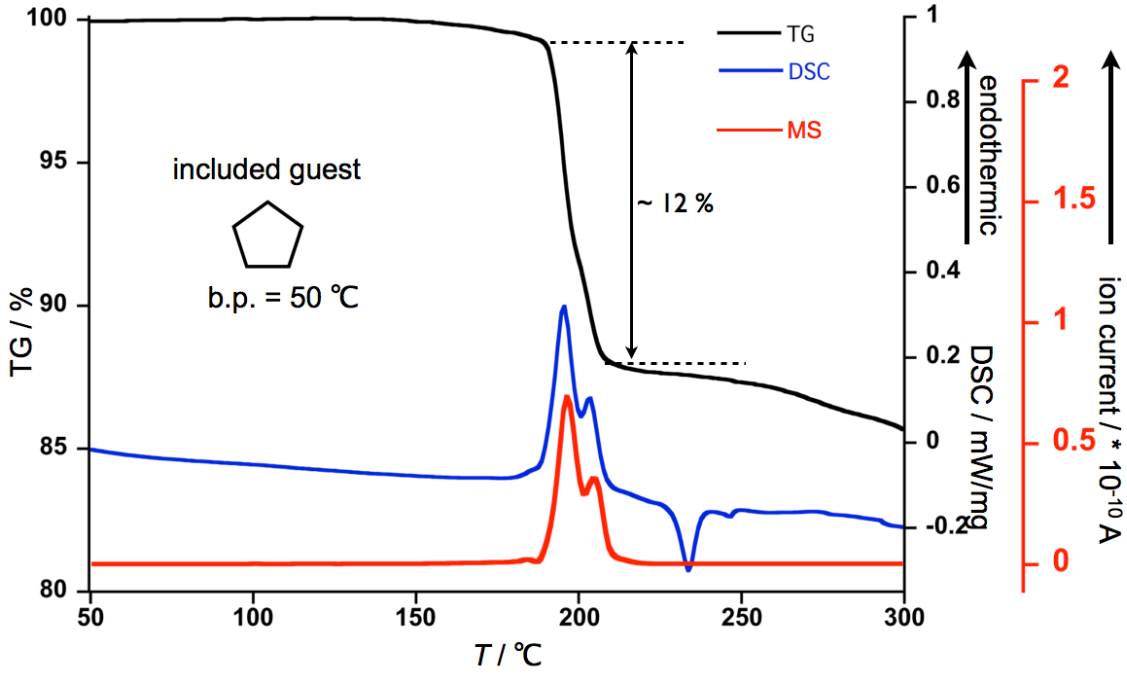

Figure S4.7. TG-DSC curves of cyclopentane complex **2⊃(5)**$_4$. (black: TG, blue: DSC, and red: mass signal intensity at *m/z* = 70) (Form SI of *Chem. Asian J.* **2013**, *8*, 2596. Reprinted with permission of Wiley-VCH)

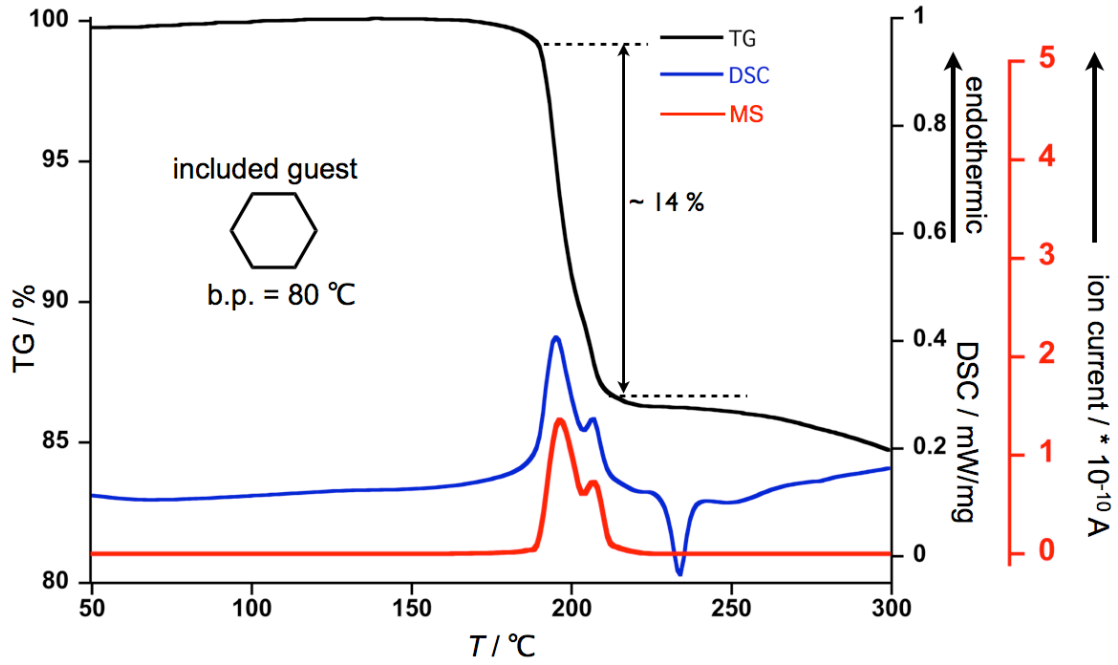

Figure S4.8. TG-DSC curves of cyclohexane complex **2⊃(6)**$_4$. (black: TG, blue: DSC, and red: mass signal intensity at *m/z* = 84)

- **Comparison of selected bond length and angle of two capsules**

Table S4.1. Selected bond length and angle

	Discrete Ru_6L_4 capsule	Networked Co_6L_4 capsules
M-M (Å)[a]	11.13–11.42, (11.27)	11.06–11.35, (11.25)
M-N_{Py} (Å)[b]	2.09–2.11, (2.10)	2.17–2.21, (2.19)
∠ N_{py}-M-N_{py}(°)[c]	85.63–86.51, (86.08)	90.86–92.08, (91.27)

[a,b]the range of the distances and average value was shown in (); [b]the range of the angle and average value was shown in ().

- **Cavity calculation**

The size of the inner cavity volumes of **1** and **2** were determined using VOIDOO calculations. The calculations were based on the crystal structure of **1⊃4** and **2⊃(4)$_4$**. A virtual probe with a radius of a radius of 1.4 Å (set by default, water-sized) was employed for **1** and **2** (Due to the large pore size of **2**, four benzene molecules were used to block the pores and prevent the probe from "falling out" of the inner sphere),[44] and the following parameters were changed from their default settings:

Maximum number of volume-refinement cycles: 30
Minimum size of secondary grid: 3
Grid for plot files: 0.1
Primary grid spacing: 0.1
Plot grid spacing: 0.1

- **The hν irradiation of acrylates in crystal**

The after washed crystals **2⊃(10)** $_2$ (40 mg) were added into 10 mL test tube, and then stood under hν irradiation (high-pressure mercury lamp from SEN LIGHTS CORP) at r.t. for 3 hours. Then, the acrylates guests were extracted with $CDCl_3$ after the decomposition of crystals with 5 M HCl, the extracted solution was analyzed by ^{1}H NMR method (Figure S4.9).

- **Control experiment of polymerization in solution**

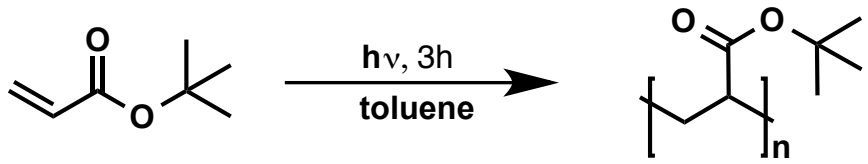

General procedures: The mixture of *t*-butyl acrylate (**10**) (64 mg, 0.5 mmol) and toluene (1 mL) were added into a 10 mL test tube and stood under hν irradiation (high-pressure mercury lamp from SEN LIGHTS CORP) at r.t. for 3 hours. The solvent and unreacted methyl acrylate monomer was evaporated and the polymer-**10** was obtained as colorless oil (46 mg, yield 67%). The averaged molecular weight of polymer-**10** (M_n = 1.00 × 10^4) was determinated by HPLC. ^{1}H NMR (500 MHz, $CDCl_3$): δ (ppm) 2.24 (br s, -CH-), 1.84 (br s, -CH_2-), 1.58-1.44 (br s, -CH_2-) and 1.44 (br s, -$C(CH_3)_3$)[50].

- **HPLC and NMR analyses**

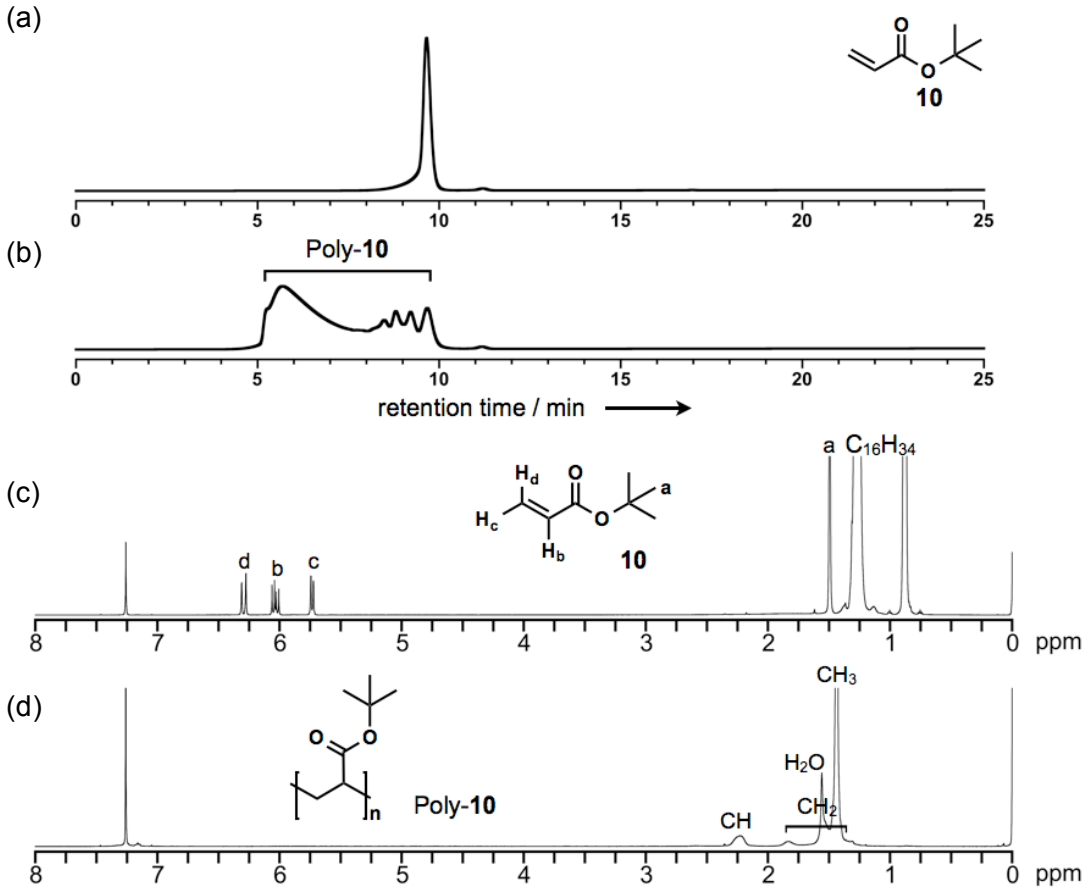

Figure S4.9. HPLC analysis of (a) pure **10**; (b) polymer-**10** using a TSKgel G2500HxI column. ^{1}H NMR spectra ($CDCl_3$, 300 K) of (c) **10** extracted from after washed simple **2⊃(10)$_2$** after hv irradiation; (d) polymer-**10**.

Averaged molecular weights of polymers were calculated from the calibration curve (Figure S6.4) obtained with a series of TSK Standard Polystyrenes (TOSOH) using a TSKgel G2500Hxl column (eluent: tetrahydrofuran (HPLC grade, WAKO)).

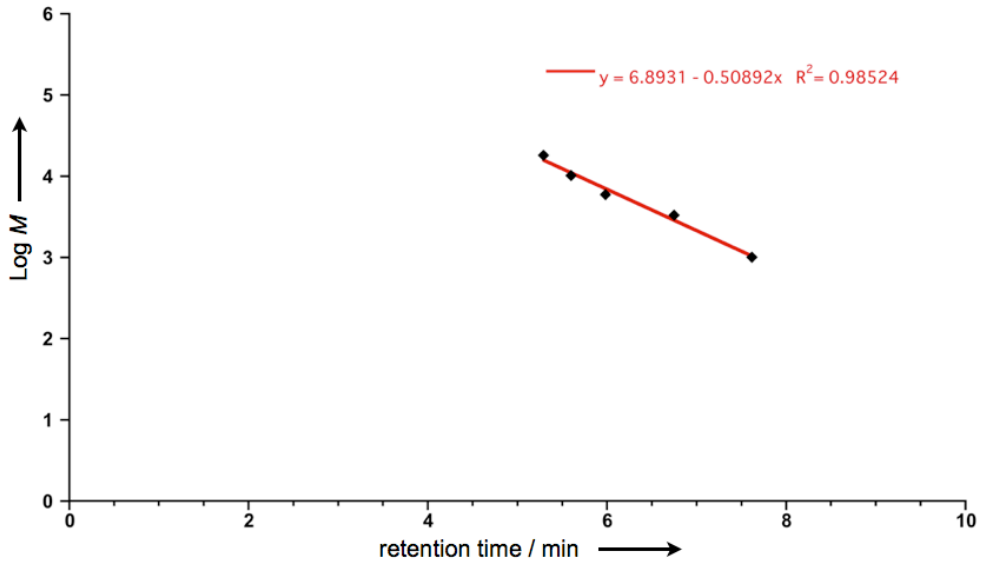

Figure S4.10. Calibration curve of TSKgel G2500Hxl column using TSK Standard Polystyrene.

- **X-ray crystallographic data**

Compound code	**2⊃(4)$_4$**	
Empirical formula	$C_{26}H_{16}N_{10}CoS_2 \bullet C_4H_8O$	
Formula weight	663.64	
Temperature	90(2) K	
Wavelength	0.71073 Å	
Crystal system	Cubic	
Space group	*Fd-3c*	
Unit cell dimensions	a = 63.8953(10) Å	α = 90°
	b = 63.8953(10) Å	β = 90°
	c = 63.8953(10) Å	γ = 90°
Volume	260860(7) Å^3	
Z	192	
Density (calculated)	0.811 g/cm^3	
Absorption coefficient	0.417 cm^{-1}	
F(000)	65472	
Crystal size	0.36 × 0.32 × 0.27 mm^3	
Theta range for data collection	2.21 to 26.42°	
Index ranges	-69≦ h ≦80, -38≦ k ≦80, -60≦ l ≦80	
Reflection collected	164654	
Independent reflections	11207	
Completeness to theta = 26.42	100 %	
Data / restraints / parameters	11207 / 444 / 160	
Goodness-of-fit on F2	2.078	
Final R indices [I > 2sigma(I)]	R_1 = 0.1319, wR_2 = 0.4200	
R indices (all data)	R_1 = 0.1616, wR_2 = 0.4646	
Largest diff. peak and hole	1.830 and -1.406 e. Å^3	

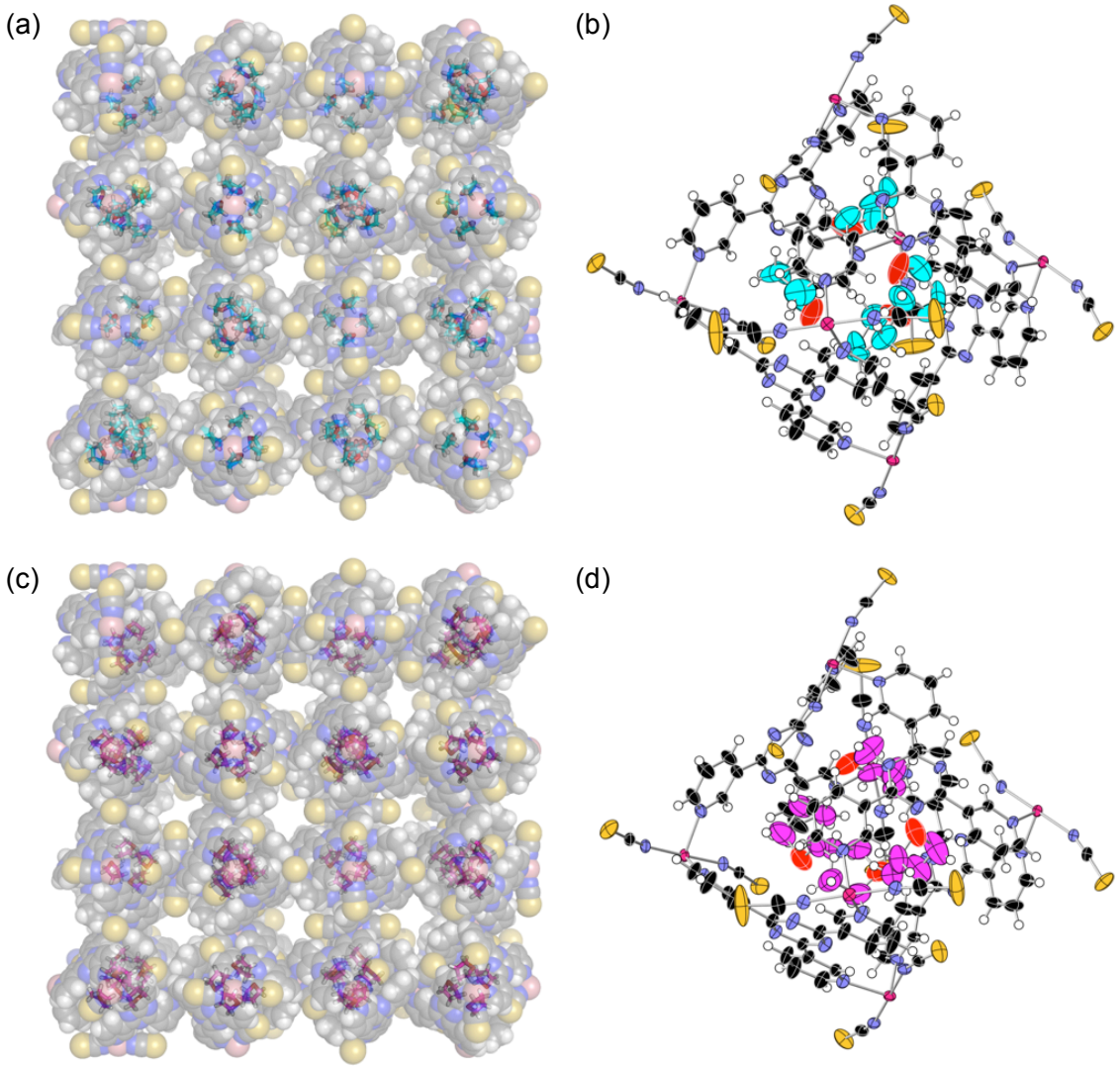

Figure S4.11. Crystal structure of networked capsules **2⊃(4)$_4$** of (a) crystal packing of disorder A; (b) ORTEP (50 % probability) drawing of one capsule unit (THF guests are drawn in cyan colour and occupancy is 48 %); (c) crystal packing of disorder B; (b) ORTEP (50 % probability) drawing of one capsule unit (THF guests are drawn in magenta colour and occupancy is 52 %).

Compound code	**2⊃(5)$_4$**	
Empirical formula	$C_{26}H_{16}N_{10}CoS_2 \bullet C_5H_{10}$	
Formula weight	661.69	
Temperature	90(2) K	
Wavelength	0.71073 Å	
Crystal system	Cubic	
Space group	*Fd-3c*	
Unit cell dimensions	a = 64.0734(17) Å	α = 90°
	b = 64.0734(17) Å	β = 90°
	c = 64.0734(17) Å	γ = 90°
Volume	263047(12) Å^3	
Z	192	
Density (calculated)	0.802 g/cm^3	
Absorption coefficient	0.412 cm^{-1}	
F(000)	65472	
Crystal size	0.36 × 0.32 × 0.28 mm^3	
Theta range for data collection	1.56 to 26.56°	
Index ranges	-49≦ h ≦80, -62≦ k ≦80, -54≦ l ≦80	
Reflection collected	167579	
Independent reflections	11457	
Completeness to theta = 26.56	100 %	
Data / restraints / parameters	11457 / 398 / 0	
Goodness-of-fit on F2	1.874	
Final R indices [I > 2sigma(I)]	R_1 = 0.1029, wR_2 = 0.3644	
R indices (all data)	R_1 = 0.1280, wR_2 = 0.4156	
Largest diff. peak and hole	1.726 and -0.780 e. Å^3	

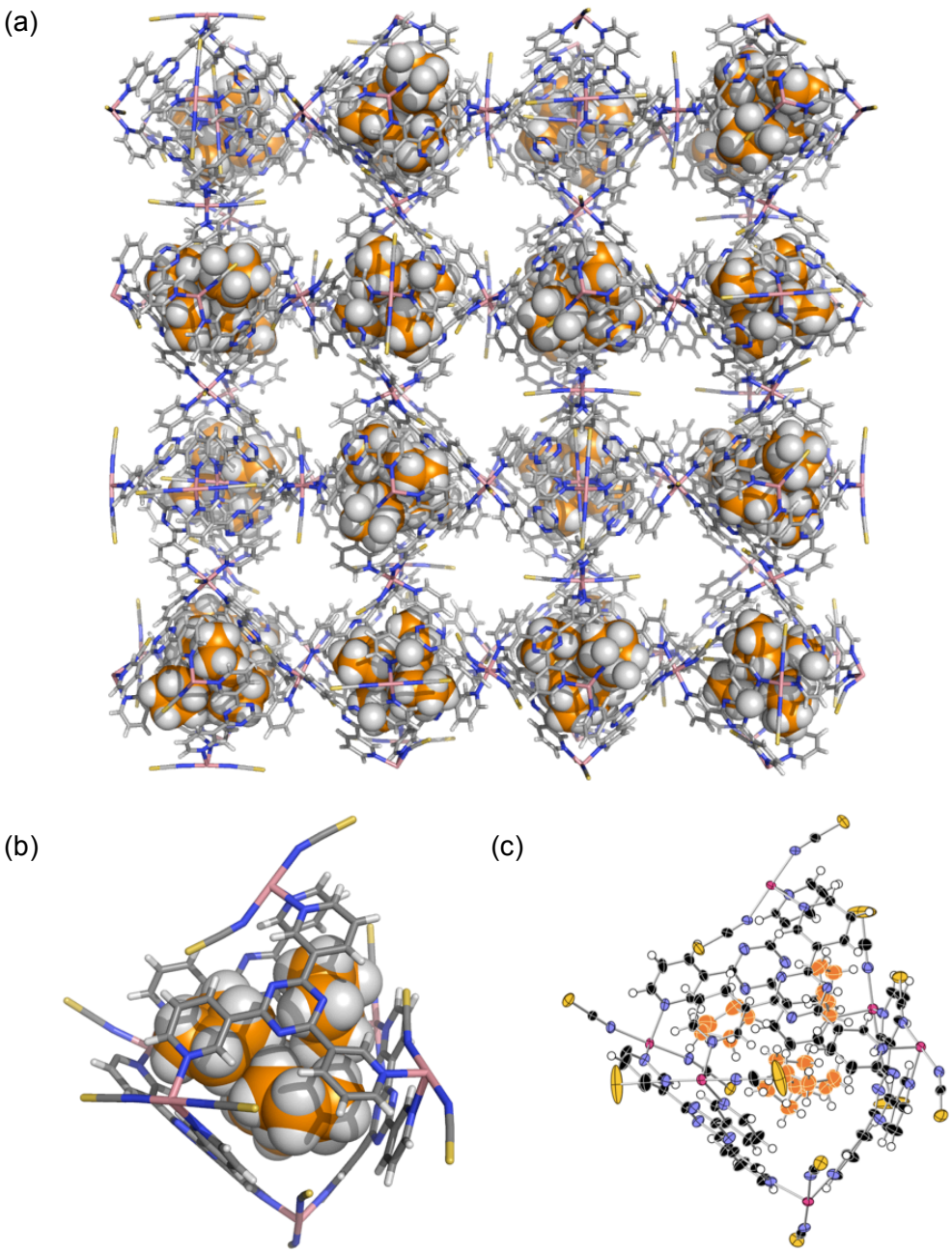

Figure S4.12. Crystal structure of networked capsules **2⊃(5)$_4$** of (a) networked structure; (b) one capsule was drawn as stick model where four cyclopentane guests was shown as CPK model; (c) ORTEP (50 % probability) drawing of one capsule unit. (cyclopentane guests are drawn in orange colour)

Compound code	**2⊃(10)$_2$**	
Empirical formula	$C_{26}H_{16}N_{10}CoS_2$•0.5($C_7H_{12}O_2$)	
Formula weight	1311.28	
Temperature	90(2) K	
Wavelength	0.71073 Å	
Crystal system	Cubic	
Space group	*Fd-3c*	
Unit cell dimensions	a = 64.235(6) Å	α = 90°
	b = 64.235(6) Å	β = 90°
	c = 64.235(6) Å	γ = 90°
Volume	265042(74) Å^3	
Z	96	
Density (calculated)	0.789 g/cm^3	
Absorption coefficient	0.410 cm^{-1}	
F(000)	64512.0	
Crystal size	0.35 × 0.33 × 0.28 mm^3	
Theta range for data collection	0.90 to 26.41°	
Index ranges	-80≦ h ≦39, -80≦ k ≦30, -80≦ l ≦80	
Reflection collected	169138	
Independent reflections	11370	
Completeness to theta = 26.42	100 %	
Data / restraints / parameters	11368 / 434 / 209	
Goodness-of-fit on F2	2.469	
Final R indices [I > 2sigma(I)]	R_1 = 0.1363, wR_2 = 0.3916	
R indices (all data)	R_1 = 0.1920, wR_2 = 0.4204	
Largest diff. peak and hole	1.840 and -0.831 e. Å^3	

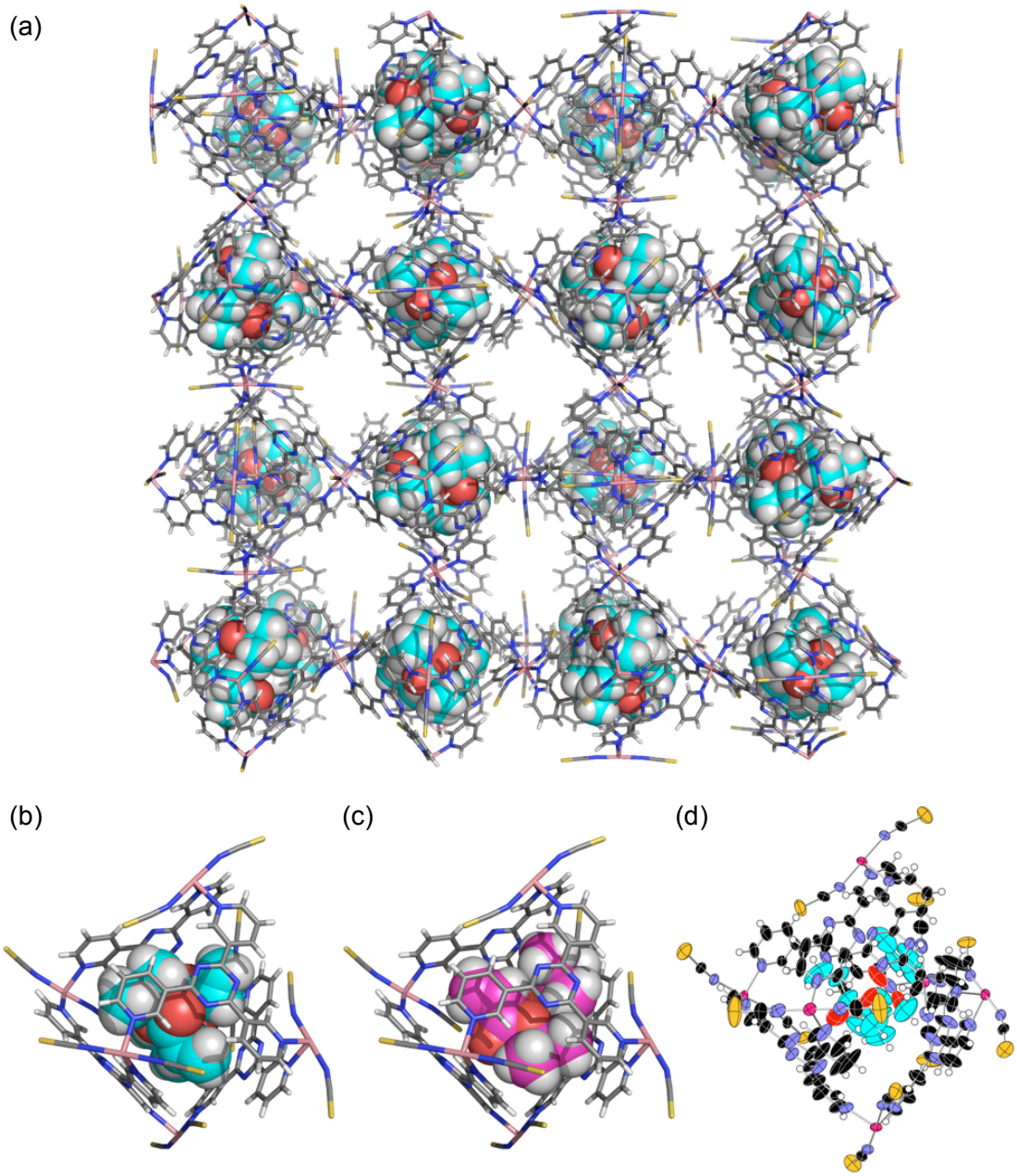

Figure S4.13. Crystal structure of networked capsules **2⊃(10)**$_2$ of (a) networked structure; Stick models of one M_6L_4 capsule unit where *tert*-butyl acrylate guests are shown in CPK models (b) disorder A in 50 % occupancy; (c) disorder B in 50 % occupancy; (d) ORTEP (50 % probability) drawing of one capsule unit. (*tert*-butyl acrylate guests are drawn in cyan colour)

Chapter 5

CH_3NCS-installed Crystalline Reagent

In this chapter I have utilized the advantages of networked capsules and bring a new idea of **'Crystalline Reagent'** for stable storage and easy handling of troublesome reagents. A highly volatile reagent, CH_3NCS, was pre-installed into networked capsules **2** in a single-crystal-to-single-crystal fashion to give crystalline reagent capsules. The tight encapsulation completely prevented reagent molecules from leaching out into the supernatant, however, introduction of aromatic amines into the crystals triggered the delivery of the CH_3NCS. Due to steric protection of the reagent by the capsules, enhanced substrate selectivity was observed in crystalline state thiocarbamoylation.

5.1 *Introduction*

Troublesome reagents, such as explosive, toxic and volatile ones, require special care during use in synthesis. Chemists are aware that if such reagents can be employed as stable, harmless solid, they would make a big contribution for synthetic chemistry. The polymer-supported reagents seems one of the solutions, however, this method has several disadvantages: (1) it is very hard to achieve exact stoichiochemistry of reactants due to the wide weight distribution of polymer; (2) different reaction needs different type of polymer-supporter; (3) it is impossible to visualize the interaction between reagent and polymer-supporter.[51] On the other hand, the chemical reactions have recently explored in the solid-state with porous coordination networks (PCNs). However, in most cases, the substrates are covalently or non-covalently fixed on the networked frameworks,[52] therefore the products cannot be isolated unless the complexes is decomposed. Through the studies in Chapter 3 and 4, the networked capsules **2** have unique properties: (1) Since the networked capsules **2** are composed of M_6L_4 capsule host units, it can act as crystalline host to accommodate guests in single-crystal-to-single-crystal (SCSC) fashion; (2) Due to the well isolation of guest molecules from external environment, the volatility of encapsulated guests (i.e. cyclopentane) is suppressed and reactivity of installed chemicals (i.e. cyclopentadiene and tetr-butyl acrylate) is controlled; (3) Due to the dynamic nature of capsule, the delivery of included guest molecules is controlled. Given these advantages of networked capsules **2**, I have an idea of 'crystalline reagent' where the reagents are pre-installed in the networked capsules **2** and desired products can be obtained by simply passing organic substrates through the pores. Such reagent-installed networked capsules are particularly useful if troublesome reagents (e.g. volatile, metastable, toxic, or explosive ones) are stably pre-installed.

In this chapter, I have introduced CH_3NCS, a highly volatile reagent, into networked capsule to give a CH_3NCS-installed capsule network that acts as non-volatile crystalline reagent and the thiourea products are readily obtained by passing the aromatic amines through the pores. In addition, the selective thiocarbamoylation in the crystalline state is achieved due to the steric protection of CH_3NCS guests by capsules.

5.2 Synthesis and Characterization

A highly volatile reagent, CH_3NCS (**11**), was introduced into the networked capsules **2** by soaking the as-synthesized crystals of **2** in saturated hexadecane solution of **11** at r.t. for 3 d. During this process, the supernatant was replaced three times with a fresh guest solution. The surplus of guests **11** remaining in the interstitial pores was washed out by treating the crystals with fresh hexadecane for 4.5 h, resulting in the reagent-installed capsule network **2⊃(11)$_4$**.

The reagent installation proceeded in SCSC fashion, and the X-ray crystallographic analysis clearly revealed that four molecules of **11** are tightly packed via CH–π and π–π interactions with **3-TPT** walls in each capsule unit. It is worthy to note that no electron density as assignable to **11** is found in the interstitial pores. These observations are in good accordance with inductively coupled plasma (ICP) analysis that determined the atomic ratio of Co/S = 1:3. Elemental analysis agreed with the formula of $\{[(Co(NCS)_2)_3(\mathbf{3\text{-}TPT})_4]\bullet\ (\mathbf{11})_3\bullet(C_{16}H_{34})_x\}_n$ (x ~ 5), indicating the presence of four molecules of **11** per capsule.

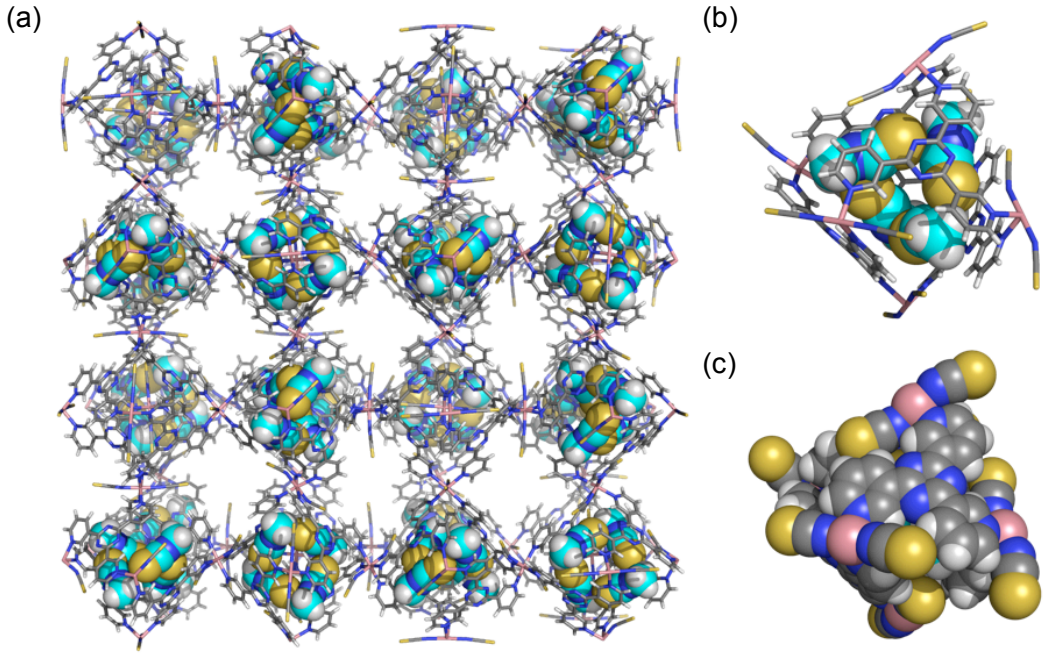

Figure 5.1. X-ray structures of **2⊃(11)$_4$** (a) networked structure; (b) stick models of one M_6L_4 capsule unit where CH_3NCS guests are shown in CPK models; (c) CPK model of one M_6L_4 capsule unit.

5.3 *Suppression of Volatility*

The X-ray data also suggested the guests **11** were well covered by the capsule walls, the strong encapsulation effect was confirmed by leaching tests of **2⊃(11)$_4$**. (1) Most importantly, guest **11** did not leach out into the supernatant after washing the crystals of **2⊃(11)$_4$** with hexadecane, a poor guest for networked capsules **2** (Figure S5.1). (2) Exposure of crystals **2⊃(11)$_4$** (*ca*. 150 mg, containing *ca.* 10 mg of **11**) to air at r.t. for 3 d caused only a very small change (<1%) in Co/S ratio. The suppressed volatility of encapsulated **11** is in striking contrast to the highly volatile nature of neat **11**: 10 mg of solid **11** sublimated within 30 min under the same conditions. (3) Thermogravimetric–differential scanning calorimetry–mass spectrometry (TG–DSC–MS) analysis indicated that guest **11** remained encapsulated up to 200 ºC; after a gentle 32 wt% loss due to the evaporation of the hexadecane solvent in the pore, a steep weight loss with a sharp endothermic peak was recorded at 205 ºC where encapsulated guest **11** (~7 wt%) were released from network **2** (Figure 5.2).

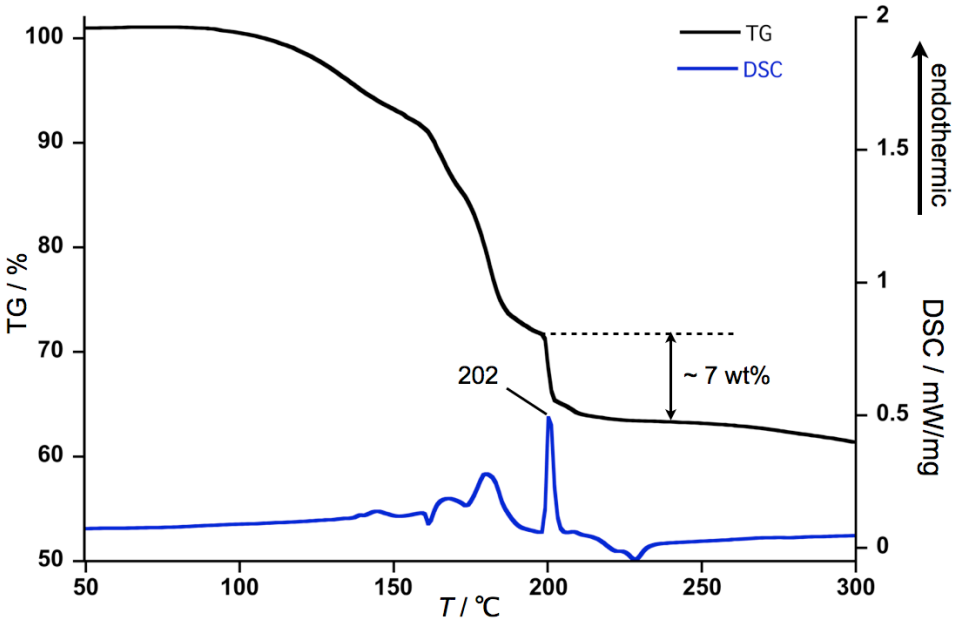

Figure 5.2. TG-DSC curves of **2⊃(11)$_4$**. (N_2 flow rate: 30 mL/min, rate of temperature increase: 5 K/min)

5.4 *Selective Thiocarbamoylation of Amines in Crystalline State*

In Chapter 4, I found although the guests were indeed strongly hold by capsules, the suitable guests or solvent (*i.e.* $CDCl_3$) could trigger the delivery of former guests. Given this result, I expected that the suitable reactant (guests) could trigger the delivery of pre-installed gusts **11** and react with them.

To my delight, the introduction of aromatic amines into the crystals indeed triggered the delivery of the encapsulated reagent **11**, and the thiocarbamoylation smoothly proceeded. Therefore the networked complex **2⊃(11)$_4$** acted as a useful crystalline reagent that can switch on upon substrate uptake.

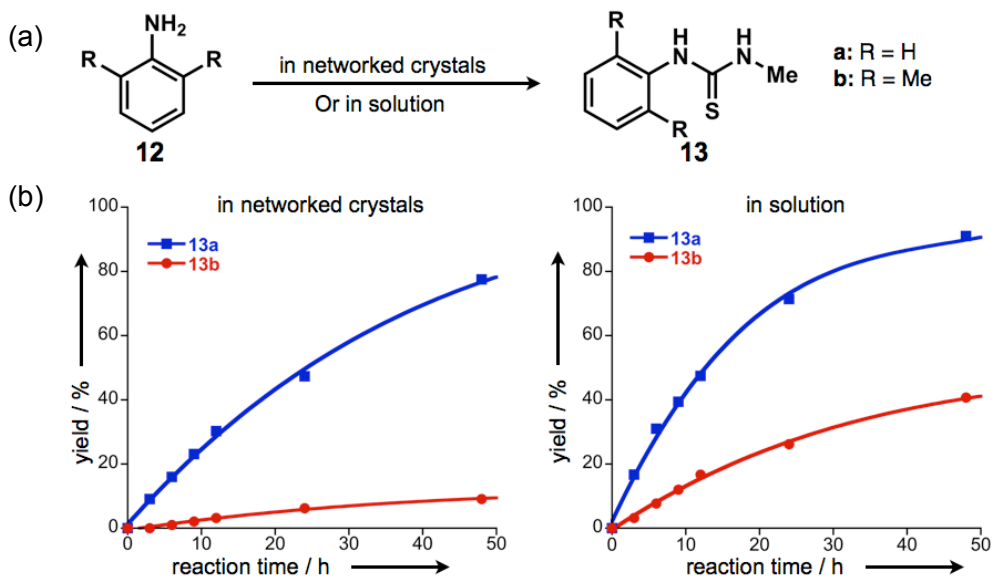

Figure 5.3. (a) Synthesis of thiourea in networked crystals of **2⊃(11)$_4$**. Product yield versus reaction time profiles (b) in networked crystals of **2⊃(11)$_4$** and (c) in solution. Initial conditions: [**12**]$_0$ = 0.24 M and [**11**]$_0$ = 0.36 M (for solution reaction). For crystalline state reactions, 1.5 equiv. of CH_3NSC was added as its inclusion complex **2⊃(11)$_4$**. The yield was determined by ^{1}H NMR spectroscopy. (From *Angew. Chem. In. Ed.* **2012**, *51*, 2379. Reprinted with permission from Wiley-VCH.)

When crystals of **2⊃(11)$_4$** were soaked in a hexadecane solution of aniline (**12a**) (0.24 M, 0.75 equiv. to CH_3NCS), **12a** was quickly enclathrated into the pores of **2**, concomitant with crystal color change from pale red to deep orange, and the thioureas were produced in situ. After 72 h, the resultant crystals were filtered, digested with HCl aq., and extracted with CH_2Cl_2 to give 1-methyl-3-phenylthiourea (**13a**) in 91%

yield. In the supernatant, neither reagent **11** nor product **13a** was detected by ^{1}H NMR spectroscopy. Thus the reaction took place only in the networked crystals.

Since the aperture size of capsule is confined, I expect the substrate selectivity can be enhanced by the steric protection of capsule. To exclude the substrate selectivity is derived from pore, the test of the selectivity of interstitial pore was preformed. The as-synthesized crystals of **2⊃(7)$_4$** was used for this test: when crystals of **2⊃(7)$_4$** were soaked in a 1:1 solution of aniline (**12a**) and a bulky aniline, 2,6-dimethylaniline (**12b**), the system reached equilibrium within 1 h, and more than 80% of the substrates were got into the crystals in almost 1:1 ratio.

Although the networked capsule **2** enclathrate **12b** as quickly as **12a**, a remarkable decrease in the reaction rate of **12a** was observed. The thioure **13b** was formed only in 11% yield after 72 h. The plot of reaction time vs. conversion allowed me to estimate the k_{11a}/k_{11b} ratio to be 10.9 (Figure 5.3b). This value is considerably larger than that in a standard solution reaction (k_{11a}/k_{11b} = 4.3; Figure 5.3c),[53] indicating that networked capsules **2⊃(11)$_4$** notably discriminate the difference in the steric bulkiness around the amino group of the substrates.

The competition experiment revealed clearer results: when a 1:1 mixture of **12a** and **12b** was treated with crystals **2⊃(11)$_4$**, thioureas **13a** and **13b** were initially formed in a 91:9 ratio, in contrast to a control experiment in solution that resulted in a 73:27 mixture (Figure S5.4). Since the inclusion of the amines into the interstitial pores of **2** is non-selective, the observed substrate selectivity is attributable to the steric protection of **11** by the capsules.

Scheme 5.1. Selective formation of thiourea **15** in networked crystals **2**

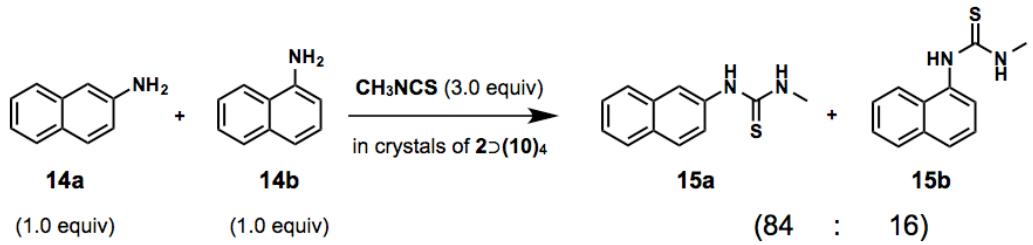

In addition, networked reagent capsules **2⊃(11)$_4$** were also able to discriminate substrate with different shape around amine group, such as 2- and 1-naphthylamine (**14a** and **14b**) in the thiocarbamoylation. When the crystals of **2⊃(11)$_4$** were immersed in an equimolar solution of **15a** and **15b**, corresponding thioureas **15a** and **15b** were

formed in 84:16 ratio over the initial 10 h (Scheme 5.1 and Figure S5.5). In contrast, the selectivity of the thiocarbamoylation in solution was very poor (**15a**:**15b** = 58:42).

Finally, I emphasize that capsule network **2** is reusable. After extraction of the products with thiophene/MeOH, reagent **11** could be reloaded into the capsule by the same procedure, and almost the same product selectivity was obtained with the recycled reagent capsules.

5.5 *Conclusion*

In summary, the networked capsules **2** can act as crystalline host to accommodate CH_3NCS, a highly volatile reagent, in a single-crystal-to-single-crystal fashion. The X-ray crystallographic analysis revealed that four CH_3NCS guests were tightly packed within the cavity of capsule, as a consequence, installed CH_3NCS guests cannot be released from capsule even washed crystals with solvent or heated up 200 ºC. To my surprise, the introduction of aromatic amine into the crystals triggered the delivery of the CH_3NCS guests. The CH_3NCS-installed capsule network is much milder reagent than the neat CH_3NCS and the enhancement of substrate selectivity is observed in the crystalline state thiocarbamoylation. Given these results, the networked capsules are promising for stable storage and easily handling of troublesome chemicals.

5.6 *Experimental Section*

- **General procedure**

Solvent and reagents were purchased from TCI, WAKO Pure Chemical Industries or Sigma-Aldrich. All the chemicals were used without any further purification except where noted. ^{1}H and ^{13}C NMR spectra were recorded on Bruker DRX-500 (500 MHz) spectrometers. All the NMR spectra were collected at 300 K, and chemical shifts were reported as the detal scale in parts per million (ppm) relative to an internal standard, tetramethylsilane (δ = 0.00 ppm for ^{1}H and ^{13}C NMR). IR measurements were carried out as KBr pellets using a DIGILAB FTS7000 instrument. Thermogravimetric analysis was performed on a SAT 409 PG/T equipped with a QMS 403C/T (NETZSCH). Elemental analysis was performed on a YANACO MT-6. ICP measurement was performed on an ICPA 6300 ICP Spectrometer (Thermo Scientific Co., Ltd.). Single crystal X-ray diffraction data were collected on a BRUKER APEX-II CCD diffractometer equipped with a focusing mirror (MoKα radiation λ = 0.71073 Å) and a N_2 generator (Japan Thermal Eng. Co., Ltd.).

- **Synthesis and characterization**

Preparation of networked capsules 2⊃(11)$_4$: As-synthesized **2⊃(7)$_4$** (200 mg) was immersed in a saturated hexadecane solution of CH_3NCS (**11**) (3 mL) and allowed to stand at room temperature for 3 d during which the supernatant was replaced three times with a freshly prepared solution of **11** by decantation. The crystals were separated by filtration (to give unwashed sample A). Subsequently the crystals were soaked in 3 mL of hexadecane and the supernatant was replaced eight times with pure hexadecane at 30 min interval. The crystals were then filtered and air-dried on the filter funnel for 15 min to give inclusion complex **2⊃(11)$_4$** quantitatively.

Elemental analysis: calculated for $\{[(Co(NCS)_2)_3(\mathbf{3\text{-}TPT})_4]\bullet 3.0(\mathbf{11})\bullet 5.0(C_{16}H_{34})\}_n$: C 63.01, H 7.32, N, 14.79; found: C 63.17, H 7.14, N 15.16. IR (KBr): 3369 (m), 3059 (m), 2924 (s), 2853 (s) 2060 (s, SCN), 1586 (s), 1525 (s), 1426 (m), 1365 (s), 1318 (m), 1194 (m), 1029 cm^{-1} (m).

General procedure for crystalline state reaction using networked reagent capsules 2⊃(11)$_4$: To a 0.24 M hexadecane solution of an aromatic amine (0.24 mL) in a 5 mL glass vial, was added inclusion complex **2⊃(11)$_4$** (*ca.* 80 mg, containing 77 μmol of CH_3NCS (**11**)). The mixture was shaken by hand for 1-2 min, and then allowed to stand at room temperature. After digestion of crystal with diluted HCl aq., the aqueous phase was neutralized with sat. $NaHCO_3$ and the reaction products were extracted with CH_2Cl_2. The organic phase was dried over Na_2SO_4, and the solvent was removed by rotary evaporator. The residual material was analyzed by ^{1}H NMR to determine the conversion yield. Pure thiourea was obtained by chromatography on silica gel.

- **Characterization of new compounds**

1-(2,6-dimethylphenyl)-3-methylthiourea (13b): R_f = 0.3 (eluent: hexane/ethyl acetate = 6:4). ^{1}H NMR (500 MHz, $CDCl_3$): δ (ppm) 7.24 (br s, 1H, NH), 7.21 (t, J = 7.5 Hz, 1H, Ar-*p*-H), 7.15 (d, J = 7.5 Hz, 2H, Ar-*m*-H), 5.38 (br s, 1H, NH), 3.11 (d, J = 5 Hz, 3H, -NH-CH_3), and 2.26 (s, 6H, Ar-CH_3); ^{13}C NMR (125 MHz, $CDCl_3$): δ 182.2 (NCS), 137.8, 133.4, 129.4, 129.3, 32.4, and 18.5. IR (KBr, cm^{-1}) 3354 (s), 3227 (s), 2989 (m), 2956 (m), 1554 (s), 1461 (m), 1256 (m), 1130 (m), and 887 (m). MALDI-TOF mass (negative mode, matrix: 9-nitroanthracene) *m/z* calcd for $C_{10}H_{14}N_2O$:

193.09 [M–H]$^-$; found: 193.07. Elemental analysis (%): calcd for $C_{10}H_{14}N_2S$: C 61.82, H 7.26, N 14.42; found: C 61.87, H 7.49, N 14.37.

1-(2-naphthyl)-3-methylthiourea (15a): R_f = 0.2 (eluent: CH_2Cl_2). ^{1}H NMR (500 MHz, $CDCl_3$): δ (ppm) 7.92 (d, J = 8.5 Hz, 1H, H^h), 7.87 (d, J = 8.0 Hz, 1H, H^g), 7.82 (d, J = 8.0 Hz, 1H, H^d), 7.75 (br s, 1H, NH^b), 7.67 (s, 1H, H^c), 7.54 (m, 2H, overlapping H^e and H^f), 7.30 (d, J = 8.5 Hz, 1H, H^i), 6.13 (br s, 1H, NH^a), and 3.17 (d, J = 5 Hz, 3H, NH-*CH₃*); ^{13}C NMR (125 MHz, $CDCl_3$): δ 181.6 (NCS), 133.7, 137.6, 131.9, 130.3, 127.8, 127.7, 127.1, 126.6, 123.7, 123.2, and 32.1. IR (KBr, cm^{-1}) 3320 (s), 1550 (s), 1467 (m), 1321 (m), 1140 (m), 1050 (m), and 864 (m). MALDI-TOF mass (negative mode, matrix: 9-nitroanthracene) *m/z* calcd for $C_{12}H_{11}N_2S$: 215.06 [M–H]$^-$; found: 214.86. Elemental analysis (%): calcd for $C_{12}H_{12}N_2S$: C 66.63, H 5.59, N 12.95; found: C 66.52, H 5.69, N 12.79.

1-(-naphthyl)-3-methylthiourea (15b): Recrystallized from EtOH. ^{1}H NMR (500 MHz, $CDCl_3$): δ (ppm) 8.01 (d, J = 7.5 Hz, 1H, H^f), 7.92 (m, 2H, overlapping H^i and H^e), 7.74 (bs, s, 1H, NH^b), 7.59 (m, 2H, overlapping H^g and H^h), 7.52 (t, J = 7.5 Hz, 1H, H^d), 7,45 (d, J = 7.5 Hz, 1H, H^c), 5.69 (br s, 1H, NH^a), 3.08 (d, J = 4.5 Hz, 3H, -NH-*CH₃*); ^{13}C NMR (125 MHz, $CDCl_3$): δ 182.6 (NCS), 134.7, 131.7, 130.1, 129.1, 128.5, 127.6, 127.2, 125.8, 125.5, 122.6, 32.2 (CH_3, N-CH_3). IR (KBr, cm^{-1}) 3279 (s), 3149 (s), 1540 (s), 1438 (m), 1274 (m), 1152 (m), 1047 (m), and 877 (m). MALDI-TOF mass (negative mode, matrix: 9-nitroanthracene) *m/z* calcd for $C_{12}H_{11}N_2S$: 215.06 [M–H]$^-$; found: 214.94. Elemental analysis (%): calculated for $C_{12}H_{12}N_2S$: C 66.63, H 5.59, N 12.95; found: C 66.60, H 5.69, N 12.85.

- **Leaching Test**

Test procedure: Sample crystals (*ca*. 20 mg) was immersed in hexadecane (*ca*. 0.3 mL) for 30 min at r.t., and an aliquot (~ 50 μL) was taken from the supernatant, diluted with $CDCl_3$, and analyzed by ^1H NMR.

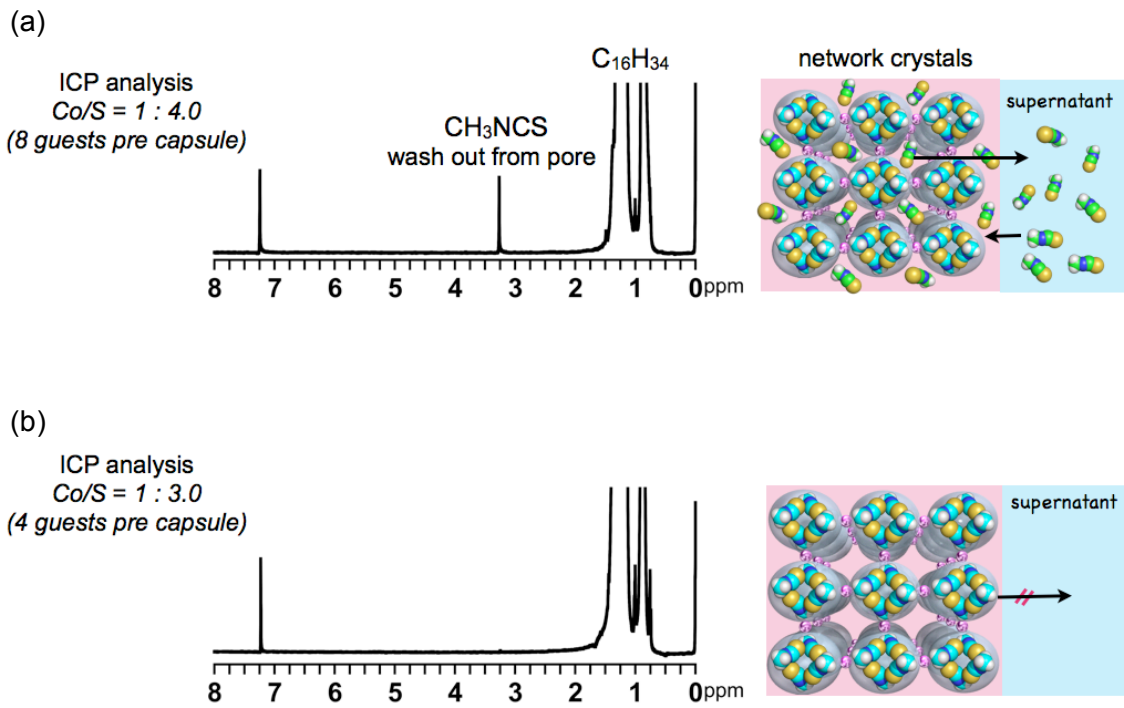

Figure S5.1. (left) ^1H NMR spectra ($CDCl_3$, 300 K) of aliquots of the supernatants in contact with (a) unwashed sample A (see above procedure) and (b) **2⊃(11)$_4$**. (right) Two cartoons showing that guests **11** in the pore readily leach out, but those in the capsules are not extracted by washing with hexadecane.

- **Comparison of initial reaction rates**

Crystalline state reactions

The reactions were carried out according to the General procedure for crystalline state reaction.

initial conditions: [aromatic amine]$_0$ = 0.24 M, network crystals **2⊃(11)$_4$** (38 mg toward 0.1 mL of aniline solution; *i.e.* 1.5 equiv. of CH_3NCS)

Solution reactions

The solution reactions were conducted in hexadecane at room temperature.

initial conditions: [aromatic amine]$_0$ = 0.24 M, [CH_3NCS] = 0.36 M

Kinetic rate constant k was determined using the equation:

$kt(a_0 - b_0) = \log[b_0(a_0 - x)/a_0(b_0 - x)]$

where, x: concentration of product, a_0 and b_0: initial concentrations of aniline and CH_3NCS, respectively.

In all runs, the plots t vs. $(a_0 - b_0)^{-1} \log[b_0(a_0 - x)/a_0(b_0 - x)]$ gave a good linear relationship, indicating that these reaction follow second-order kinetics during the early stages.

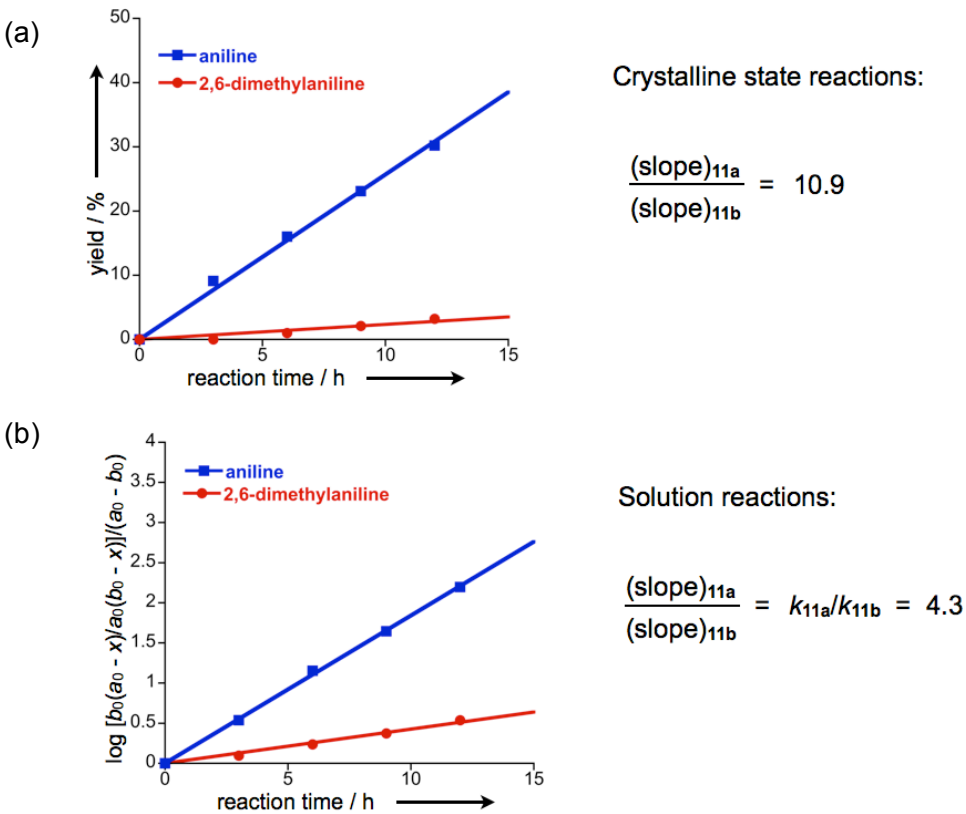

Figure S5.2. Estimation of initial relative rates for the reaction between aniline **12** and CH_3NCS (**11**) in (a) network **2** and (b) solution. (From SI of *Angew. Chem. In. Ed.* **2012**, *51*, 2379. Reprinted with permission from Wiley-VCH.)

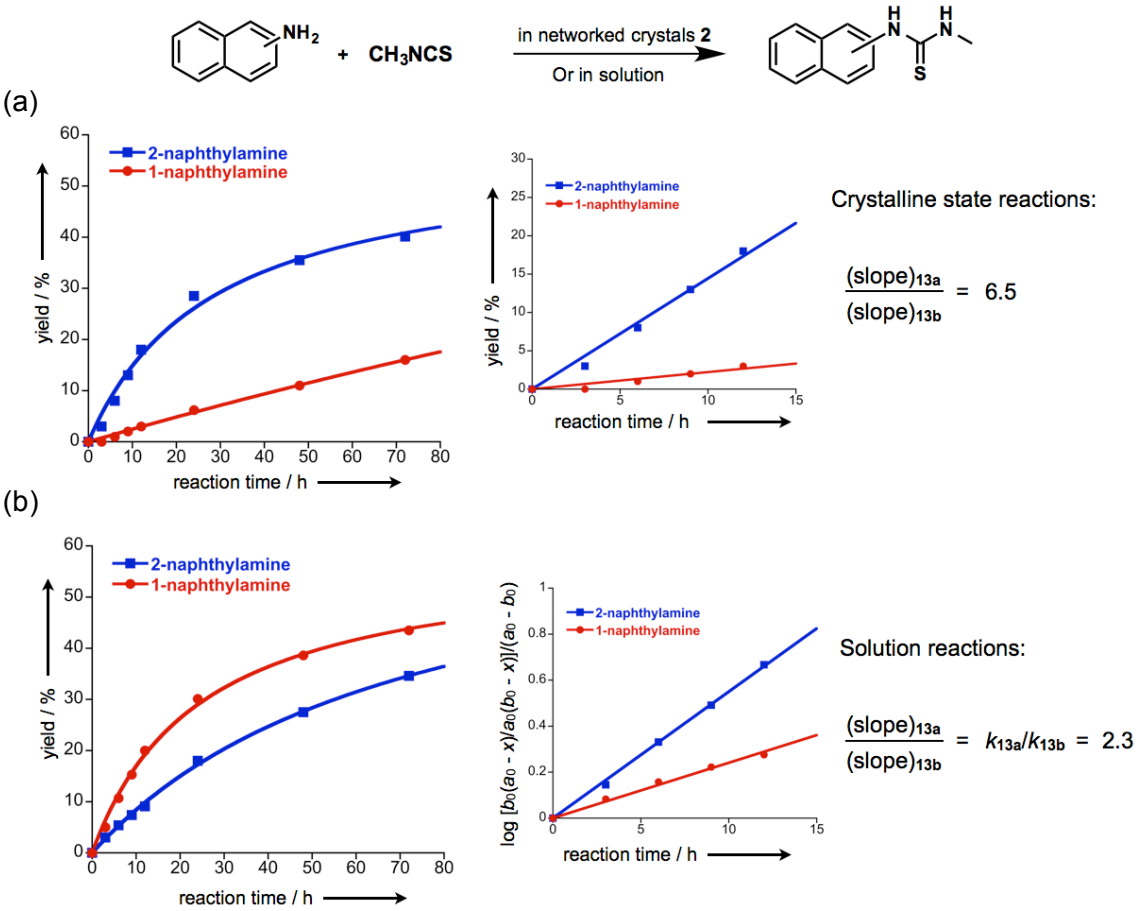

Figure S5.3. Estimation of initial relative rates for the reaction between 2- or 1-naphthylamine **14** and CH_3NCS (**11**) in (a) network **2** and (b) solution. (From SI of *Angew. Chem. In. Ed.* **2012**, *51*, 2379. Reprinted with permission from Wiley-VCH.)

- **Competition reactions with a mixture of aromatic amines**

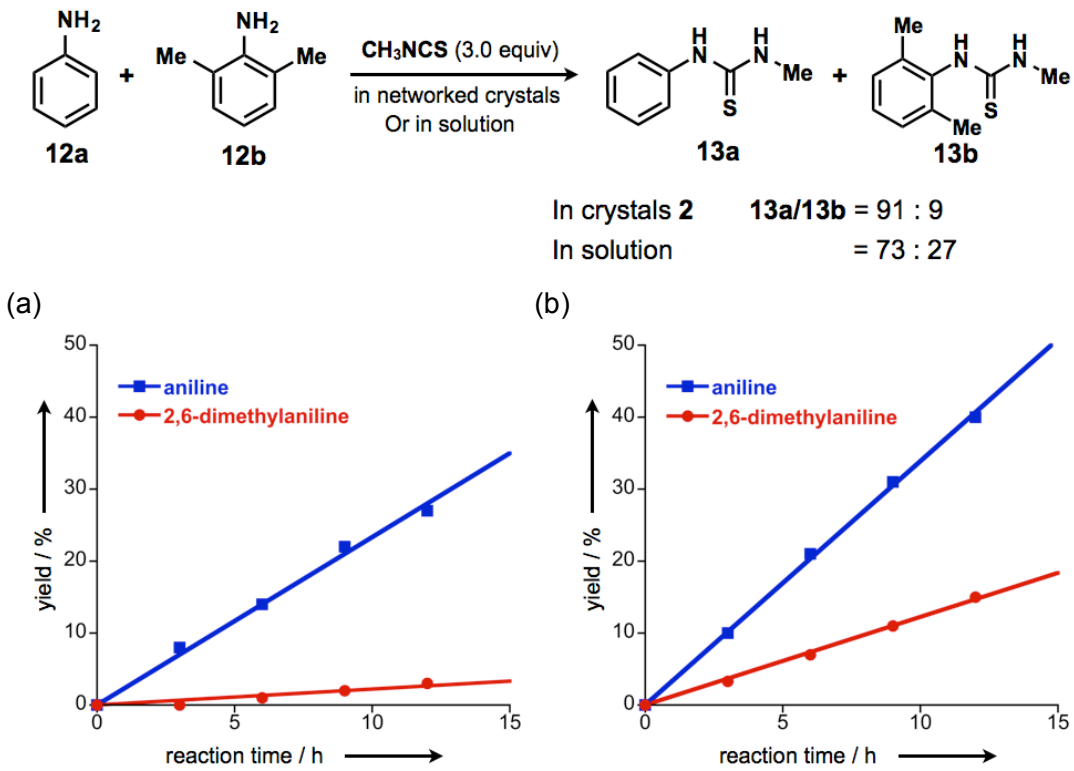

Figure S5.4. Results of competition experiments between aniline **12** and CH_3NCS (**11**). Initial conditions: $[\mathbf{12a}]_0$ = $[\mathbf{12b}]_0$ = 0.12 M (in hexadecane). 3.0 equiv of CH_3NCS (**11**) was added (a) as networked capsules **2⊃(11)$_4$** and (b) as its pure solid. (From SI of *Angew. Chem. In. Ed.* **2012**, *51*, 2379. Reprinted with permission from Wiley-VCH.)

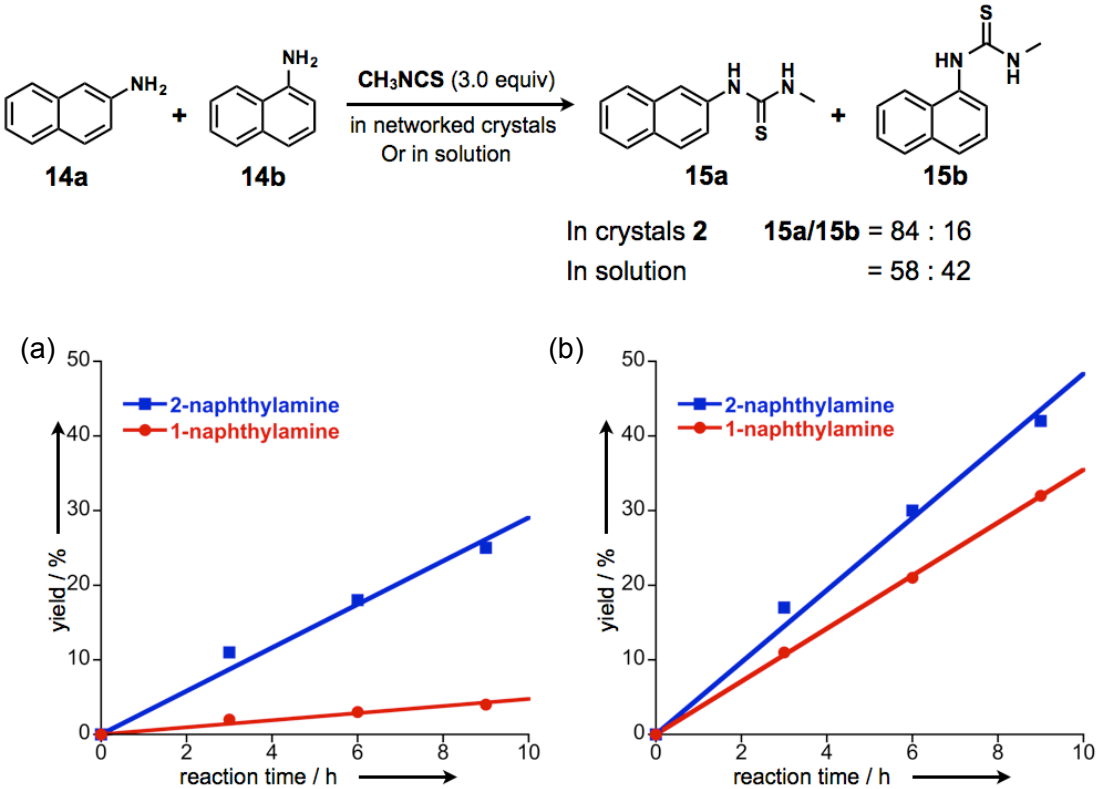

Figure S5.5. Results of competition experiments between 2- or 1-naphthylamine **14** and CH_3NCS (**11**). Initial conditions: $[\mathbf{14a}]_0 = [\mathbf{14b}]_0 = 0.12$ M (in hexadecane/toluene =1:1). 3.0 equiv of CH_3NCS (**11**) was added a) as networked capsules $\mathbf{2}\supset(\mathbf{11})_4$ and b) as its pure solid. (From SI of *Angew. Chem. In. Ed.* **2012**, *51*, 2379. Reprinted with permission from Wiley-VCH.)

- **X-ray crystallographic data**

Compound code	**2⊃(11)$_4$**	
Empirical formula	$C_{26}H_{16}N_{10}CoS_2$•0.36(C_2H_3NS)	
Formula weight	617.88	
Temperature	90(2) K	
Wavelength	0.71073 Å	
Crystal system	Cubic	
Space group	*Fd-3c*	
Unit cell dimensions	a = 64.0580(3) Å	α = 90°
	b = 64.0580(3) Å	β = 90°
	c = 64.0580(3) Å	γ = 90°
Volume	262853(21) Å^3	
Z	192	
Density (calculated)	0.749 g/cm^3	
Absorption coefficient	0.423 cm^{-1}	
F(000)	60419	
Crystal size	0.33 × 0.32 × 0.28 mm^3	
Theta range for data collection	0.90 to 26.42°	
Index ranges	-80≦ h ≦80, -80≦ k ≦80, -80≦ l ≦80	
Reflection collected	674910	
Independent reflections	11287	
Completeness to theta = 26.42	100 %	
Data / restraints / parameters	11287 / 390 / 24	
Goodness-of-fit on F2	2.141	
Final R indices [I > 2sigma(I)]	R_1 = 0.1424, wR_2 = 0.4141	
R indices (all data)	R_1 = 0.1777, wR_2 = 0.4772	
Largest diff. peak and hole	4.440 and -0.674 e. Å^3	

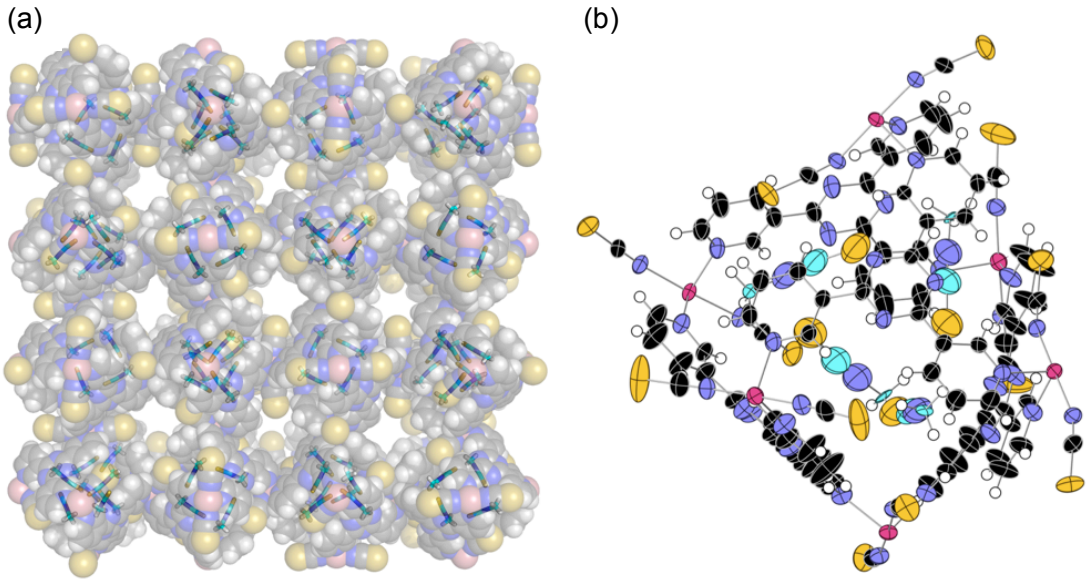

Figure S5.6. Crystal structure of networked capsules **2⊃(11)$_4$** of (a) networked structure; (b) ORTEP (50 % probability) drawing of one capsule unit. (CH_3NCS guests are drawn in cyan colour)

Chapter 6

Summary and Perspective

In this thesis, a complementary pair of dynamic capsules in solution and in crystals were designed and prepared by self-assembly of common flexible organic linker, **3-TPT**, with different metal ion (Ru(II) for solution capsule and Co(II) for crystalline capsule) (Figure 7.1). Due to the cavity equivalency and similar dynamic behavior of two capsules, the bridge of solution and the solid-state host-guest chemistry was achieved: (1) Common guest encapsulation; (2) Common host-guest properties including suppression of volatility, control of reactivity and control of guest delivery.

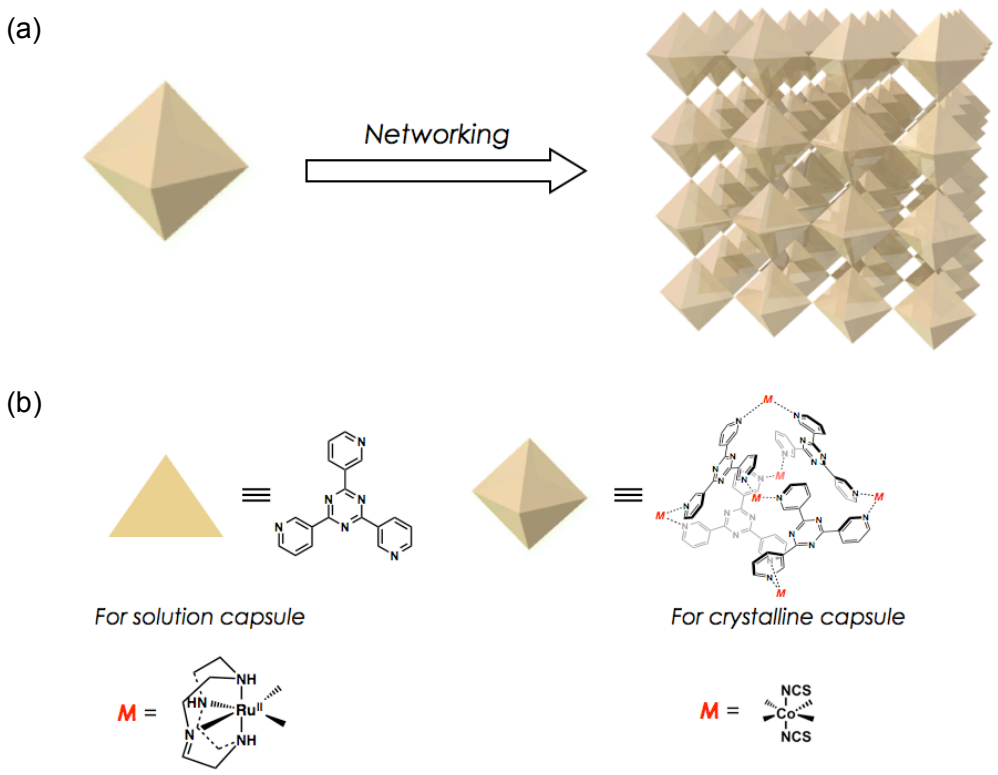

Figure 6.1 (a) Conceptual scheme of the networking of discrete capsule to networked capsules (b) the structure of solution and crystalline capsule

The applications of solution host have faced many problems, however, the applications of crystalline host are much easier (table 6.1). Therefore, in this thesis, I have discovered the unique properties for networked capsules quickly through the

solution studies, and then bring a new idea 'crystalline reagent' for application of networked capsules: Pre-installation of troublesome reagents (i.e. CH_3NCS) into networked capsules has afforded crystalline reagents that the encapsulated troublesome chemicals can be stably stored and easily handled.

Table 6.1. The comparison of solution or crystalline hosts for application

	Solution host	Crystalline host
Density	Low	High
Cost	High	Low
Scale up	Difficult	Easy
Reusability	Low	High

In Chapter 2, the synthesis and dynamic behaviors of Ru_6L_4 capsule in solution were discussed. In Chapter 3, the synthesis and dynamic host-guest chemistry of networked Co_6L_4 capsules in crystalline state were investigated. In these two chapters, the solution and crystalline capsules both were capable of isolating guest molecules from the external environment confirmed by X-ray crystallographic analysis (the window size is much narrower than the guest size). In Chapter 4, the comparison of X-ray structure of two capsules revealed that discrete capsule was isostructural with the subunit of networked capsules (M_6L_4 capsule topology) and they offer similar hydrophobic environment for guest binding through similar host-guest interactions (e.g. CH-π, van der Waals interactions and hydrophobic effects). Due to cavity equivalency and similar dynamic behavior, the bridge of solution and crystalline state chemistry were achieved with a pair of capsule hosts. In Chapter 5, take the advantages of dynamic nature of M_6L_4 capsule, the networked capsules acted as crystalline host to stabilize volatile reagents, CH_3NCS, without lose of their reactivity, therefore the encapsulated CH_3NCS could be used as crystalline solid in a simple way.

Although only qualitatively same host-guest chemistry were observed in solution and in crystals due to the intrinsic different, especially cavity volumes, the benefits from the bridge of solution and the solid-state chemistry with two dynamic capsules are

obvious: (1) The 'networking strategy' is a promising method for design and synthesis of a pair of solution and crystalline metallo-organic hosts. (2) The applications of 'cream skimming' of host-guest chemistry in solution and in crystals allow me to quick screening suitable guests and fast discovery of host-guest properties for crystalline capsule through the solution studies. On the other hand, 'cream skimming' also allow me to the visualize the solution host-guest chemistry, especially when single crystals of host-guest inclusion complex did not obtained in solution, by X-ray analysis with crystalline capsules.

This thesis has just disclosed the tip of the iceberg of bridge of host-guest chemistry in solution and in crystals. In the future, I think some investigations will be very valuable in this area:

1. Since the dynamic or flexible nature is key factor of solution host-guest chemistry, the construction of dynamic host cavity must be achieved in crystals. In this research, the dynamic behavior of capsules was transferred into crystalline-state partially (solution capsules is more flexible than crystalline capsules). In the future, the construction of dynamic or flexible host cavity in crystals that is exactly same with solution host is still a challenge.
2. Although the organic ligand is key factor for construction of same molecular space in solution and in crystals, the effects of metals should be also considered (in this research, the Ru(II) for solution and Co(II) for crystalline state, resulting different charge for host cavity (+12 for solution capsule and natural for crystalline capsules)). In the future, design of solution and crystalline host using same organic ligand and metal ion is also a challenge.
3. Since most of synthetic hosts in solution have a hydrophobic molecular space, the solvent is very important for guest binding. I believed that the synthesis of water stable crystalline host can improve the guest binding ability and similarity between solution and crystalline-state host-guest chemistry.

References:

[1] For some reviews: a) D. J. Cram, "Molecular container compounds" *Nature* **1992**, *356*, 29-36; b) F. Hof, S. L. Craig, C. Nuckolls, J. Rebek, Jr., "Molecular Encapsulation" *Angew. Chem. Int. Ed.* **2002**, *41*, 1488-1508; c) R. Warmuth, "The Inner Phase of Molecular Container Compounds as a Novel Reaction Environment" *J. Incl. Phenom. Macrocycl. Chem.* **2000**, *37,* 1-38; d) J. Rebek, Jr., "Simultaneous Encapsulation: Molecules Held at Close Range" *Angew. Chem. Int. Ed.* **2005**, *44*, 2068-2078.

[2] A. Jasat, J. C. Sherman, "Carceplexes and Hemicarceplexes" *Chem. Rev.* **1999**, *99*, 931-967.

[3] J. C. Sherman, D. J. Cram, "Carcerand Interiors Provide a New Phase of Matter" *J. Am. Chem. Soc.* **1989**, *111*, 4527-4528.

[4] D. J. Cram, M. E. Tanner, R. Thomas, "The Taming of Cyclobutadiene" *Angew. Chem. Int. Ed.* **1991**, *30*, 1024-1027.

[5] R. Warmuth, "*o*-Benzyne Strained Alkyne or Cumulene? − NMR Characterization in a Molecular Container" *Angew. Chem. Int. Ed.* **1997**, *36*, 1347-1350.

[6] L. R. MacGillivray, J. L. Atwood, "A Chiral Spherical Molecular Assembly Held Together by 60 Hydrogen Bonds" *Nature* **1997**, *389*, 469-472.

[7] G. W. V. Cave, J. Antesberger, L. J. Barbour, R. M. McKinlay, J. L. Atwood, "Inner Core Structure Responds to Communication between Nanocapsule Walls" *Angew. Chem. Int. Ed.* **2004**, *43*, 5263-5266.

[8] N. Branda, R. Wyler, J. Rebek, Jr., "Encapsulation of Methane and Other Small Molecules in a Self-Assembling Superstructure" *Science* **1994**, *263*, 1267-1268.

[9] R. S. Meissner, J. Rebek, Jr., J. Mendoza, "Auto encapsulation Through Intermolecular Forces: A Synthetic Self-Assembling Spherical Complex" *Science* **1995**, *264*, 1485-1488.

[10] T. Heinz, D. M. Rudkevich, J. Rebek, Jr., "Pairwise Selection of Guests in a Cylindrical Molecular Capsule of Nanometre Dimensions" *Nature* **1998**, *394*, 764-767.

[11] D. Ajami, J. Rebek, Jr., "More Chemistry in Small Spaces" *Acc. Chem. Res.* **2012**, *46*, 990-999.

[12] J. Kang, J. Rebek, Jr., "Acceleration of a Diels-Alder reaction by a Self-assembled Molecular Capsule" *Nature* **1997**, *385*, 50-52.

[13] A. Shivanyuk, J. Rebek, Jr., "Social Isomers in Encapsulation Complexes" *J. Am. Chem. Soc.* **2002**, *124*, 12074-12075.

[14] D. L. Caulder, K. N. Raymond, " The Self-Assembly of a Predesigned Tetrahedral M_4L_6 Supramolecular Cluster" *Angew. Chem. Int. Ed.* **1998**, *37*, 1840-1843.

[15] M. Ziegler, J. L. Brumaghim, K. N. Raymond, "Stabilization of a Reactive Cationic Species by Supramolecular Encapsulation" *Angew. Chem. Int. Ed.* **2000**, *39*, 4119-4121.

[16] P. Mal, B. Breiner, K. Rissanen, J. R. Nitschke, "White Phosphorus Is Air-Stable Within a Self-Assembled Tetrahedral Capsule" *Science* **2009**, *324*, 1697-1699.

[17] M. Fujita, D. Oguro, M. Miyazawa, H. Oka, K. Yamaguchi, K. Ogura, "Self-Assembly of 10 Molecules into Nanometer-sized Organic Host Frameworks" *Nature* **1995**, *378*, 469-471.

[18] S. Horiuchi, T. Murase, M. Fujita, "Noncovalent Trapping and Stabilization of Dinuclear Ruthenium Complexes within a Coordination Cage" *J. Am. Chem. Soc.* **2011**, *133*, 12445-12447.

[19] J. L. Atwood, J. E. D. Davies, D. D. Macnicol, F. Vögtle, J.-M. Lehn, , Volume 7 in 'Comprehensive Supramolecular Chemistry', Elsevier Science, New York, **1996**.

[20] J. A. Incavo, P. K. Dutta, "Zeolite Host-Guest Interactions: Optical Spectroscopic Properties of Tris(bipyridine)ruthenium(II)in Zeolite Y Cages" *J. Phys. Chem.* **1990**, *94*, 3075-3081.

[21] For reviews, see: a) S. R. Batten, R. Robson, "Interpenetrating Nets: Ordered, Periodic Entanglement" *Angew. Chem., Int. Ed.* **1998**, *37*, 1460–1494; b) O. M. Yaghi, M. O'Keeffe, N. W. Ockwig, H. K. Chae, M. Eddaoudi, J. Kim, "Reticular Synthesis and the Design of New Materials" *Nature* **2003**, *423*, 705–714; c) S. Kitagawa, R. Kitaura, S. Noro, "Functional Porous Coordination Polymers" *Angew. Chem., Int. Ed.* **2004**, *43*, 2334–2375; d) M. Kawano, M. Fujita, "Direct Observation of Crystalline-State Guest Exchange in Coordination Networks" *Coord. Chem. Rev.* **2007**, *151*, 2592–2605; e) G. Férey, " Hybrid Porous Solids: Past, Present, Future" *Chem. Soc. Rev.* **2008**, *37*, 191–214; f) B. Moulton, M. J. Zaworotko, "From Molecules to Crystal Engineering: Supramolecular Isomerism and Polymorphism in Network Solids" *Chem. Rev.* **2001,** *101*, 1629–1658.

[22] H. Deng, S. Grunder, K. E. Cordova, C. Valente, H. Furukawa, M. Hmadeh, F.

Gándara, A. C. Whalley, Z. Liu, S. Asahina, H. Kazumori, M. O'Keeffe, O. Terasaki, J. F. Stoddart, O. M. Yaghi, "Large-Pore Apertures in a Series of Metal-Organic Frameworks" *Science* **2012**, *336*, 1018-1023.

[23] S. S.-Y. Chui, S. M.-F. Lo, J. P. H. Charmant, A. G. Orpen, I. D. Williams, "A Chemically Functionalizable Nanoporous Material $[Cu_3(TMA)_2(H_2O)_3]_n$" *Science* **1999**, *283*, 1148-1150.

[24] J. L. C. Rowsell, O. M. Yaghi, "Effects of Functionalization, Catenation, and Variation of the Metal Oxide and Organic Linking Units on the Low-Pressure Hydrogen Adsorption Properties of Metal–Organic Frameworks" *J. Am. Chem. Soc.* **2006**, *128*, 1304-1315.

[25] M. Dincă, W. S. Han, Y. Liu, A. Dailly, C. M. Brown, J. R. Long, "Observation of Cu^{2+}–H_2 Interactions in a Fully Desolvated Sodalite-Type Metal–Organic Framework" *Angew. Chem. Int. Ed.* **2007**, *46*, 1419-1422.

[26] R. Custelcean, B. A. Moyera, B. P. Hay, "A Coordinatively Saturated Sulfate Encapsulated in a Metal–Organic Framework Functionalized with Urea Hydrogen-Bonding Groups" *Chem. Commun.* **2005**, *48*, 5971-5973.

[27] T. Mitra, K. E. Jelfs, M. Schmidtmann, A. Ahmed, S. Y. Chong, D. J. Adams, A. I. Cooper, "Molecular Shape Sorting Using Molecular Organic Cages" *Nat. Chem.* **2013**, *5*, 276-281.

[28] M. Fujita, J. Yazaki, K. Ogura, "Macrocyclic Polynuclear Complexes $[(en)M(4,4'\text{-bpy})]]_4(NO_3)_8$ (M = Pd or Pt) as Inorganic Cycophane."Their Ability for Molecular Recognition"" *Tetrahedron Lett.* **1991**, *32*, 5589-5592.

[29] M. Fujita, Y. J. Kwon, S. Washizu, K. Ogura, "Preparation, Clathration Ability, and Catalysis of a Two-Dimensional Square Network Material Composed of Cadmium(II) and 4,4'-Bipyridine" *J. Am. Chem. Soc.* **1994**, *116*, 1151-1152.

[30] Y. Inokuma, T. Arai, M. Fujita, "Networked Molecular Cages as Crystalline Dponges for Fullerenes and other Guests" *Nat. Chem.* **2010**, *2*, 780-783.

[31] S. Hiraoka, M. Fujita, " Guest-Selected Formation of Pd(II)-Linked Cages from a Dynamic Receptor Library" *J. Am. Chem. Soc.* **1999**, *121*, 10239-10240.

[32] A. V. Davis, K. N. Raymond, "The Big Squeeze: Guest Exchange in an M_4L_6 Supramolecular Host" *J. Am. Chem. Soc.* **2005**, *127*, 7912-7919.

[33] For reviews a) S. Kitagawa, K. Uemura, " Dynamic Porous Properties of Coordination Polymers Inspired by Hydrogen Bonds" *Chem. Soc. Rev.* **2005**, *34*,

109-119; b) G. Férey, C. Serre, "Large Breathing Effects in Three-dimensional Porous Hybrid Matter: Facts, Analyses, Rules and Consequences" *Chem. Soc. Rev.* **2009**, *38*, 1380-1399.

[34] K. Biradha, M. Fujita, "A Spring-like 3D-Coordination Network that Shrinks/Swells in Crystal-to-Crystal Manner upon Guest Removal and Exchange" *Angew. Chem. Int. Ed.* **2002**, *41*, 3392-3395.

[35] S. K. Ghosh, S. Bureekaew, S. Kitagawa, "A Dynamic, Isocyanurate Functionalized Porous Coordination Polymer" *Angew. Chem. Int. Ed.* **2008**, *47*, 3403-3406.

[36] B. Therrien, " Coordination Chemistry of 2,4,6-tri(pyridyl)-1,3,5-triazine Ligands" *J. Organomet. Chem.* **2011**, *696*, 637-651.

[37] J. Freudenreich, J. Furrer, G. Süss-Fink, B. Therrien, "Template-Directed Synthesis of Hexanuclear Arene Ruthenium Complexes with Trigonal-Prismatic Architecture Based on 2,4,6-Tris(3-pyridyl)triazine Ligands" *Organometallic* **2011**, *30*, 942-951.

[38] C.- Y. Hung, A. S. Singh, C.- W. Chen, Y.- S. Wen, S.- S. Sun, "Colorimetric and Luminescent Sensing of F^- Anion through Strong Anion–π Interaction inside the π-acidic Cavity of a Pyridyl-triazine Bridged Trinuclear Re(I)–tricarbonyl Diimine Complex" *Chem. Commun.* **2009**, *45*, 1511-1513.

[39] P. Govindaswamy, G. Süss-Fink, B. Therrien, "Self-Assembled Chloro-Bridged (Arene)ruthenium Metallo-Prisms: Synthesis and Molecular Structure of Cationic Complexes of the Type $[Ru_6(\eta^6\text{-arene})_6(\mu_3\text{-tpt-K}N)_2(\mu\text{-Cl})_6]^{6+}$ (tpt) 2,4,6-tris(pyridinyl)-1,3,5-triazine)" *Organometallic* **2007**, *26*, 915-924.

[40] S.- Y. Yu, T. Kusukawa, K. Biradha, M. Fujita, "Hydrophobic Assembling of a Coordination Nanobowl into a Dimeric Capsule which Can Accommodate up to Six Large Organic Molecules" *J. Am. Chem. Soc.* **2000**, *122*, 2665-2666.

[41] M. Fujita, S.- Y. Yu, T. Kusukawa, H. Funaki, K. Ogura, K. Yamaguchi, "Nanometer-Sized Macrotricyclic Complexes Self-Assembled from Ten Small Component Moleules" *Angew. Chem. Int. Ed.* **1998**, *37*, 2082-2085.

[42] K. Q. Ferreira, F. G. Santos, Z. N. Rocha, T. Guaratini, R. S. Silva, E. Tfouni, "Conformational Isomers of *Cis*-chloro(nitrosyl)(1,4,7,10-tetraazacyclododecene) ruthenium(II), *Cis*-$[Ru^{II}Cl(imcyclen)(NO^+)]^{2+}$. Oxidation of the Coordinated 1,4,7,10-tetraazacyclododecane (cyclen) Ligand" *Inorg. Chem. Commun.* **2004**, *7*, 204-208.

[43] L. A. Berben, M. C. Faia, N. R. M. Crawford, J. R. Long, "Angle-Dependent Electronic Effects in 4,4′-Bipyridine-Bridged Ru_3 Triangle and Ru_4 Square Complexes" *Inorg. Chem.* **2006**, *45*, 6378-6386.

[44] G. J. Kleywegt, T. A. Jones, "Detection, Delineation, Measurement and Display of Cavities in Macromolecular Structures" *Acta Crystallogr.* **1994**, D50, 178-185.

[45] a) Spek, A. L. *PLATON – A Multipurpose Crystallographic Tool*; Utrecht University, Utrecht, The Netherlands, 2003; b) P. V. Sluis, Spek, A. L. "Bypass: An Effective Method for the Refinement of Crystal Structures Containing Disordered Solvent Regions" *Acta. Cryst., Sect. A*, **1990**, 46, 194-201.

[46] Y. Inokuma, S. Yoshioka, M. Fujita, "A Molecular Capsule Network: Guest Encapsulation and Control of Diels–Alder Reactivity" *Angew. Chem. Int. Ed.* **2010**, *49,* 8912–8914.

[47] R. A. Bilbeisi, J. K. Clegg, N. Elgrishi, X. Hatten, M. Devillard, B. Breiner, P. Mal, J. R. Nitschke, "Subcomponent Self-Assembly and Guest-Binding Properties of Face-Capped $Fe_4L_4^{8+}$ Capsules" *J. Am. Chem. Soc.* **2012**, *134*, 5110–5119.

[48] a) H.-J. Schneider, "Mechanisms of Molecular Recognition: Investigations of Organic Host-Guest Complexes" *Angew. Chem. Int. Ed.* **1991**, *30,* 1417–1436; b) C. A. Hunter, J. K. M. Sanders, "The Nature of π–π interactions" *J. Am. Chem. Soc.* **1990**, *112*, 5525–5534; c) J. C. Ma, D. A. Dougherty, "The Cation–π Interaction" *Chem. Rev.* **1997**, *97*, 1303-1324; d) M. Nishio, " CH/π Hydrogen Bonds in Crystals" *CrystEngComm*, **2004**, *6*, 130-158.

[49] T. Ohara, T. Sato, N. Shimizu, G. Prescher, H. Schwind, O. Weiberg, K. Marten, H. Greim, **2003**. "Acrylic Acid and Derivatives" *Ullmann's Encyclopedia of Industrial Chemistry*.

[50] M. Suchoparek, J. Spevacek, "Characterization of the Stereochemical Structure of Poly(tert-butyl acrylate) by One- and Two-dimensional NMR Spectroscopy" *Macromolecules* **1993**, *26*, 102– 106.

[51] a) G. Manecke, P. Reuter, "Reactions on and with Polymers" *Pure Appl. Chem.* **1979**, *51*, 2313-2330; b) D. Hudson, "Matrix Assisted Synthetic Transformations: A Mosaic of Diverse Contributions. I. The Pattern Emerges" *J. Combin. Chem.* **1999**, *1,* 333-360; c) D. Hudson, "Matrix Assisted Synthetic Transformations: A Mosaic of Diverse Contributions. II. The Pattern Is Completed" *J. Combin. Chem.* **1999**, *1,* 403-457.

[52] Examples of crystalline state reactions within porous coordination networks in which substrates or catalysts are embedded before the reaction: a) S. M. Cohen, Z. Q. Wang, "Postsynthetic Modification of Metal–Organic Frameworks" *Chem. Soc. Rev.* **2009**, *38*, 1315–1329; b) Y. Inokuma, M. Kawano, M. Fujita, "Crystalline Molecular Flasks" *Nat. Chem.* **2011**, *3*, 349–358; c) J. S. Seo, D. Whang, H. Lee, S. I. Jun, J. Oh, Y. J. Jeon, K. Kim, "A Homochiral Metal–Organic Porous Material for Enantioselective Separation and Catalysis" *Nature* **2000**, *404*, 982–986; d) W. B. Lin, L. Q. Ma, C. Abney, "Enantioselective Catalysis with Homochiral Metal–Organic Frameworks" *Chem. Soc. Rev.* **2009**, *38*, 1248–1256; e) T. Kawamichi, T. Haneda, M. Kawano, M. Fujita, "X-ray Observation of A Transient Hemiaminal Trapped in A Porous Network" *Nature* **2009**, *461*, 633–635; f) S. C. Jones, C. A. Bauer, "Diastereoselective Heterogeneous Bromination of Stilbene in a Porous Metal-Organic Framework" *J. Am Chem. Soc.* **2009**, *131*, 12516–12517; g) K. Ohara, Y. Inokuma, M. Fujita, "The Catalytic Z to E Isomerization of Stilbenes in a Photosensitizing Porous Coordination Network" *Angew. Chem. Int. Ed.* **2010**, *49*, 5507–5509; h) J. M. Falkowski, C. Wang, S. Liu, W. Lin, "Actuation of Asymmetric Cyclopropanation Catalysts: Reversible Single Crystal to Single Crystal Reduction of Metal–Organic Frameworks" *Angew. Chem. Int. Ed.* **2011**, *50*, 8674-8678.

[53] a) Harper and Row, "*Chemical Kinetics*" 3rd ed. (Ed. K. J. Laidler), New York, **1987**; b) E. Dyer, J. F. Glenn, "The Kinetics of the Reactions of Phenyl Isocyanate with Certain Thiols" *J. Am. Chem. Soc.* **1957**, *79*, 366–369.

List of Publication

Publication related to this thesis:

1. **Guo-Hong Ning**, Yasuhide Inokuma, and Makoto Fujita*; Dynamic Behavior of M_6L_4 Capsule in Solution and Crystalline State, *Chem. Asian. J.* **2013**, *8,* 2596 – 2599.

   (Chapter 2~4)

2. Yasuhide Inokuma, **Guo-Hong Ning**, and Makoto Fujita*; Reagent-Installed Capsule Network: Selective Thiocarbamoylation of Aromatic Amines in Crystals with Preinstalled CH_3NCS, *Angew. Chem. Int. Ed.* **2012**, *51*, 2379 – 2381.

   (Chapter 5)

3. **Guo-Hong Ning**, Yasuhide Inokuma and Makoto Fujita*; Stable Encapsulation of Acrylates in Networked Molecular Capsules, *Chem. Asian. J.* **2014**, *9,* 466 – 468,

   (Chapter 4)

Other Publications:

4. **Guo-Hong Ning**, Ting-Zheng Xie, Yuan-Jiang Pan, Yi-Zhi Li, Shu-Yan Yu*; Self-Assembly of Bowl-Like Metallo-macrocycles, *Dalton, Trans.,* **2010**, *39*, 3203–3211.

5. **Guo-Hong Ning**, Liao-Yuan Yao, Li-Xia Liu, Ting-Zheng Xie, Yi-Zhi Li, Yu Qin, Yuan-Jiang Pan, Shu-Yan Yu*; Self-Assembly and Host-Guest Interaction of Metallo-marcocycles Using Fluorescent Dipyrazole Linker with Dimetallic Clips, *Inorg. Chem.,* **2010**, *49*, 7783-7792.

6. **Guo-Hong Ning**, Yi-Zhi Li, Shu-Yan Yu*; Synthesis, Spectroscopic Properties and Crystal Structure of 3,3′-(Anthracene- 9,10-diyl)bis(1-phenylpropan-1-one), *Chinese J. Struct. Chem.,* **2010**, *12*, 1780-1783.

7. Mingrui Li, Chunyan Deng, Chao Chen, Limei Peng, **Guohong Ning**, Qingji Xie*, Shouzhuo Yao; An Amperometric Hydrogen Peroxide Biosensor Based on a Hemoglobin-Immobilized Dopamine-Oxidation Polymer/Prussian Blue/Au Electrode, *Electroanalysis,* **2006**, *18*, 2210-2217.

Acknowledgement

First of all, I would like to give my sincere thanks to my supervisor, Professor Makoto Fujita, for his constructive guidance (e.g. His big-picture view of the research help me to keeps it moving forward smoothly) and continuous support throughout this thesis. As a foreign student, I also very appreciate his kind support in my personal life that I am able to devote myself to academic research in his group.

I am so luck to work with Assistant Professor Yasuhide Inokuma, a talented young chemist who teaches me how to become an independent researcher that I am still working on. I want to thank him for his valuable advices, inspirited discussions and encouragement all through my doctoral research. His professional and broad knowledge in chemistry has provided me instructive suggestions for my experiments.

Big thanks should be given to Dr. Qingfu Sun, Mr. Koki Ikemoto, Mr. Shota Yoshioka and Mr. Tatsuhiko Arai for introducing me the X-ray structure refinement technic and help me in the X-ray facility; I also thank to Dr. Junji Iwasa, Mr. Tkafumi Osuga and Miss. Eri Numata for the assistance of mass measurement and analyses; I also appreciated Dr. Kate Harris for valuable proofreading and comments on my manuscripts; I would like to further thank Mr. Yu Fang and Mr. Ryosuke Takeuchi for help me so much in my daily life.

I am very grateful to Lecturer Sota Sato, Assistant Professor Takashi Murase, Assistant Professor Tomohisa Sawada, Mr. Yuh Kohyoma, Dr. Shinnosuke Horiuchi Mr. Hiroki Takezawa, Mr. Jinu Jeong, Miss. Junko Ariyoshi and all the other members in the Fujita group for their kind helps on the experiments, discussions and encouragement in the past three years.

I especially appreciate the secretaries of the Fujita group, Miss Yukari Ara, Mrs. Ayano Oishi and Miss Noriki Yamaguchi for their kind assistance and support not only in my Lab-work, but also in my personal life.

I would like to acknowledge The University of Tokyo Global COE program and

the Japan Society for the Promotion of Science (JSPS) for financial support.

Lastly, I would like to dedicate this thesis to my family and friends. Without their supports and helps, I would not possible to accomplish my doctoral research in past three years.

Guo-Hong Ning
August 2013